Tissue-Specific effects of Pregnane X Receptor (PXR) and Estrogen Sulfotransferase (EST) on Hemorrhagic Shock-Induced Multiple Organ Injuries

by

Yang Xie

Bachelor of Science, China Pharmaceutical University, 2011

Master of Science, China Pharmaceutical University, 2014

Submitted to the Graduate Faculty of the

School of Pharmacy in partial fulfillment

of the requirements for the degree of

Doctor of Philosophy

University of Pittsburgh

2020

UNIVERSITY OF PITTSBURGH

SCHOOL OF PHARMACY

This dissertation was presented

by

Yang Xie

It was defended on

March 3, 2020

and approved by

Xiaochao Ma, PhD, Associate Professor, Pharmaceutical Sciences

Christian Fernandez, PhD, Assistant Professor, Pharmaceutical Sciences

Jie Fan, MD, PhD, Professor, Surgery

Melanie Scott, MD, PhD, Associate Professor, Surgery

Dissertation Advisor: Wen Xie, MD, PhD, Pharmaceutical Sciences

Tissue-Specific effects of Pregnane X Receptor (PXR) and Estrogen Sulfotransferase (EST) on Hemorrhagic Shock-Induced Multiple Organ Injuries

Yang Xie, PhD

University of Pittsburgh, 2020

Hemorrhagic shock (HS) is a life-threatening condition associated with tissue hypoperfusion. HS may lead to dysfunction of multiple organs, including the liver and lung, as a result of oxidative stress and a secondary inflammatory stimulus. Pregnane X receptor (PXR) is a species-specific xenobiotic receptor that regulates the expression of drug-metabolizing enzymes (DMEs) such as the cytochrome P450 3A (CYP3A). Many clinical drugs, including those often prescribed to trauma patients, are known to activate PXR and induce CYP3A. However, it is unclear whether and how PXR plays a role in the regulation of DMEs in the setting of HS and HS-induced hepatic and extrahepatic injury. The estrogen sulfotransferase (EST, or SULT1E1) is a conjugating enzyme that sulfonates and deactivates estrogens. We have previously reported that the expression of EST is highly inducible in the livers of mouse models of multiple diseases, including obesity and type 2 diabetes, liver ischemia and reperfusion, and sepsis. The induction of EST by these disease conditions led to attenuated estrogen responses and have impact on the outcome of these diseases through varied mechanisms and often in a sex- and tissue-specific manner. It is unclear whether and how EST plays a role in HS-induced liver and lung injury. In this dissertation study, I studied the tissue-specific effects of PXR and EST on HS-induced hepatic injury and acute lung injury, respectively. My results demonstrated that (1) activation of PXR sensitizes mice to HS-induced hepatic injury but not acute lung injury. The unavoidable use of PXR-activating drugs in trauma patients has the potential to exacerbate HS-induced hepatic injury, which can be mitigated by the co-administration of anti-oxidative agents, CYP3A inhibitors, or

PXR antagonists. (2) Genetic ablation or pharmacological inhibition of Est effectively protected female mice from HS-induced acute lung injury. The pulmonoprotective effect of Est ablation or inhibition was sex- and tissue-specific. HS-induced hepatic injury was not affected in Est knockout ($Est^{-/-}$) mice. Pharmacological inhibition of EST may represent an effective approach in female patients to manage HS-induced acute lung injury. In summary, my dissertation research has uncovered the tissue-specific effects of PXR and EST on HS-induced multiple organ injuries.

Table of Contents

List of Tables

List of Figures

Preface

From time to time, I keep imagining that day where I can finally say: “I did it!” And now I’m proud to say, “I did it! I never gave up!” For the past six years, I have been very fortunate to pursue my PhD training at the University of Pittsburgh, School of Pharmacy. This is so far the best time and the most difficult but exciting adventure I have ever had which I will surely treasure for the rest of my life.

First, my sincere gratitude goes to my dear advisor, Dr. Wen Xie, for his dedicated mentorship and tremendous support since 2014. Dr. Xie was the first one to offer the olive branch, which encouraged me to continue my academic dream. His trust and support to allow me to pursue my own research interest made me see myself in doing research. His encouragement and understanding in the time of difficulties made me feel of being cared and cherished. His great mentorship lighted a fire of ambition again in my academic career. Without his mentoring in science and life, I would not be where I am today. I, like any one of your students, will always love you.

It was also my great pleasure to work with so many lab mates in Xie lab who shape my training and accompany me as family: Songrong Ren, Meishu Xu, Mengxi Jiang, Jiong Yan, Peipei Lu, Yuhan Bi, Xinran Cai, Anne Barbosa, Hung-Chun Tung, Jingyuan Wang, Gregory Young, Xinyun Chen, Yunqi An, Wojciech Garbacz, Yueshui Zhao, You-Jin Choi, Junjie Zhu, Pengfei Xu, Jibin Guan, Xuan Qin, Yan Guo, Zhihui Zheng, Zanmei Zhao, Dan Xu, Yongdong Niu, Li Gao, Ye Feng, Bin Li, Ziteng Zhang, Yingjie Guo, Zihui Fang, Yue Xi, and Jing Li.

I would also thank my committee members, Dr. Xiaochao Ma, Dr. Christian Fernandez, Dr. Jie Fan, and Dr. Melanie Scott, for their insightful comments from various perspectives to help

improve my research, the precious time and efforts they have committed. It is our numerous discussions that inspired this dissertation piece by piece.

I would also acknowledge my dearest friends and colleagues in School of Pharmacy: Chenxiao Tang, Adriana Zakrzewska, Amina Shehu, Yuemin Bian, Yankang Jing, Ruichao Xu, Ziheng Hu, Lingjue Li, Junyi Li, Alex Prokopienko, Yoko Frenchetti, Zhuoya Wan, and Xin Tong, who made my time at Pitt wonderful and lively.

I'd also like to thank the fellows in the Center of Pharmacogenetics, the staff, faculty, and students in the School of Pharmacy, in particular, I want to sincerely thank Bill, Maggie and Lori for their readiness for help whenever it was.

Finally, I give my heartful gratitude to my family for their unconditional love, dedication and support. I want to thank my parents, Liping Xie and Yizhi Yang, and in-laws for their tremendous support and understanding. I also want to thank my beloved husband, Changrui Xing, my best friend and soul mate, with whom I shared joys and tears all over the years. We made so many memories in Pittsburgh that will last forever. Our marriage and our lovely son, Eddie, are the best gifts during my graduate study, as well as for the rest of my life. With the power of love, I will keep marching forward on my way of life and career regardless of trials and hardships.

1.0 Introduction

Hemorrhagic shock (HS), a life-threatening condition when the body loses more than 20% of its blood or fluid supply, is the leading cause of death and disability in patients younger than 54 years of age (Krug et al., 2000). During the acute phase of hemorrhage, in addition to stopping bleeding, fluid resuscitation is a therapeutic priority in the clinic. Although the modern resuscitation techniques developed in the 1960s have led to an improved immediate survival, the emergence of subsequent organ failure remains a major health issue that may lead to late death (Minei et al., 2012). Among the mechanisms of HS-induced tissue injury, an exaggerated inflammatory response and oxidative stress generated through resuscitation are the major contributors to cellular membrane damage, cell death and tissue damage (Toklu and Tumer, 2015). The liver (Yu et al., 2008; Wetzel et al., 2014) and lung (Rubenfeld et al., 2005; Villar et al., 2014) are organs sensitive to HS-induced injury. A growing body of evidence has also put the xenobiotic receptors, such as PXR, and metabolic enzymes, such as EST, in the physiological and pathological context beyond the classical functions, such as endobiotic metabolism and immune responses. These newest findings propel us to do further investigation on the novel functions of PXR and EST in the underlying molecular mechanisms of HS-induced multiple organ injuries.

1.1 Hypothesis and Specific Aims

Studies by others have suggested that PXR and EST play fundamental roles in exogenous and endogenous metabolism, which impact on multiple diseases, including drug-induced liver

injury, obesity and type 2 diabetes, hepatic ischemia and reperfusion, and sepsis. The dissertation work was dedicating to the novel hepatic/extrahepatic function of PXR and EST in HS-induced multiple organ injures. The overall hypothesis is that 1) activation of PXR sensitizes hemorrhagic shock-induced liver injury via inducing the expression of CYP3A and oxidative stress, but shows no effects on HS-induced acute lung injury; 2) hepatic EST distantly sensitizes mice to HS-induced acute lung injury in a sex-specific manner, but shows very limited impact on HS-induced hepatic injury.

There are two specific aims in the dissertation study:

For the specific Aim 1, we have investigated the role of PXR in the regulation of drug metabolism enzymes (DMEs) in the setting of HS, and whether activation of PXR is beneficial or detrimental to HS-induced hepatic injury. PXR transgenic, knockout, and humanized mice were subject to hemorrhagic shock and resuscitation (HS/R). The liver injury, as well as lung injury, was assessed histologically and biochemically. The expression and/or activity of PXR and CYP3A were manipulated genetically or pharmacologically in order to determine their effects on HS-induced hepatic injury. Our results showed that genetic or pharmacological activation of PXR sensitized wild-type (WT) and hPXR/CYP3A4 humanized mice to HS-induced hepatic injury, whereas knockout of PXR protected mice from HS-induced hepatic injury. The manipulation of PXR showed little impact on HS-induced acute lung injury which can be explained by the low expression of PXR in the lung. Mechanistically, the sensitizing effect on liver injury of PXR activation was accounted for by PXR-responsive induction of CYP3A and increased oxidative stress in the liver. The sensitizing effect of PXR was attenuated by ablation or pharmacological inhibition of CYP3A, treatment with the antioxidant *N*-acetylcysteine amide (NACA), or treatment with a PXR antagonist. In this specific study, we have uncovered a novel function of PXR in HS-

induced hepatic injury. Our results suggest that the unavoidable use of PXR-activating drugs in trauma patients has the potential to exacerbate HS-induced hepatic injury, which can be mitigated by the co-administration of anti-oxidative agents, CYP3A inhibitors, or PXR antagonists.

For the specific Aim 2, we have investigated the role of liver EST in HS-induced acute lung injury through sulfonating and deactivating estrogens. In this specific study, we showed that the expression of Est was markedly induced in the liver, but not in the lung of female mice subject to HS/R. Genetic ablation or pharmacological inhibition of Est effectively protected female mice from HS-induced acute lung injury, including interstitial edema, neutrophil mobilization and infiltration, and inflammation, while showed limited protection from HS-induced hepatic injury. The pulmonoprotective effect Est ablation or inhibition was sex-specific, because the HS-induced acute lung injury was not affected in male Est$^{-/-}$ mice. Mechanistically, the pulmonoprotective phenotype in female Est$^{-/-}$ mice was accompanied by increased lung and circulating levels of estrogens, attenuated pulmonary inflammation, and inhibition of neutrophil mobilization from the bone marrow and infiltration to the lung, whereas the pulmonoprotective effect was abolished upon ovariectomy, suggesting that the pulmonoprotective effect was estrogen dependent. The pulmonoprotective effect of Est ablation was also tissue-specific, as loss of Est had little effect on HS-induced hepatic injury. Moreover, transgenic reconstitution of human EST in the liver of global Est$^{-/-}$ mice abolished the pulmonoprotective effect, suggesting that it is the EST in the liver that contributes to HS-induced acute lung injury. Taken together, our results revealed a sex- and tissue-specific role of EST in HS-induced acute lung injury. Pharmacological inhibition of EST may represent an effective approach in female patients to manage HS-induced acute lung injury.

1.2 Dissertation Outline

The contents of the dissertation include:

Chapter I. Introduction (this chapter) is a concise description of the dissertation, including research background, overall research hypothesis, and specific aims with general research approaches.

Chapter II. Pregnane X receptor and hemorrhagic shock-induced hepatic injury is a complete research report for the specific Aim 1 that describes the study background, methodology, experimental results, and discussion and conclusion.

Chapter III. Estrogen sulfotransferase and hemorrhagic shock-induced acute lung injury includes literature review of estrogen sulfotransferases in liver diseases and a complete research report for the specific Aim 2 that describes the study background, methodology, experimental results, and discussion and conclusion.

Chapter IV. Summary is a conclusive overview for the sex- and tissue-specific role of PXR and EST in the hemorrhagic shock-induced multiple organ injuries, including liver and lung.

2.0 Pregnane X receptor and hemorrhagic shock-induced hepatic injury

2.1 Research Background

Hemorrhagic shock (HS), a life-threatening condition when the body loses more than 20% of its blood or fluid supply, is the leading cause of death and disability in patients younger than 54 years of age (Krug et al., 2000). During the acute phase of hemorrhage, in addition to stopping bleeding, fluid resuscitation is a therapeutic priority in the clinic. Although the modern resuscitation techniques developed in the 1960s have led to an improved immediate survival, the emergence of subsequent organ failure remains a major health issue that may lead to late death (Minei et al., 2012). The pathogenesis of HS-induced tissue injury is dynamic, including the hypoperfusion and hypoxia resulted from deprivation of blood supply during acute phase and oxidative stress introduced during the restoration of blood volume upon resuscitation (Figure 1). The free radicals generated through oxidative stress leads to cellular membrane damage and cell death and trigger secondary tissue and organ injury (Toklu and Tumer, 2015). The liver is an organ sensitive to HS-induced injury (Yu et al., 2008; Wetzel et al., 2014). In the liver, the cytochrome P450 (CYP) enzymes in the hepatocytes represent an important source of reactive oxygen species (ROS), which may lead to mitochondrial dysfunction and cell necrosis upon HS (Jaeschke, 2011; Tsai et al., 2015; Logsdon et al., 2016). CYP3A is the most abundant hepatic P450. Although the effect of CYP3A on ROS generation might be substrate dependent, it is believed that CYP3A plays a major role in the overall ability of the human liver to generate ROS (Puntarulo and Cederbaum, 1998).

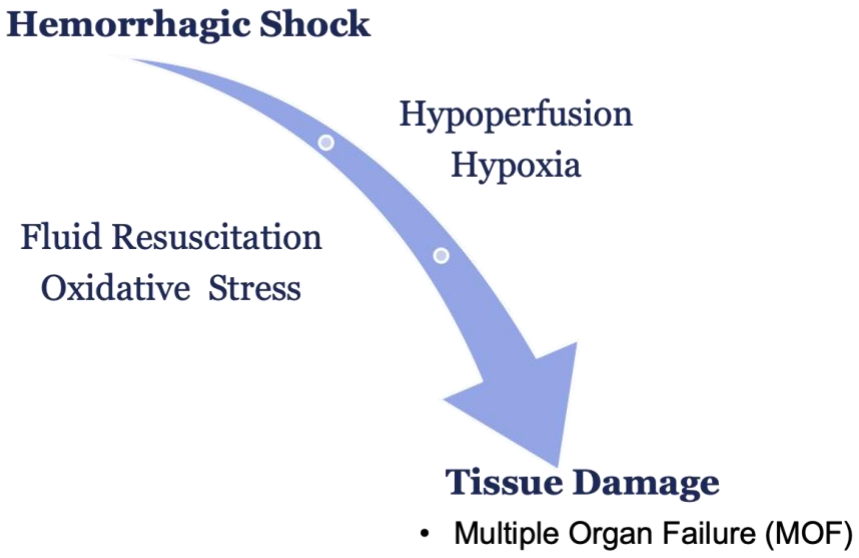

Figure 1. Pathogeneis of Hemorrhagic Shock.

Pregnane X receptor (PXR) is a species specific xenobiotic receptor that regulates the expression of drug-metabolizing enzymes (DEMs) with CYP3A as its primary target gene (Yan and Xie, 2016). Like other nuclear receptors, PXR is characterized by ligand binding domain and and DNA binding domain. It can be activated by a range of endogenous and exogenouse compounds, such as pregnanes, progesterone, corticosterone, testosterone, lithocholic acids, and the steroid-like xenobiotic dexamethasone (Xue et al., 2007). Upon activation, PXR would form a heterodimer with retinoid X receptor (RXR) and bind to the responsive element in the promoter area of regulated genes (Xie et al., 2000b; Willson and Kliewer, 2002).

Seriously injured trauma patients are uniformly prescribed with multiple medications, including common ICU medications, such as fentanyl, protonix, dexamethasone (DEX) (Grinstein-Nadler and Bottoms, 1976; Zingarelli et al., 1994), benzodiazepines (Abel and Reis, 1971), and other medications, such as Tylenol and oxycodone for post-surgery pain management, statins and fibrates for trauma patients with hyperlipidemia, and the antibiotic rifampicin (RIF) for reducing deep surgical site infections (Shiels et al., 2018; Tyas et al., 2018) or for the treatment of

tuberculosis. Many of these drugs are known to activate PXR and induce the expression of CYP3A before or after the onset of HS. For example, DEX, RIF, statins and fibrates are typical agonists that preferentially activate the mouse and human PXR, respectively (Blumberg et al., 1998; Kliewer et al., 1998; Xie et al., 2000a). Besides regulating DMEs, activation of PXR has been shown to sensitize normal and cancerous tissues to oxidative cellular damage, but the mechanism is yet to be defined (Gong et al., 2006). Although the expression of PXR and DEMs has been reported to be dynamically regulated by HS (Edmonds et al., 2011), it is unclear whether and how PXR plays a role in the regulation of DMEs in the setting of HS and if so, whether activation of PXR is beneficial or detrimental to HS-induced hepatic injury.

Another reason for our interests in PXR is that cytochrome P450 3A4 (CYP3A4) is the primary downstream gene regulated by PXR. CYP3A4 is a major member of cytochrome P450 drug metabolism enzymes, who can oxidize small molecules such as steroids, fatty acids and drugs. Beyond mitochondria electron transport chain, P450-dependent microsomal electron transport system is believed to be another major endogenous source of ROS. It was reported as the most active P450 in catalyzing the formation of ROS, such as NADPH oxidation and the production of superoxide anion radicals (Hrycay and Bandiera, 2015), which are known to be important contributors to tissue damage after HS. CYP3A4 also presents high amount in human liver microsome. Therefore, we believe induction of CYP3A4 might be a critical factor in HS-induced liver injury through generating ROS.

In this study, a fixed-pressure HS model (Figure 2) is used instead of fixed volume hemorrhage and uncontrolled hemorrhage, because the extent of hypotension, duration and the volume can be controlled. In this HS model, we did bilateral femoral artery cannulation and withdraw around 0.6 cc of blood from one side of artery and maintained the mean arterial pressure

at 25 mmHg for 2 h before resuscitation. Animals were sacrificed at 24 h after the initial of HS. Details can be found in **2.2 Experimental Procedures**.

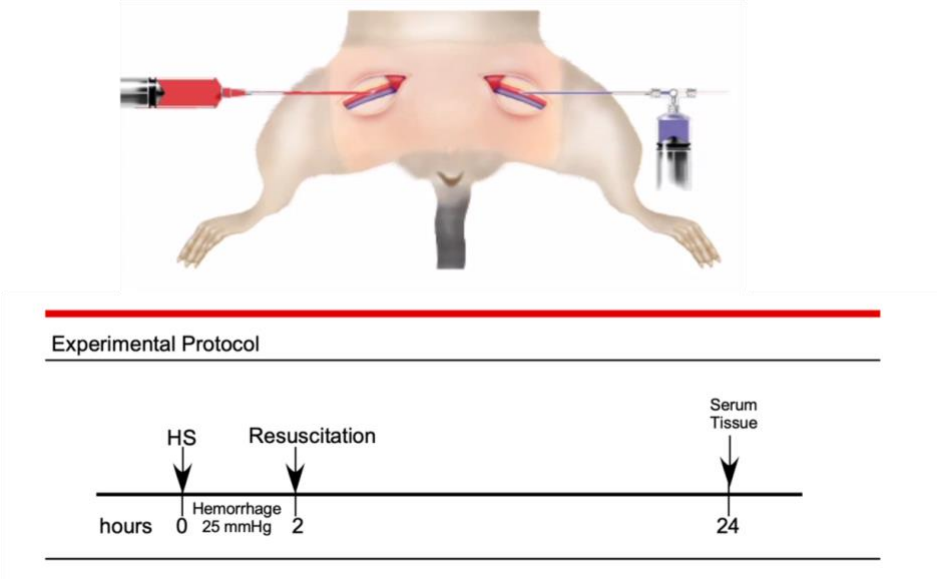

Figure 2. The murine model of HS.

Our results showed that activation of PXR sensitized both the wild-type and hPXR/CYP3A4 humanized mice to HS-induced hepatic injury in a CYP3A dependent manner. The sensitizing effect of PXR on HS-induced hepatic injury can be mitigated by inhibition of CYP3A, or treatment with an antioxidant, or a PXR antagonist.

2.2 Experimental Procedures

Animals and hemorrhagic shock

The Pxr$^{-/-}$ (Xie et al., 2000a), VP-PXR transgenic (Xie et al., 2000a), and hPXR/CYP3A4 humanized mice (Ma et al., 2008) were previously described. VP-PXR/Cyp3a$^{-/-}$ mice were generated by breeding the VP-PXR transgene into the Cyp3a$^{-/-}$ background (van Herwaarden et al., 2007). Eight-week old mice were used for hemorrhagic shock. Under anesthesia, catheters

were placed in both femoral arteries. To initiate HS, approximately 0.6 ml of blood were withdrawn using a syringe pump during which the blood pressure was maintained at approximately 25 mmHg. After a 2-h pressure-controlled HS, mice were resuscitated using Lactated Ringers solution at a volume of 3x each animal's shed blood volume given over a 15-min period using a syringe pump. In the sham control mice, the femoral arteries were exposed but not catheterized. Serum and tissue samples were collected 22 hours after resuscitation. The use of mice in this study complied with the relevant federal guidelines and institutional policies.

Chemicals

Ketoconazole (KET), dexamethasone (DEX) and pregnenolone 16α-carbonitrile (PCN) were purchased from Sigma-Aldrich (St. Louis, MO). KET was prepared for i.p. or oral administration by dissolution in ethanol and Tween 80 (1:1(v/v)) and then further dilution with saline. SPA70, the human PXR antagonist, is a kind gift from Dr. Taosheng Chen's lab (St. Jude Children's Research Hospital, Memphis). SPA70 was prepared for i.p. administration by dissolution in 30% PEG-400 dissolved in saline.

Histology, immunohistochemistry, and immunofluorescence

Five-micron thick tissue paraffin sections were stained with hematoxylin-eosin for general histology. Necrosis was estimated by dividing the necrotic area by the entire histological section using ImageJ software. Sections were scored from 0-4 for sinusoidal congestion, hydropic degeneration, necrosis, neutrophilic infiltration, and steatosis, and these parameters were used to calculate the Suzuki score as described (Suzuki et al., 1993) . For 4-hydroxynonenal (4-HNE) immunostaining, liver paraffin sections were incubated with the primary 4-HNE antibody

(Ab48506 from Abcam, Cambridge, MA) at 1:25 dilution overnight at 4 °C. The secondary antibody used was anti-mouse monoclonal at 1:500 dilution. The signal was visualized by peroxidase reaction using 3,3′-diaminobenzidine as the chromogen substrate. Hematoxylin was used as a nuclear counterstain. At least three mice were used for each treatment group or genotype, and for each sample at least four non-contiguous regions were photographed and analyzed. For 8-hydroxyguanosine (8-OHdG) immunofluorescence, liver paraffin sections were incubated with primary 8-OHdG antibody (Ab48508 from Abcam, Cambridge, MA) at 1:200 dilution overnight at 4 °C. The secondary antibody used was a Cy3 (Cyanine 3) conjugated donkey anti-mouse monoclonal at 1:500 dilution. DAPI was used as a nuclear counterstain.

Real-time PCR and Western Blot analysis

Total RNA was extracted from tissues using the TRIzol reagent. Total RNA was treated with RNase-free DNase I and reverse transcribed into single stranded cDNA. Real-time PCR using the SYBR Green-based assay was performed with the ABI 7300 Real-Time PCR System. For Western blotting, 20 μg of total protein for each sample were separated on 10% SDS-polyacrylamide gel. The primary antibody was a monoclonal mouse antibody against 4-HNE (1:200) from Abcam (Ab48506). The primary antibody of Cyp2b10 (1:200) was a polyclonal rabbit antibody from Abcam (Ab9916), while the primary antibody of Cyp3a11/CYP3A4 (1:200) was a monoclonal mouse antibody obtained from Dr. Frank J Gonzalez's lab (National Cancer Institue, NIH).

Serum chemistry

Blood samples were collected by cardiac puncture. Serum aminotransferase (ALT) levels were measured using an assay kit from Stanbio (Boerne, TX).

Analysis of microsomal metabolism of midazolam and oxycodone

Microsomes were prepared from the mouse livers as described (Matsubara et al., 1974). Fifty mg liver tissue was homogenized with buffer A (0.1 M phosphate buffer, pH7.5; 0.25 M sucrose; 0.154 M KCl; 1mM protease inhibitor) and centrifuged at 100,000 g for 25 min at 4 °C. The pellets were washed once with buffer B (0.1 M phosphate buffer, 20% v/v glycerol) and resuspended in 200 µl buffer B. The metabolisms of midazolam and oxycodone were measured by incubating 0.5 mg/ml microsomes with 30 µM midazolam or 0.1 mg/ml microsome with 300 µM oxycodone in a tube containing 0.1 mM PBS (pH=7.4). The incubation was initiated by adding 1 mM NADPH. After incubation for 10 min at 37 °C for midazolam or 120 min at 37 °C for oxycodone, 100 µl ice-cold methanol was added to stop the reaction. The samples were vortexed for 30 s, then centrifuged at 15000 rpm for 10 min. One hundred µl of supernatant was transferred to an autosampler vial for UPLC-MS analysis. The UPLC-MS analysis was performed as described (Fang et al., 2013; Tien et al., 2015).

Statistical analysis

Results are expressed as mean ± SE. Differences between two individual groups were determined by Student's *t* test. Differences between multiple groups were evaluated using one-way analysis of variance followed by post-hoc multiple comparison according to the Student-Newman-Keuls test. Statistical significance was accepted at $p < 0.05$.

2.3 Experimental Results

2.3.1 Genetic activation of PXR and Pxr ablation sensitize mice to and protect mice from HS-induced hepatic injury, respectively

To investigate the role of PXR in hepatic injury following hemorrhagic shock and resuscitation (HS/R), we established a 2-h fixed pressure model of HS/R in which mice were sacrificed 22 h after the resuscitation (Kohut et al., 2011). As expected (Yu et al., 2008; Wetzel et al., 2014), HS led to hepatic injury, as evidenced by histological necrosis (Figure 3A), apoptosis of hepatocytes adjacent to the central vein (CV) (Figure 3B) that was consistent with the peri-CV expression of Cyp3a11 (Figure 3C), and increased serum level of alanine aminotransferase (ALT) (Figure 3D). In addition, qRT-PCR results showed that the expression of *Pxr* and several of its target genes, including *Cyp3a11*, *Cyp2b10*, *Cyp2d22* and *Cyp2c29*, was down-regulated (Figure 3E). The downregulation of Cyp3a11 was verified by Western blotting (Figure3). The down-regulation of DMEs was also confirmed at the enzymatic level, because compared to the sham group, liver microsomes isolated from the HS group showed a decreased metabolism of sedative midazolam, a substrate of CYP3A (Figure 3G) and analgesic oxycodone, a substrate of both CYP3A and CYP2D (Figure 3H). Interestingly, we observed an intact expression of Pxr and a modest but significant increase in the expression of Cyp3a11 at the mRNA (Figure 3I) and protein (Figure 3J) levels in mice that were subject to a 2-h HS but without a resuscitation. These results suggested that the suppression of Pxr and Cyp3a in mice subject to HS/R may have been secondary to the liver injury; whereas the activation of PXR and induction of Cyp3a11 in the HS phase may have played a pathogenic role in the liver injury.

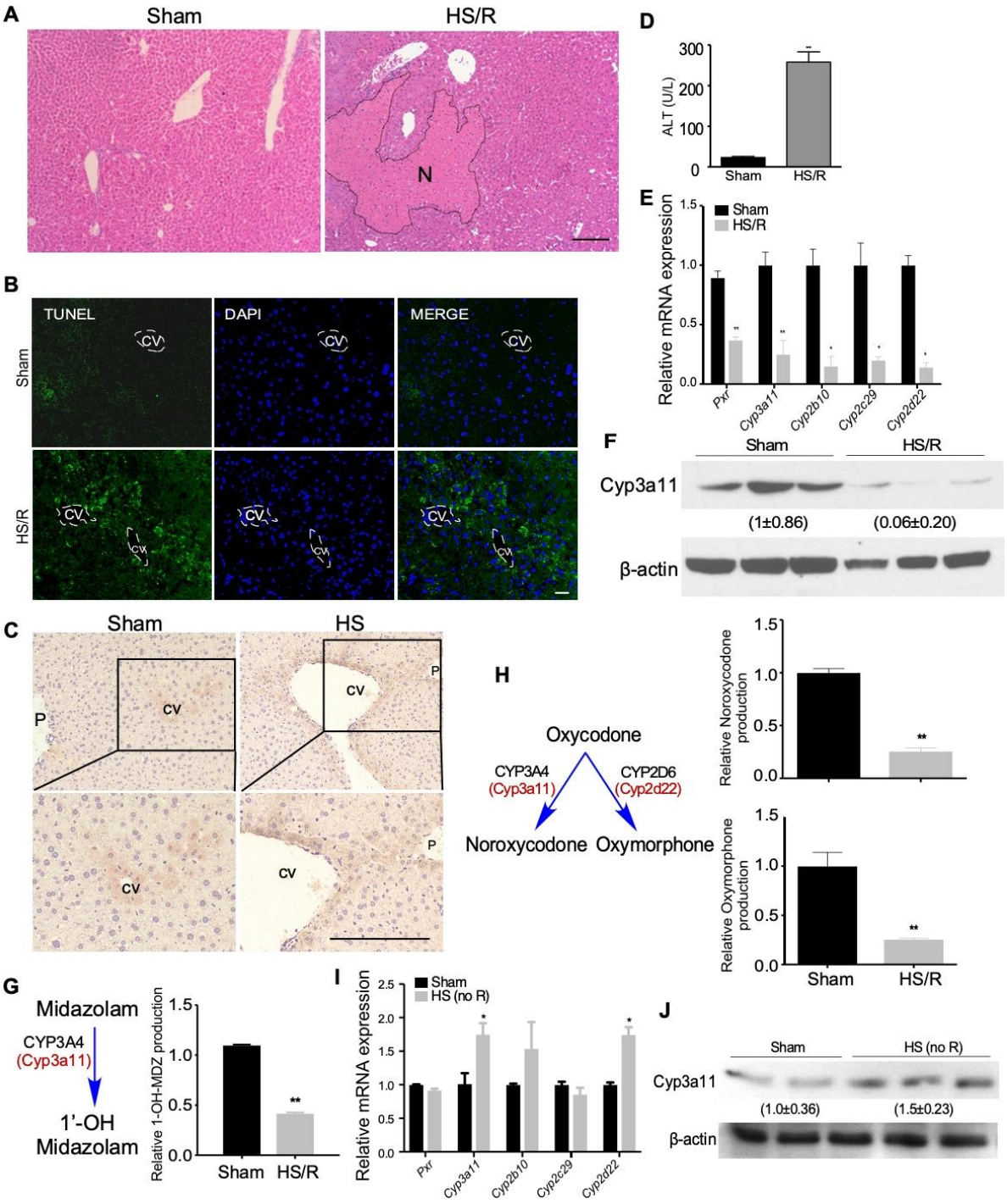

Figure 3. Hemorrhagic shock causes hepatic injury and affects the expression and activity of DMEs.

(A) Liver histology of WT mice subject to sham surgery or HS/R was analyzed by H&E staining. The "N"s within the dotted circle indicate the necrotic areas. **(B)** Apoptosis was analyzed by TUNEL staining. CV, central vein. **(C)** The hepatic expression of Cyp3a11 was measured by immunostaining. **(D)** Mice are the same as in (A). Shown are

the serum levels of ALT. **(E)** The hepatic gene expression was measured by qRT-PCR. **(F)** The hepatic expression of Cyp3a11 was measured by Western blotting. **(G)** Schematic presentation of midazolam metabolism by CYP3A4 in human and Cyp3a11 in mice (left). The liver microsomal formation of 1'-OH midazolam was measured by UPLC-MS (right). **(H)** Schematic presentation of oxycodone metabolism by CYP3A4 in human (Cyp3a11 in mice) and CYP2D6 in human (Cyp2d22 in mice) (left). The liver microsomal formations of noroxycodone and oxymorphone were measured by UPLC-MS (right). **(I)** The hepatic gene expression was measured by qRT-PCR in WT mice subject to sham surgery or HS without resuscitation. **(J)** Mice are the same as in (H). The hepatic protein expression of Cyp3a11 was measured by Western blotting. Results are presented as mean ±SE. n=4~5 for each group. *, $p < 0.05$; **, $p < 0.01$, compared to the sham groups.

To determine the effect of PXR activation on HS-induced tissue injury, WT, Alb-VP-PXR transgenic, and Pxr$^{-/-}$ mice were subject to HS/R before being analyzed for their injury in the liver and lung, two tissues known to be sensitive to HS (Yu et al., 2008; Wen et al., 2014; Wetzel et al., 2014). The Alb-VP-PXR transgenic mice express the constitutively activated PXR (VP-PXR) under the control of the liver-specific albumin gene promoter (Xie et al., 2000a). Wild type mice subject to HS/R showed hepatic injury, as shown by H&E staining (Figure 4A), quantification of necrotic area (Figure 4B), Suzuki score of the histology based on hydropic degeneration and steatosis (Suzuki et al., 1993) (Figure 4C), and the serum ALT level (Figure 4D). Compared to WT mice, VP-PXR transgenic mice showed heightened hepatic injury with a significant larger liver necrotic area and elevated serum ALT level when subjected to HS; while Pxr$^{-/-}$ mice showed attenuated hepatic injury (Figure 4A-4D). The expression of both *Cyp3a11* and *Cyp2b10* was induced in sham VP-PXR transgenic mice as expected, but the expression of both genes was suppressed upon HS/R (Figure 4E). Interestingly, the effect of PXR on HS-induced tissue injury was liver-specific, because there were no appreciable differences in HS-induced lung injury, including interstitial edema and infiltration of cells into the interstitial and alveolar spaces, among

the three genotypes (Figure 4F). Compared to the liver, the lung had a very low expression of either *Pxr* or *Cyp3a11* (data not shown).

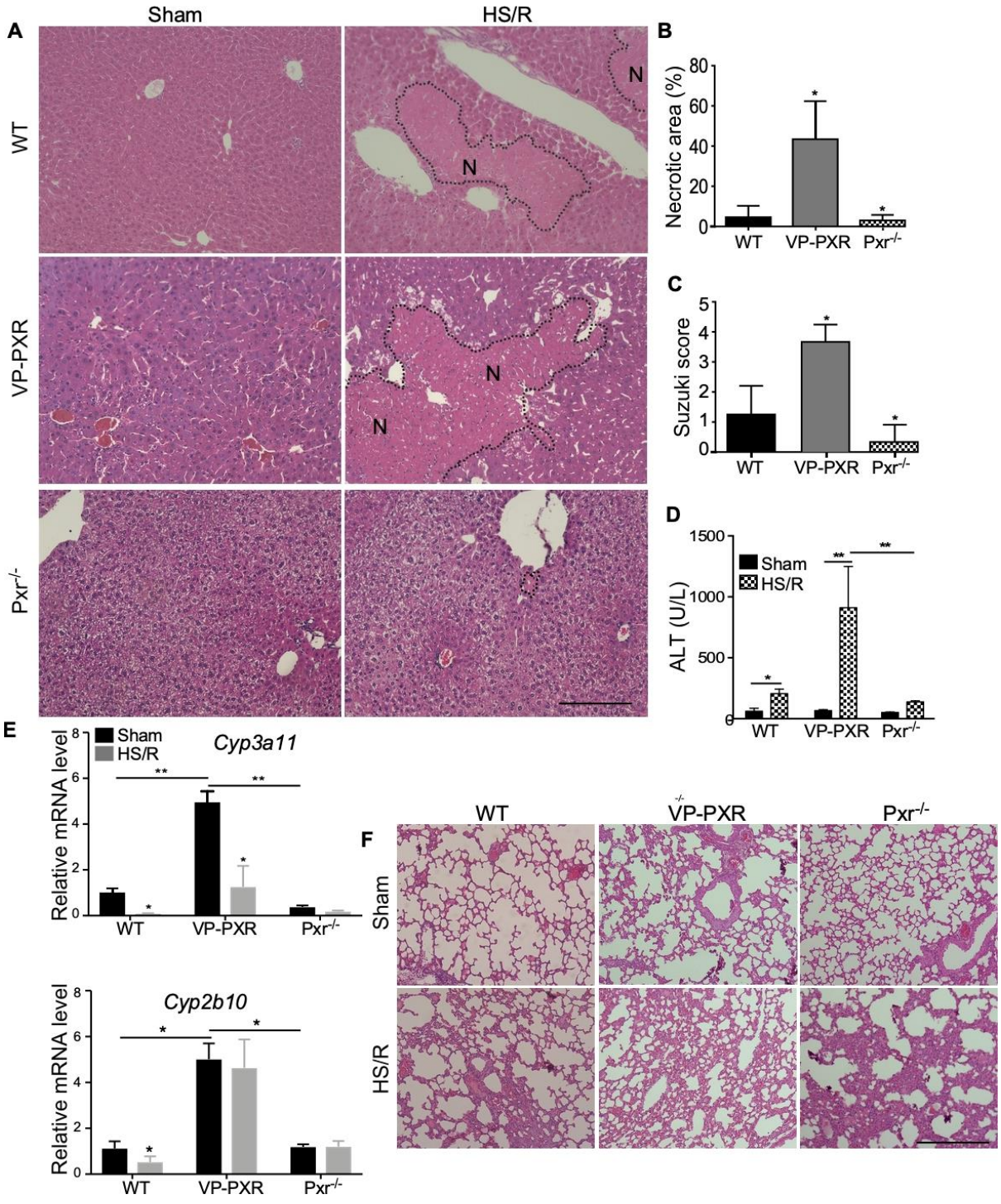

Figure 4. Genetic activation of PXR and Pxr ablation sensitize mice to and protect mice from HS-induced hepatic injury, respectively.

(A) WT, VP-PXR transgenic, and Pxr$^{-/-}$ mice subject to sham surgery or HS/R were analyzed for liver injury by H&E staining. The "N"s within the dotted circle indicate the necrotic areas. Bar is 100 μm. **(B-E)** Mice are the same as in (A). Shown are quantification of necrotic areas (B), Suzuki scores of the liver damage (C), and serum levels of ALT (D), and hepatic expression of *Cyp3a11* and *Cyp2b10* (E). **(F)** Mice in (A) were analyzed for lung injury by H&E staining (F). n=4~5 for each group. *, $p < 0.05$; **, $p < 0.01$, compared to the WT (B and C), or the comparisons are labeled (D and E).

2.3.2 Pharmacological activation of PXR, but not CAR, sensitizes mice to HS-induced hepatic injury

Since many clinical drugs, including those often prescribed to trauma patients, can activate PXR, we investigated whether a pharmacological activation of PXR can also sensitize mice to HS-induced hepatic injury. WT and Pxr$^{-/-}$ mice were pre-treated with PCN (40 mg/kg per day, i.p.) or DEX (20 mg/kg per day, i.p.) for two days before receiving the HS/R surgery. PCN is a prototypical mouse Pxr agonist, whereas DEX is a mouse-preferred Pxr agonist and a widely-prescribed glucocorticoid (Grinstein-Nadler and Bottoms, 1976; Zingarelli et al., 1994; Blumberg et al., 1998; Kliewer et al., 1998; Xie et al., 2000a). When PCN was used as outlined in Figure 5A, treatment of WT mice with PCN induced the expression of Cyp3a11 and Cyp2b10 at the mRNA (Figure 5B), protein (Figure 5C), and enzymatic (Figure 5D) levels in the sham group. PCN also induced the expression of Cyp3a11 in the HS/R group, which overrode the suppressive effect of HS/R on Cyp3a11 (Figure 5B-5D). As expected, PCN had little effect on the expression of Cyp3a11 in Pxr$^{-/-}$ mice regardless of HS/R (Figure 5B). Consistent with the results from the VP-PXR transgenic mice, treatment with PCN also sensitized mice to HS-induced hepatic injury as shown by H&E staining, quantification of necrotic area, and Suzuki scores (Figure 5E), and the serum ALT level (Figure 5F). The sensitizing effect of PCN was abolished in Pxr$^{-/-}$ mice (Figure

5E-5H). A similar pattern of Pxr-dependent sensitization was observed in mice pre-treated with DEX (Figure 6).

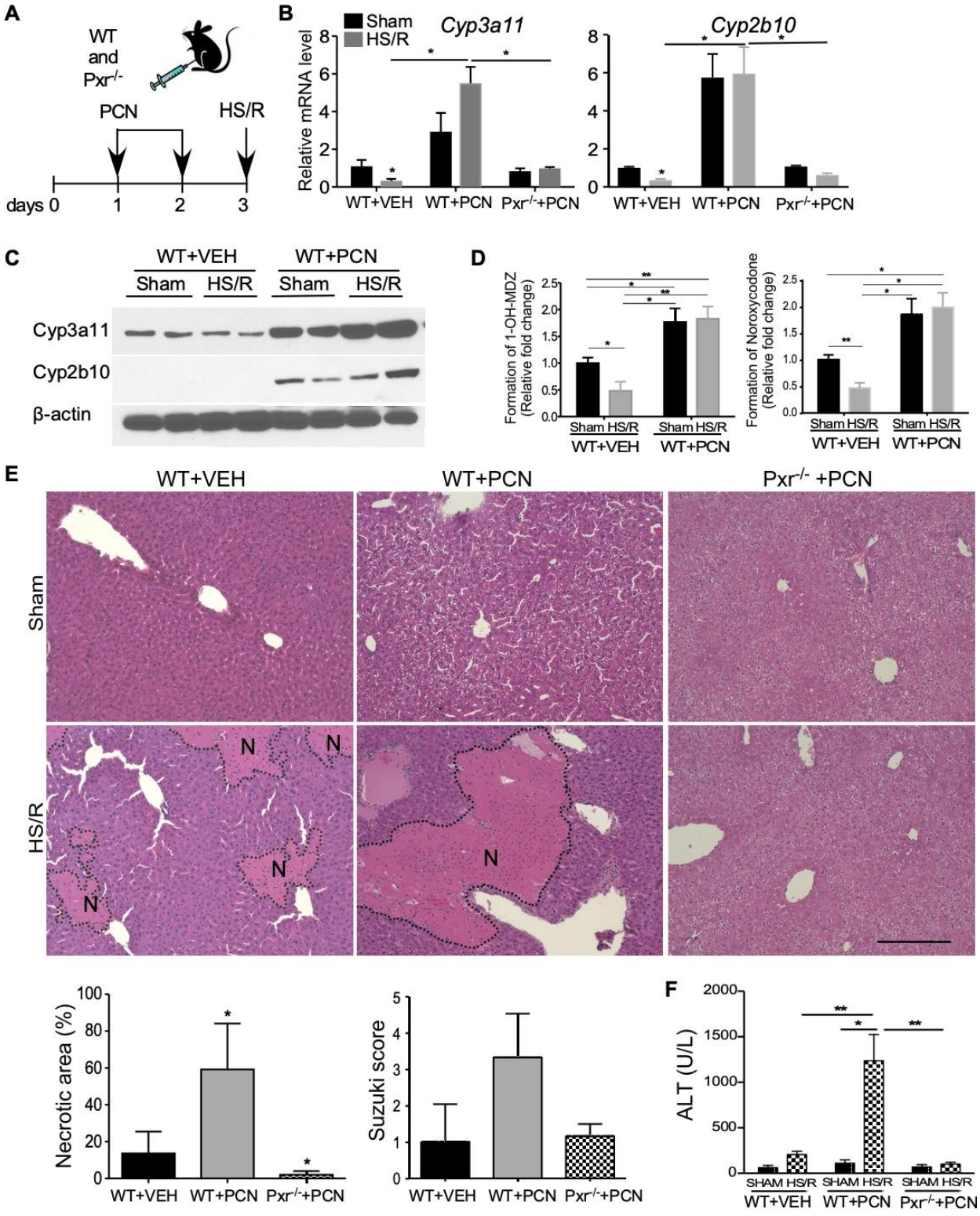

Figure 5. Pharmacological activation of PXR sensitizes mice to HS-induced hepatic injury.

(A) Schematic representation of the PCN pre-treatment model. WT and Pxr-/- mice were intraperitoneally injected with PCN (40 mg/kg per day) for two days before receiving the sham surgery or HS/R. **(B and C)** The hepatic mRNA (B) and protein (C) expression of Cyp3a11 and Cyp2b10 were measured by qRT-PCR and Western blotting, respectively. **(D)** The liver microsomal productions of 1'-OH midazolam (left) and noroxycodone (right) were measured by UPLC-MS analysis. **(E)** Liver histology was analyzed by H&E staining. Bar is 100 μm. Shown below are quantification of necrotic areas and Suzuki scores. **(F)** Serum levels of ALT. n=4~5 for each group. *, $p < 0.05$; **, $p < 0.01$, the comparisons are labeled (B, D and F), or compared to the WT+VEH group (E).

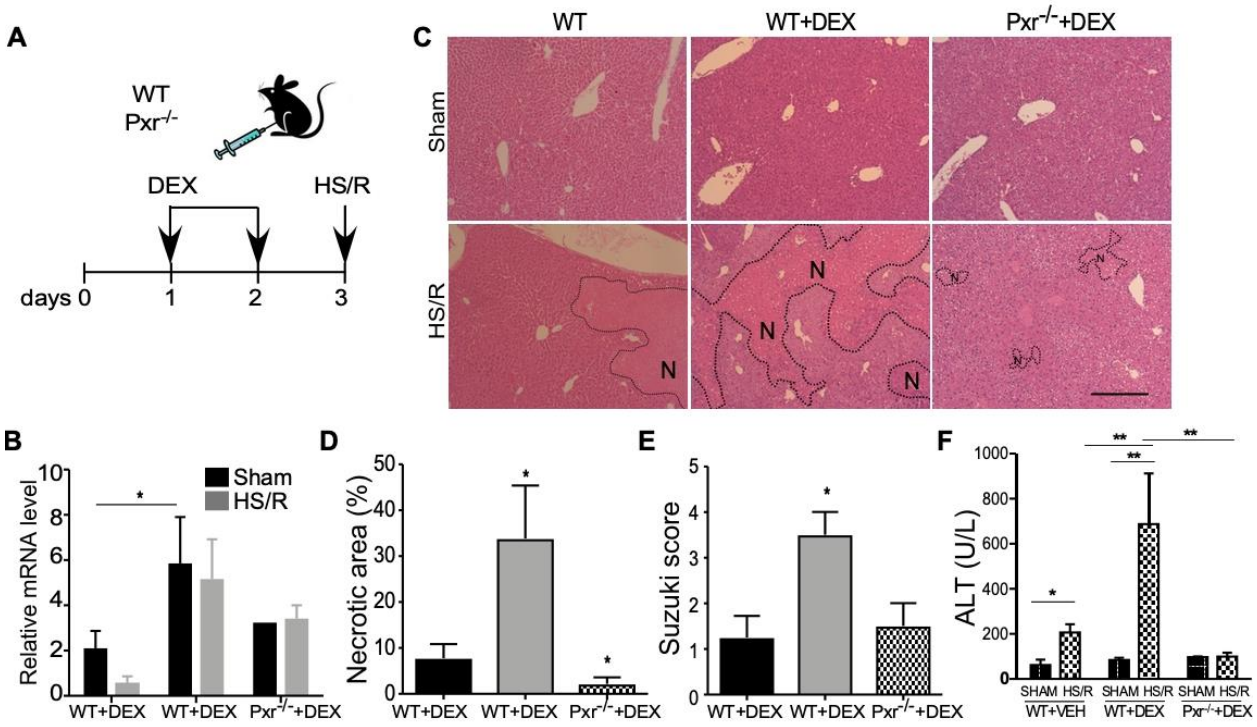

Figure 6. Treatment with DEX sensitizes mice to HS-induced hepatic injury in a PXR-dependent manner.

(A) Schematic representation of the DEX pre-treatment model. WT and Pxr-/- mice were intraperitoneally injected with DEX (20 mg/kg per day) for two days before receiving the sham surgery or HS/R. **(B)** The hepatic mRNA expression of *Cyp3a11* was measured by qRT-PCR. **(C)** Liver histology was analyzed by H&E staining. Bar is 100 μm. **(D-F)** Mice are the same as in (C). Shown are quantification of necrotic areas (D), Suzuki scores (E), and serum levels of ALT (F) in mice subject to HS/R. Results are presented as mean ±SE. n=4~5 for each group. *, $p < 0.05$; **, $p < 0.01$, the comparisons are labeled (B and F), or compared to WT+VEH (D and E).

The constitutive androstane receptor (CAR) is a sister xenobiotic receptor of PXR. To determine whether activation of CAR can also sensitize mice to HS-induced hepatic injury, WT mice were pre-treated with TCPOBOP (0.25 mg/kg, i.p.), a potent CAR agonist, for 3 days before the HS/R surgery (Figure 7A). As expected, TCPOBOP induced the expression of *Cyp2b10*, a primary target gene of CAR (Figure 7B). However, TCPOBOP had little effect on HS-induced hepatic injury, as shown by histology (Figure 7C-7E). These results suggested that the sensitizing effect was PXR specific.

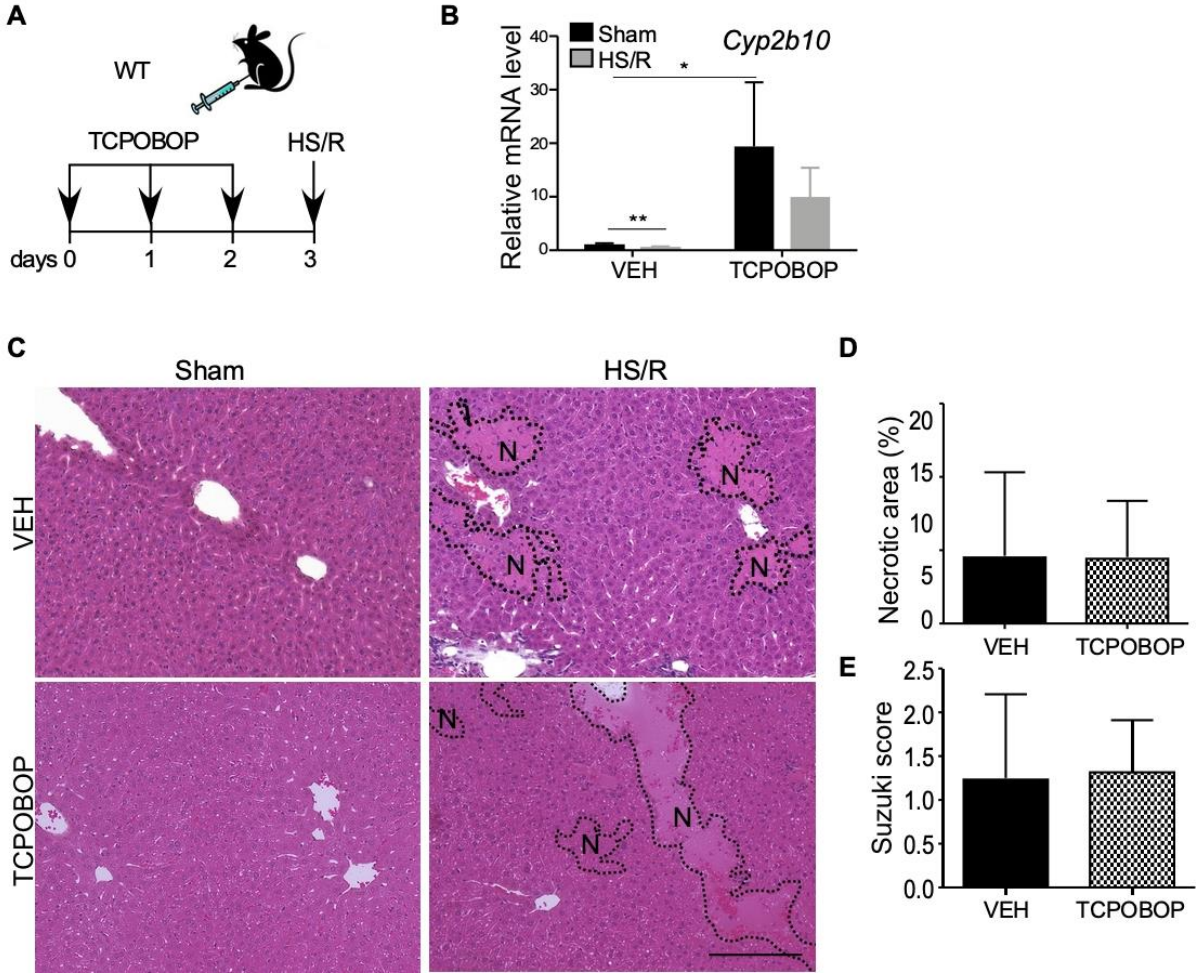

Figure 7. Treatment with the CAR agonist TCPOBOP fails to sensitize mice to HS-induced hepatic injury.

(A) Schematic representation of the TCPOBOP pre-treatment model. WT mice were intraperitoneally injected with TCPOBOP (0.25 mg/kg per day) for three days before receiving the sham surgery or HS/R. **(B)** The hepatic mRNA

expression of *Cyp2b10* was measured by qRT-PCR. **(C)** Liver histology was analyzed by H&E staining. Bar is 100 μm. **(D and E)** Mice are the same as in (C). Shown are quantification of necrotic areas (D) and Suzuki scores (E) in mice subject to HS/R. Results are presented as mean ±SE. n=4~5 for each group. *, $p < 0.05$; **, $p < 0.01$, the comparisons are labeled.

2.3.3 Induction of CYP3A is required for the sensitizing effect of PXR activation on HS-induced hepatic injury

Since CYP3A is the primary target gene of PXR and a major source of ROS production that contributes to liver damage (Puntarulo and Cederbaum, 1998; Jaeschke, 2011; Tsai et al., 2015; Logsdon et al., 2016), we went on to use CYP3A loss-of-function models to determine whether the expression and regulation of CYP3A were required for the heightened HS-induced hepatic injury in VP-PXR transgenic mice. The inhibition of CYP3A was achieved pharmacologically by treating mice with ketoconazole (KET) (Anderson and Blaschke, 1986), or genetically by using the Cyp3a knockout (Cyp3a$^{-/-}$) mice that bear the deletion of a cluster of mouse Cyp3a genes (van Herwaarden et al., 2007; Ma et al., 2008). In the pharmacological model, WT and VP-PXR transgenic mice were pre-treated with vehicle or KET (95 mg/kg per day, p.o.) for three days before receiving the HS/R surgery (Figure 8A). KET attenuated HS-induced hepatic injury in WT mice, and this attenuating effect was more dramatic in VP-PXR transgenic mice, as shown by histology (Figure 8B and 8C) and serum ALT level (Figure 8D).

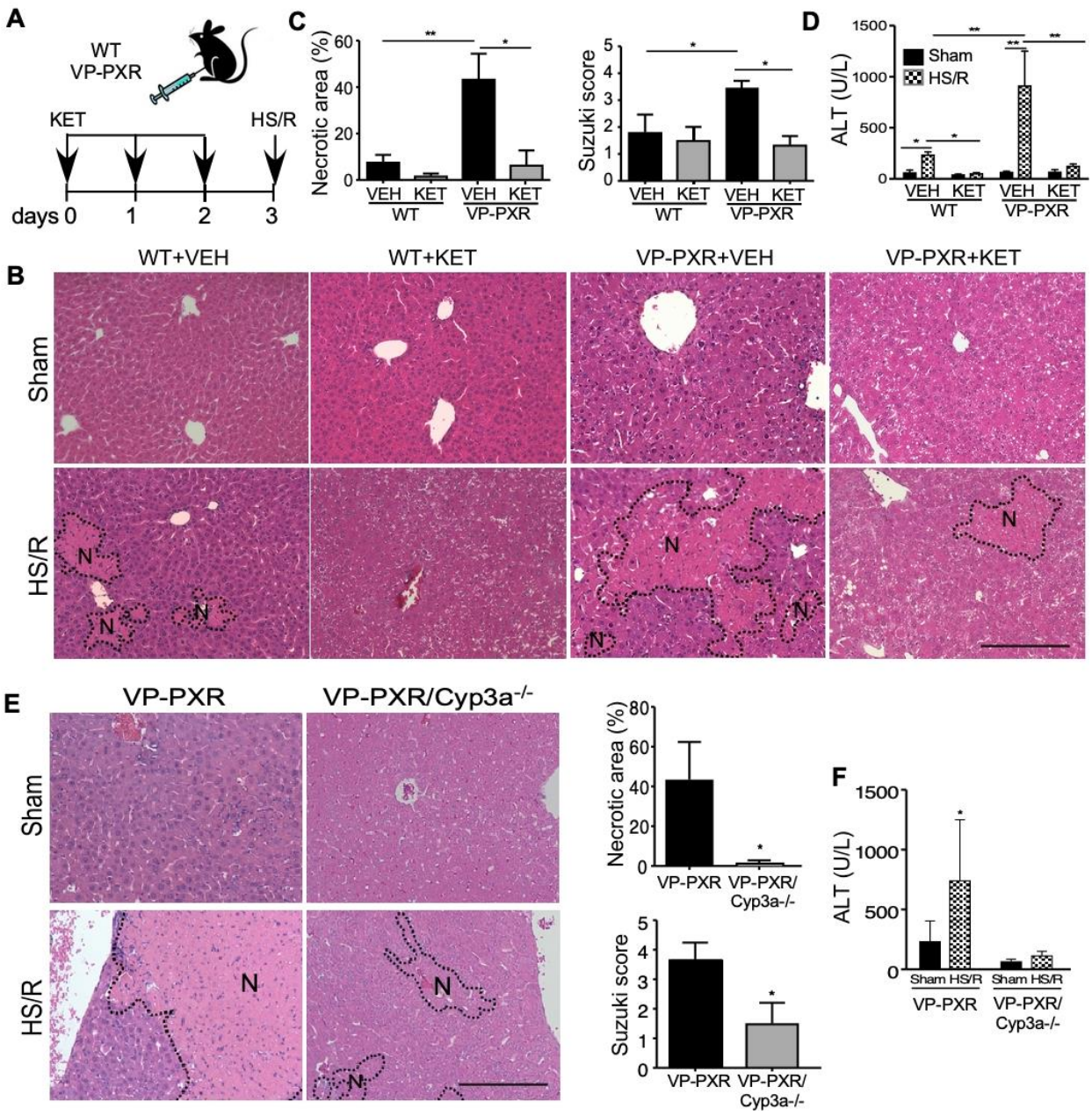

Figure 8. Induction of CYP3A is required for the sensitizing effect of PXR activation on HS-induced hepatic injury.

(A) Schematic representation of the ketoconazole (KET) pre-treatment model. WT and VP-PXR transgenic mice were treated with KET (20 mg/kg per day) for two days before receiving the sham surgery or HS/R. **(B and C)** Liver histology was analyzed by H&E staining (B, Bar is 100 μm), and quantification of necrotic areas and Suzuki scores (C). **(D)** Serum levels of ALT. **(E)** VP-PXR and VP-PXR/Cyp3a$^{-/-}$ mice subject to the sham surgery or HS/R were analyzed for liver histology by H&E staining. Shown on the right are quantification of necrotic areas and Suzuki

scores. **(F)** Serum levels of ALT. n=4~5 for each group. *, $p < 0.05$; **, $p < 0.01$, the comparisons are labeled (C, D, and F), or compared to the VP-PXR group (E).

Since trauma patients often receive treatment after their admissions to ICU, we evaluated the effect of post-HS treatment of KET on PCN-induced and HS/R responsive hepatic injury. Two time points of post-HS KET treatment were chosen: 2 h after the initiation of HS and right before resuscitation when Cyp3a11 was induced (Figure 3I and 3J), and 12 h after the initiation of HS when the suppression of Cyp3a11 became obvious (Figure 9A). The designs of the experiment are outlined in Figure 9B. Treatment with KET at the 2-h time point, but not the 12-h time point, was effective to attenuate HS-induced hepatic injury as shown by histology (Figure 9C-9E) and the serum ALT level (Figure 9F). The loss of protection at the 12-h time point was likely due to the suppression of Cyp3a11. Nevertheless, these results suggested that the effect of post-HS treatment of KET was time-sensitive.

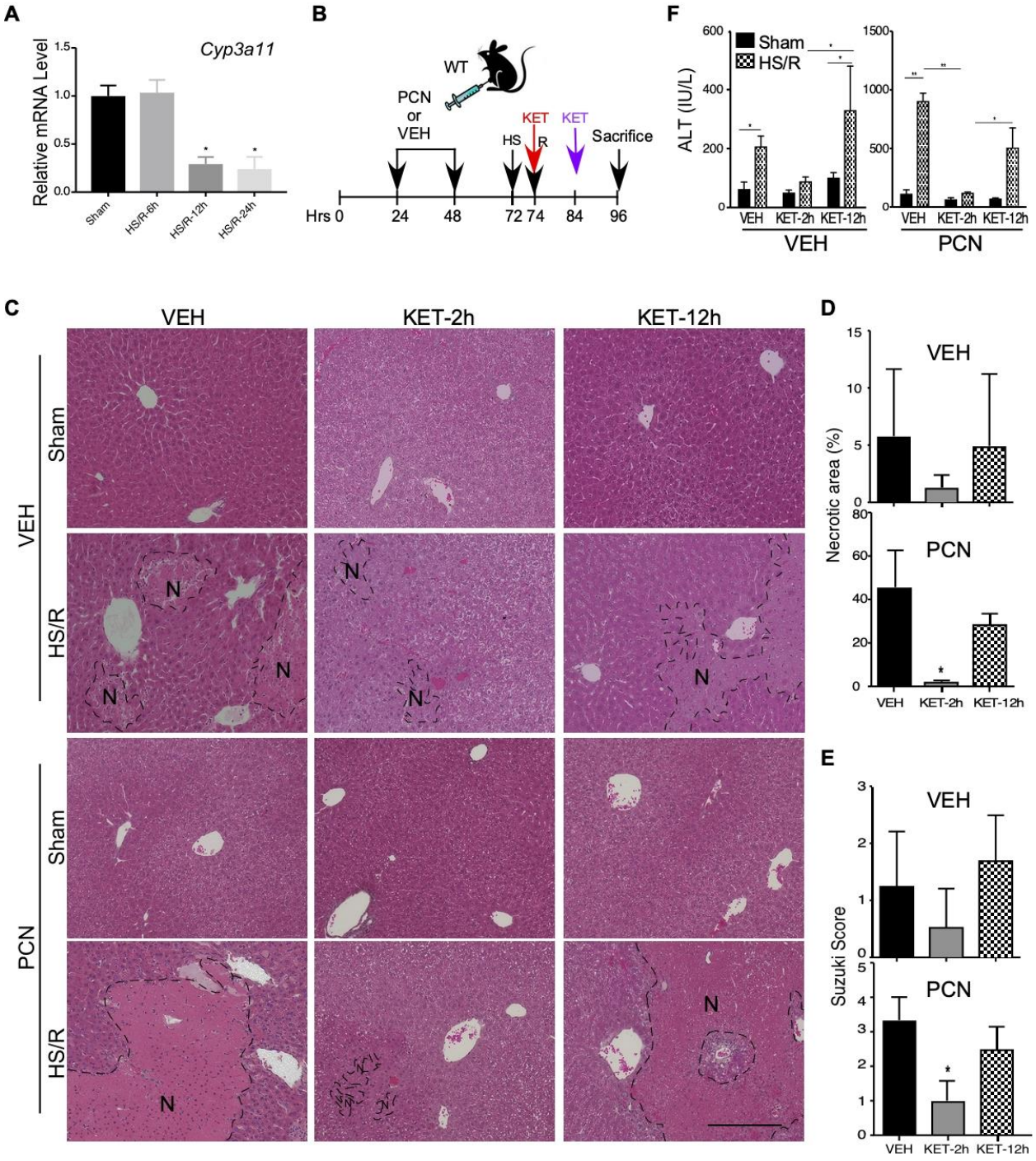

Figure 9. Post-hemorrhagic shock treatment of CYP3A inhibitor KET attenuates HS-induced hepatic injury.

(A) The hepatic mRNA expression of *Cyp3a11* at indicated time points after HS was measured by qRT-PCR. **(B)** Schematic representation of the KET post-HS treatment model. WT mice were intraperitoneally injected with PCN (40 mg/kg) or VEH for two days before receiving the sham surgery or HS/R. KET (95 mg/kg) or VEH was given either 2-h after the initiation of HS (at 72 h), or 12-h after the initiation of HS (at 84 h). **(C)** Liver histology was

analyzed by H&E staining. Bar is 100 μm. **(D-F)** Mice are the same as in (C). Shown are quantification of necrotic areas (D), Suzuki scores (E), and serum ALT levels (F) in mice subject to HS/R. Results are presented as mean ±SE. n=3 for each group. *, $p < 0.05$; **, $p < 0.01$, compared to VEH (D and E), or the comparisons are labeled (F).

In the genetic model, we generated the VP-PXR/Cyp3a$^{-/-}$ mice by breeding the VP-PXR transgene into the Cyp3a$^{-/-}$ background. The VP-PXR and Cyp3a$^{-/-}$ alleles were verified by PCR genotyping (Figure 10A) and the loss of Cyp3a expression was confirmed by qRT-PCR (Figure 10B). In the same VP-PXR/Cyp3a$^{-/-}$ mice, the expression of *Cyp2b10* was induced (Figure 10B), consistent with the notion that *Cyp2b10* is a PXR target gene. Compared to their VP-PXR counterparts, VP-PXR/Cyp3a$^{-/-}$ mice showed attenuated liver injury upon HS/R (Figure 8E and 8F). These results suggested that the sensitizing effect of the VP-PXR transgene was Cyp3a11 dependent, but independent of Cyp2b10. Ablation of Cyp3a also attenuated the sensitizing effect of PCN (Figure 10C-10F).

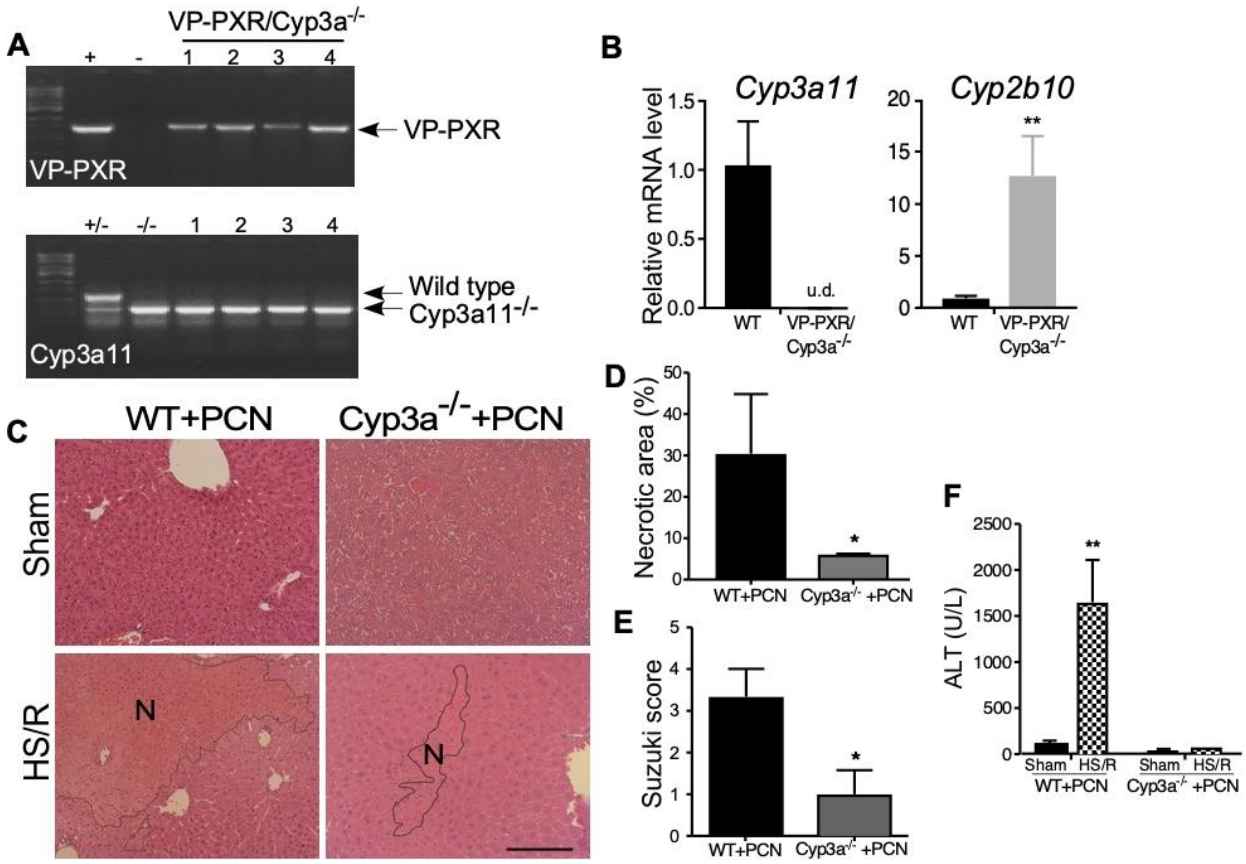

Figure 10. Ablation of Cyp3a abolishes the sensitizing effect of PCN.

(A) PCR genotying to validate the creation of VP-PXR/Cyp3a$^{-/-}$ mice. **(B)** The hepatic mRNA expression of *Cyp3a11* and *Cyp2b10* was measured by qRT-PCR. **(C)** Liver histology was analyzed by H&E staining in PCN-treated WT and Cyp3a$^{-/-}$ mice subject to sham surgery or HS/R. Bar is 100 μm. **(D-F)** Mice are the same as in (C). Shown are quantification of necrotic areas (D), Suzuki scores (E), and serum levels of ALT (F) in mice subject to HS/R. Results are presented as mean ±SE. n=3 for each group. *, $p < 0.05$; **, $p < 0.01$, compared to WT.

2.3.4 Pharmacological activation of hPXR sensitizes the hPXR/hCYP3A4 humanized mice to HS-induced hepatic injury in a CYP3A-dependent manner

The drug induction of DMEs is known to have species specificity, and original hPXR humanized mice showed that the species origin of the PXR receptor is the determining factor for

the species specificity (Xie et al., 2000a). The second-generation of humanized mice were subsequently created by humanizing both hPXR and human CYP3A4. The humanization of CYP3A4 was achieved by introducing the CYP3A4 transgene into the Cyp3a$^{-/-}$ background (Ma et al., 2008). We used the hPXR/hCYP3A4 humanized mice and the control hPXR/Cyp3a$^{-/-}$ mice to determine whether activation of hPXR by RIF, an antibiotic and potent hPXR-specific agonist, can sensitize mice to HS-induced hepatic injury and whether this sensitization is CYP3A dependent. The humanized mice were pre-treated with RIF (10 mg/kg per day, i.p.) for 4 days before the HS/R surgery (Figure 11A). Treatment with RIF was efficient in inducing CYP3A4 as expected (Figure 11B), and the massive induction of CYP3A4 caused the loss of zonal expression of CYP3A4 (Figure 11C). The humanized mice showed a basal sensitivity to HS-induced hepatic injury similar to WT mice, and the liver injury was exacerbated by the treatment of RIF, as shown by histology (Figure 11D) and serum ALT level (Figure 11E). The sensitizing effect of RIF was attenuated in hPXR/Cyp3a$^{-/-}$ mice, suggesting that the sensitizing effect was CYP3A dependent (Figure 11D and 11E).

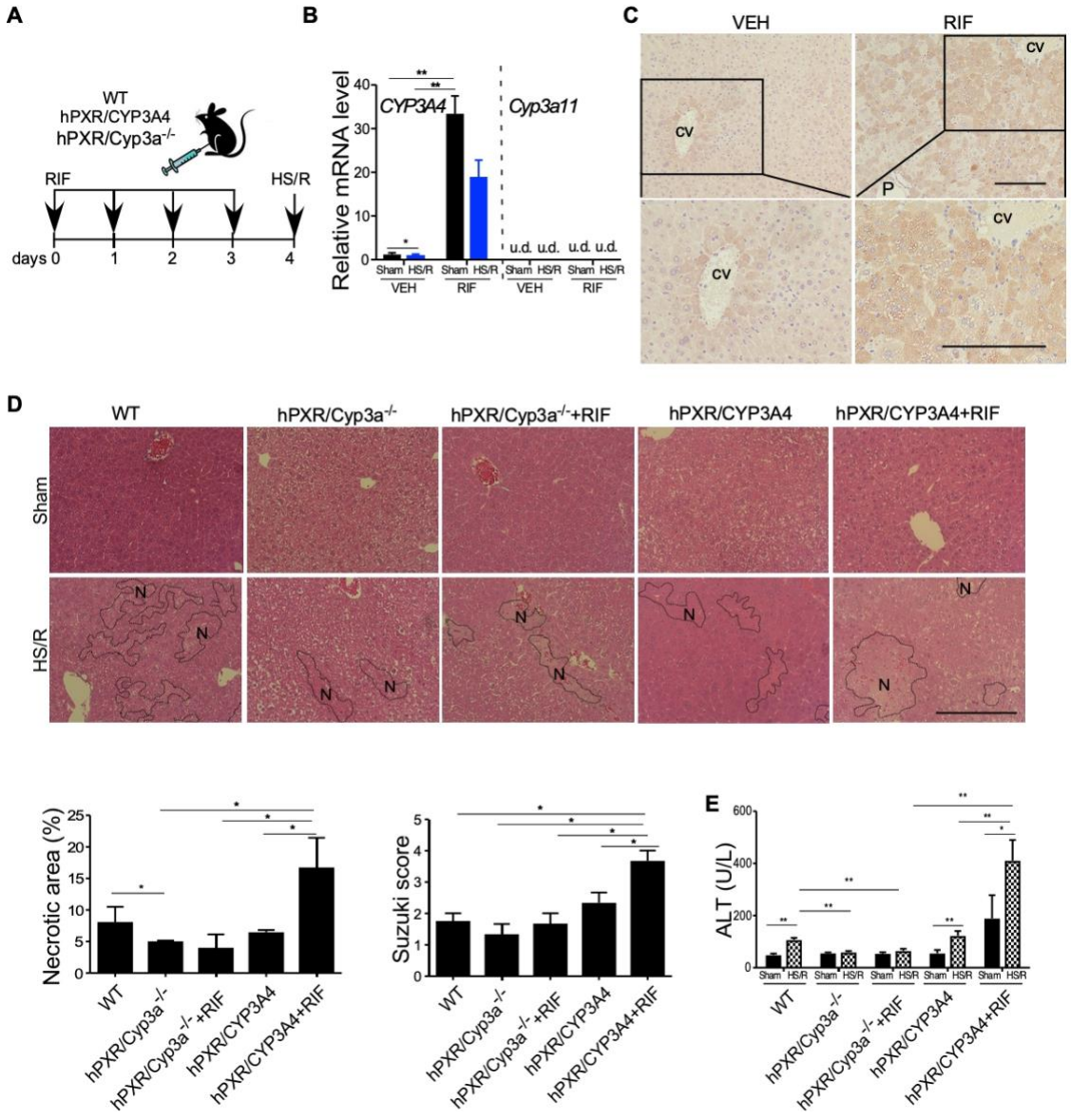

Figure 11. Pharmacological activation of hPXR sensitizes the hPXR/hCYP3A4 humanized mice to HS-induced hepatic injury in a CYP3A-dependent manner.

(A) Schematic representation of the rifampicin (RIF) pre-treatment model. WT, hPXR/CYP3A4 and hPXR/Cyp3a-/- mice were treated with RIF (10 mg/kg per day) for four days before receiving the sham surgery or HS/R. **(B)** The hepatic mRNA expression of human *CYP3A4* and mouse *Cyp3a11* was measured by qRT-PCR. **(C)** The hepatic expression of CYP3A4 was measured by immunostaining. CV, central vein; P, portal vein. **(D)** Liver histology was analyzed by H&E staining. Bar is 100 μm. Shown below are quantification of necrotic areas and Suzuki scores. **(E)** Serum levels of ALT. n=4~5 for each group. *, $p < 0.05$; **, $p < 0.01$, the comparisons are labeled.

2.3.5 The sensitizing effect of PXR on HS-induced hepatic injury is accompanied by increased oxidative stress

CYP3A-mediated oxidation is an important source of ROSs (Puntarulo and Cederbaum, 1998; Jaeschke, 2011; Tsai et al., 2015; Logsdon et al., 2016). Activation of PXR has been reported to sensitize mice to oxidative stress, such as those triggered by the oxidative toxicant paraquat (Gong et al., 2006). Having shown that induction of CYP3A is required for the sensitizing effect of PXR on HS-induced hepatic injury, we went on to determine whether the sensitizing effect of PXR was associated with an increased oxidative stress. Upon HS/R and compared to WT mice, the immunostaining of 4-hydroxynonenal (4-HNE), the α,β-unsaturated hydroxyalkenal produced by lipid peroxidation and an oxidative stress biomarker (Tjalkens et al., 1999), was increased in VP-PXR transgenic mice and PCN-treated WT mice, but decreased in Pxr$^{-/-}$ mice (Figure 12A). The respective increased and decreased oxidative stress in HS/R-treated VP-PXR and Pxr$^{-/-}$ mice were further verified by Western blot analysis of 4-HNE (Figure 12B) and immunofluorescence of 8-hydroxy-2'-deoxyguanosine (8-OHdG), a biomarker for free radicals induced by oxidative DNA lesions (Valavanidis et al., 2009) (Figure 12C). Consistent with the notion that Cyp3a enzymes reside in the endoplasmic reticulum, the hepatic expression of activating transcription factor 3 (Atf3) (Figure 12D) and C/EBP homologous protein (Chop) (Figure 12E), two ER stress sensors (Edagawa et al., 2014; Dai et al., 2017), was increased in VP-PXR mice upon HS/R. The increased HS-responsive oxidative stress in VP-PXR transgenic mice and RIF-treated hPXR/hCYP3A4 humanized mice was Cyp3a dependent, because these effects were abolished in VP-PXR/Cyp3a$^{-/-}$ mice and hPXR/Cyp3a$^{-/-}$ mice (Figure 12F), respectively, as shown by immunofluorescence of 8-OHdG.

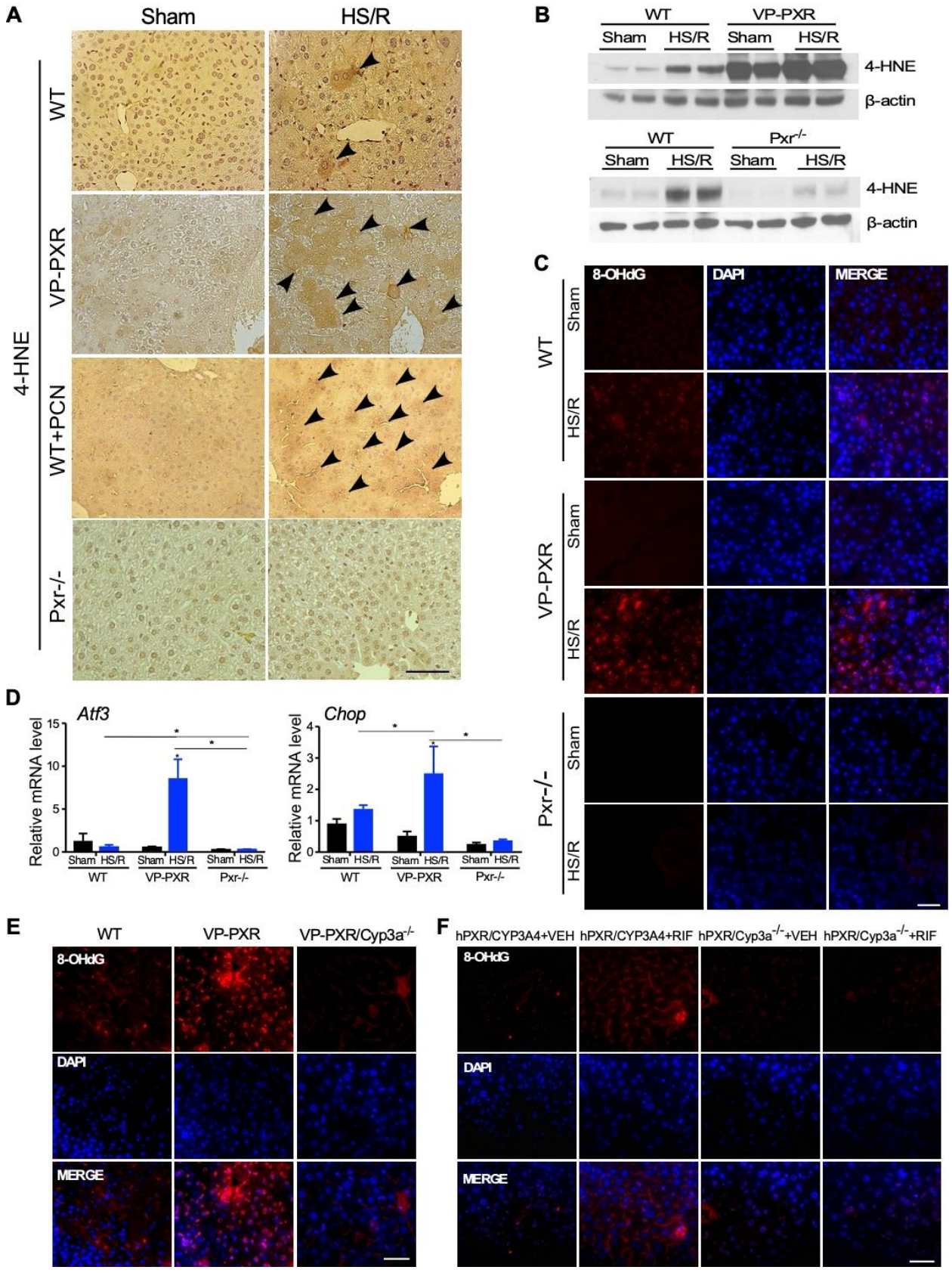
A
Sham
HS/R
4-HNE
WT
VP-PXR
WT+PCN
Pxr-/-
B
WT
VP-PXR
Sham
HS/R
4-HNE
β-actin
WT
Pxr-/-
C
8-OHdG
DAPI
MERGE
D
Atf3
Chop
Relative mRNA level
E
WT
VP-PXR
VP-PXR/Cyp3a-/-
F
hPXR/CYP3A4+VEH
hPXR/CYP3A4+RIF
hPXR/Cyp3a-/-+VEH
hPXR/Cyp3a-/-+RIF

Figure 12. The sensitizing effect of PXR on HS-induced hepatic injury is accompanied by increased oxidative stress.

(A) Immunostaining of 4-HNE in liver tissues from WT, VP-PXR, WT+PCN, and Pxr$^{-/-}$ mice subject to the sham surgery or HS/R. Arrowheads indicate positive staining. **(B)** The level of 4-HNE was measured by Western blotting. **(C)** Immunofluorescent staining of 8-OHdG in liver tissue from WT, VP-PXR and Pxr$^{-/-}$ mice. **(D)** The hepatic expression of *Atf3* and *Chop* was measured by qRT-PCR. **(E and F)** Immunofluorescent staining for 8-OHdG in liver tissues from WT, VP-PXR and VP-PXR/Cyp3a$^{-/-}$ mice that were subject to HS/R (E), or VEH- or RIF-treated hPXR/CYP3A4 and hPXR/Cyp3a$^{-/-}$ mice that were subject to HS/R (F). Bars are 100 μm. n=4~5 for each group. *, $p < 0.05$; **, $p < 0.01$, the comparisons are labeled.

Treatment with the antioxidant NACA attenuates the sensitizing effect of PXR on HS-induced hepatic injury

To determine whether treatment with an antioxidant can attenuate the sensitizing effect of the VP-PXR transgene, VP-PXR transgenic mice were pre-treated with the antioxidant *N*-acetylcystein amide (NACA, 200 mg/kg, i.p.) (Guo et al., 2015) one hour before the initiation of HS/R. Treatment with NACA attenuated HS-induced hepatic injury, as shown by histology (Figure 13A-13C) and serum ALT level (Figure 13D). The HS-induced increase of 4-HNE immunostaining in the transgenic mice was also attenuated upon the NACA treatment (Figure 13E). Treatment of WT mice with NACA also attenuated the sensitizing effect of PCN and DEX on HS-induced hepatic injury (Figure 14). Co-treatment of the VP-PXR transgenic mice with KET and NACA fully abolished the HS-induced hepatic injury (Figure 15).

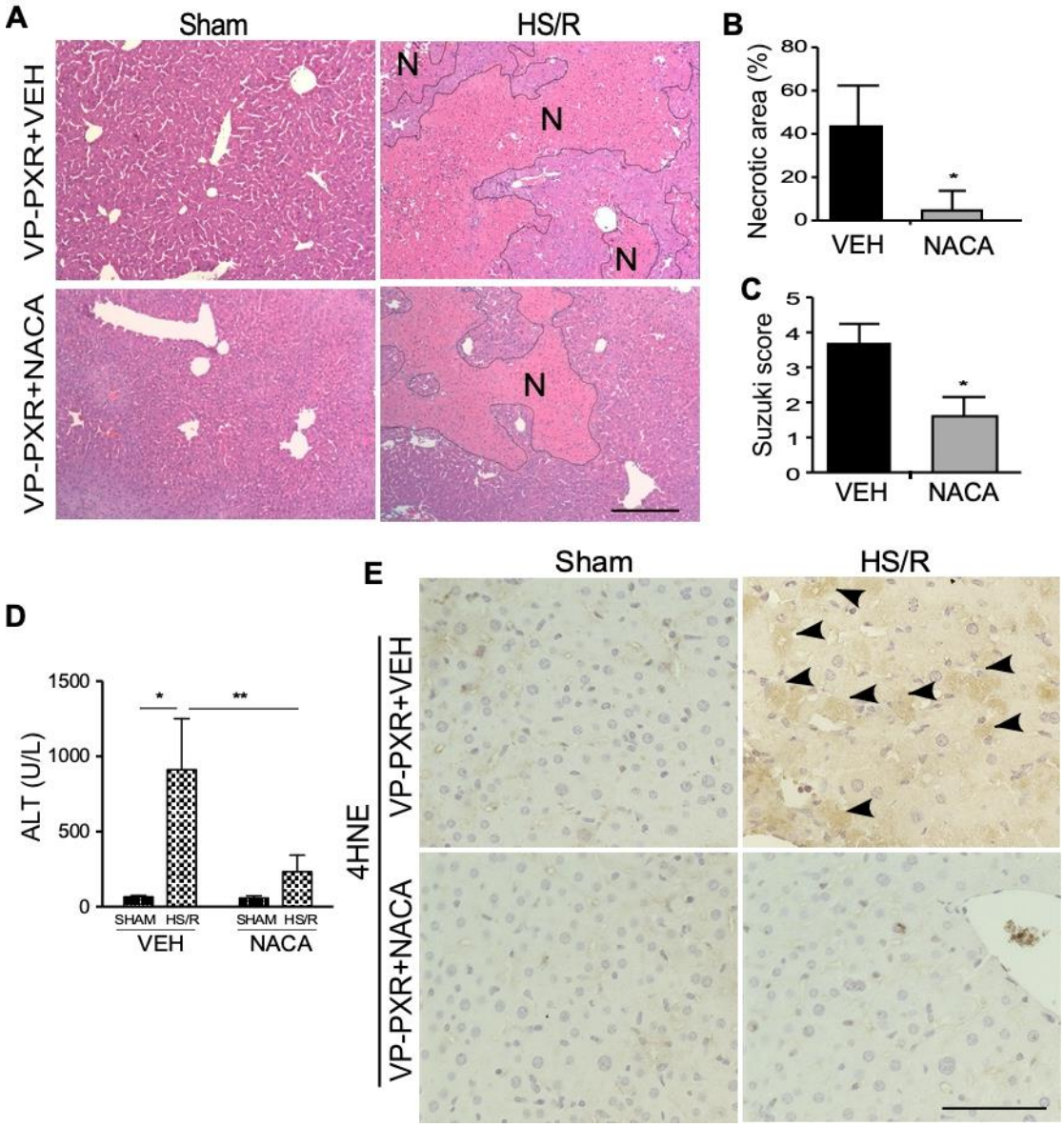

Figure 13. Treatment with the antioxidant NACA attenuates the sensitizing effect of PXR on HS-induced hepatic injury.

(A) Liver histology was analyzed by H&E staining in VEH- or NACA-treated VP-PXR mice that were subject to the sham surgery or HS/R. Bar is 100 μm. **(B to D)** Mice are the same as in (A). Shown are quantification of necrotic areas (B), Suzuki scores (C), and serum levels of ALT (D) in mice subject to HS/R. **(E)** Mice are the same as in (A). The level of 4-HNE was measured by immunostaining with the positive staining indicated by arrowheads. Bar is 100 μm. n=4~5 for each group. *, $p < 0.05$; **, $p < 0.01$, compared to the VEH group (B and C), or the comparisons are labeled (D).

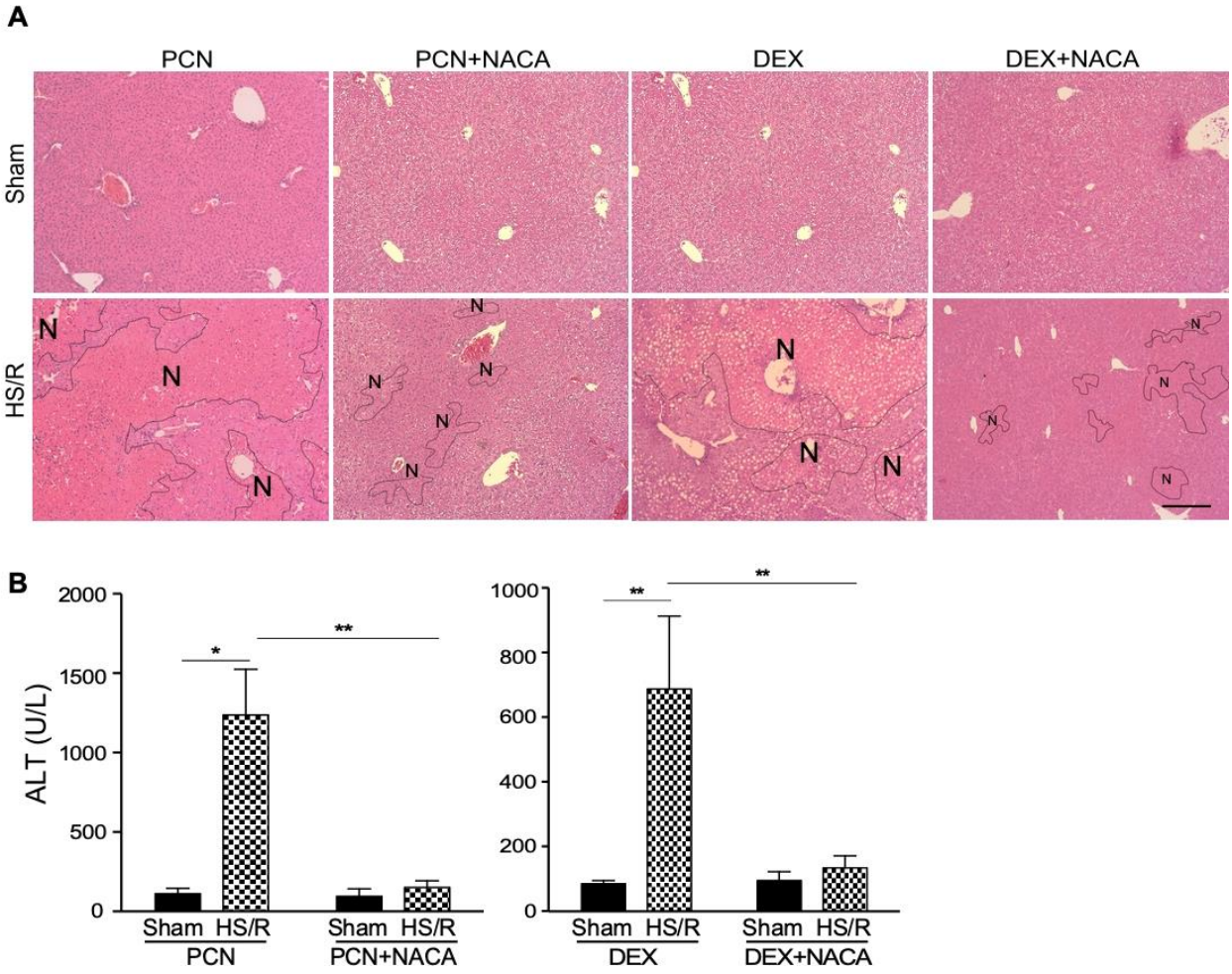

Figure 14. Treatment with the antioxidant NACA attenuates the sensitizing effect of PCN and DEX on HS-induced hepatic injury.

(A-B) WT mice were treated with PCN or DEX, in the absence or presence of NACA, before receiving the sham surgery or HS/R. (A) Liver histology was analyzed by H&E staining. Bar is 100 μm. (B) Serum levels of ALT. Results are presented as mean ±SE. n=4 for each group. *, $p < 0.05$; **, $p < 0.01$, the comparisons are labeled.

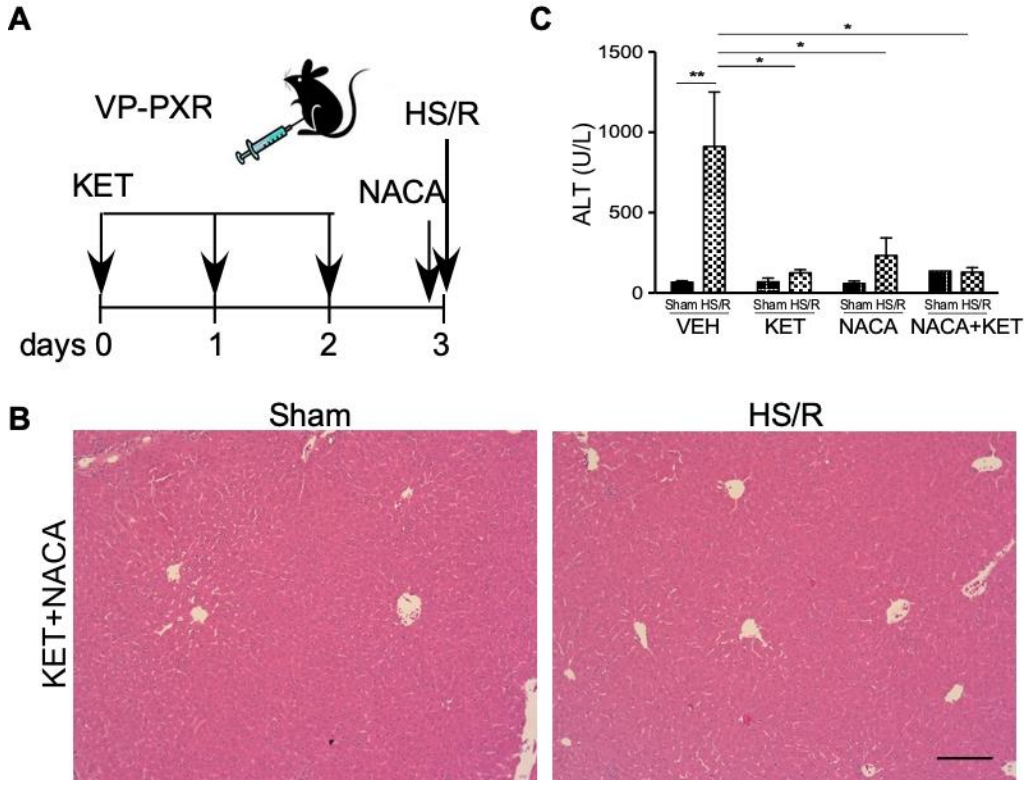

Figure 15. Co-treatment of the VP-PXR transgenic mice with CYP3A inhibitor KET and antioxidant NACA abolishes HS-induced hepatic injury.

(A) Schematic representation of the KET and NACA co-treatment model. VP-PXR transgenic mice were pre-treated with KET (95 mg/kg per day) for three days and intraperitoneally injected with NACA one hour before the sham surgery or HS/R. **(B)** Liver histology was analyzed by H&E staining. Bar is 100 μm. **(C)** Serum levels of ALT. Results are presented as mean ±SE. n=3 for each group. *, $p < 0.05$; **, $p < 0.01$, the comparisons are labeled.

To evaluate the therapeutic potential of NACA, we conducted the post-HS treatment of NACA 2 h after HS but before the initiation of resuscitation (Figure 16A). Post-HS treatment of NACA also attenuated PCN-induced and HS-responsive hepatic injury, as shown by histology (Figure 16B-16D) and serum ALT level (Figure 16E).

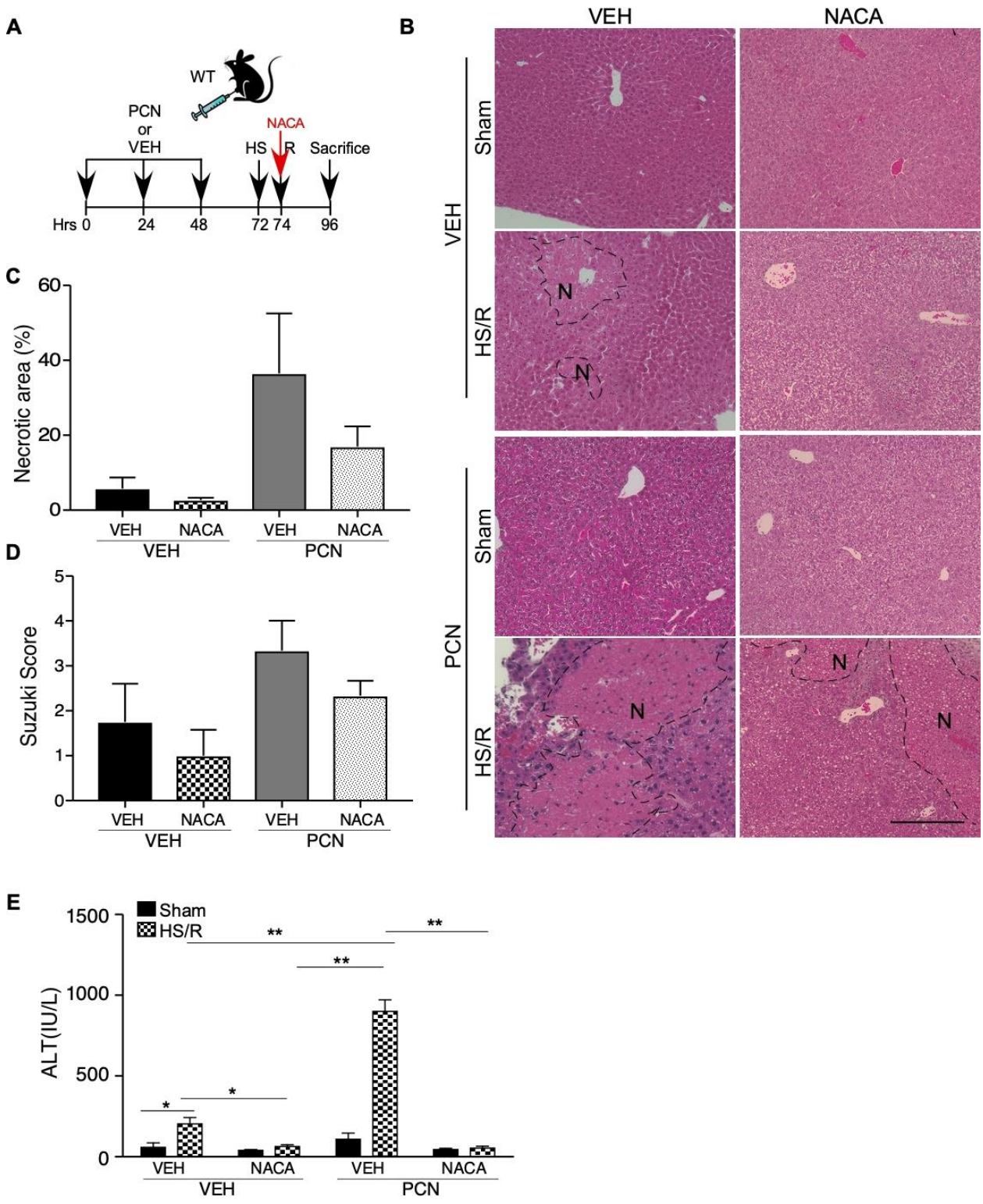

Figure 16. Post-hemorrhagic shock treatment of NACA attenuates HS-induced hepatic injury.

(A) Schematic representation of the NACA post-HS treatment model. WT mice were intraperitoneally injected with PCN (40 mg/kg) or VEH for two days before receiving the sham surgery or HS/R. NACA (200 mg/kg) or saline was given 2 hours after the initiation of HS and before the resuscitation. **(B)** Liver histology was analyzed by H&E staining. Bar is 100 μm. **(C-E)** Mice are the same as in (B). Shown are quantification of necrotic areas (C), Suzuki scores (D), and serum levels of ALT (E) in mice subject to HS/R. Results are presented as mean ±SE. n=3 for each group. *, $p < 0.05$; **, $p < 0.01$, the comparisons are labeled.

2.3.6 Post-hemorrhagic shock activation of PXR sensitizes mice to HS-induced hepatic injury

Since many trauma patients receive PXR-activating drugs upon their admissions to ICU, we investigated whether post-HS pharmacological activation of PXR can also sensitize mice to HS-induced hepatic injury. In this experiment, WT mice were subject to the HS surgery first, and right before the resuscitation, mice received a single intraperitoneal injection of PCN (40 mg/kg) or DEX (20 mg/kg) (Figure 17A). The activation of PXR and induction of Cyp3a11 were verified by qRT-PCR (Figure 17B). Post-HS treatment with PCN or DEX also exacerbated HS-induced hepatic injury as shown by histology (Figure 17C) and serum ALT level (Figure 17D). Post-HS treatment with PCN or DEX also increased HS-responsive oxidative stress as shown by immunofluorescence of 8-OHdG (Figure 17E). When the post-HS treatment of PCN was repeated in Cyp3a$^{-/-}$ mice, we found that PCN can no longer sensitize these mice to HS-induced hepatic injury (Figure 18), suggesting that the sensitizing effect of post-HS activation of PXR was also Cyp3a dependent.

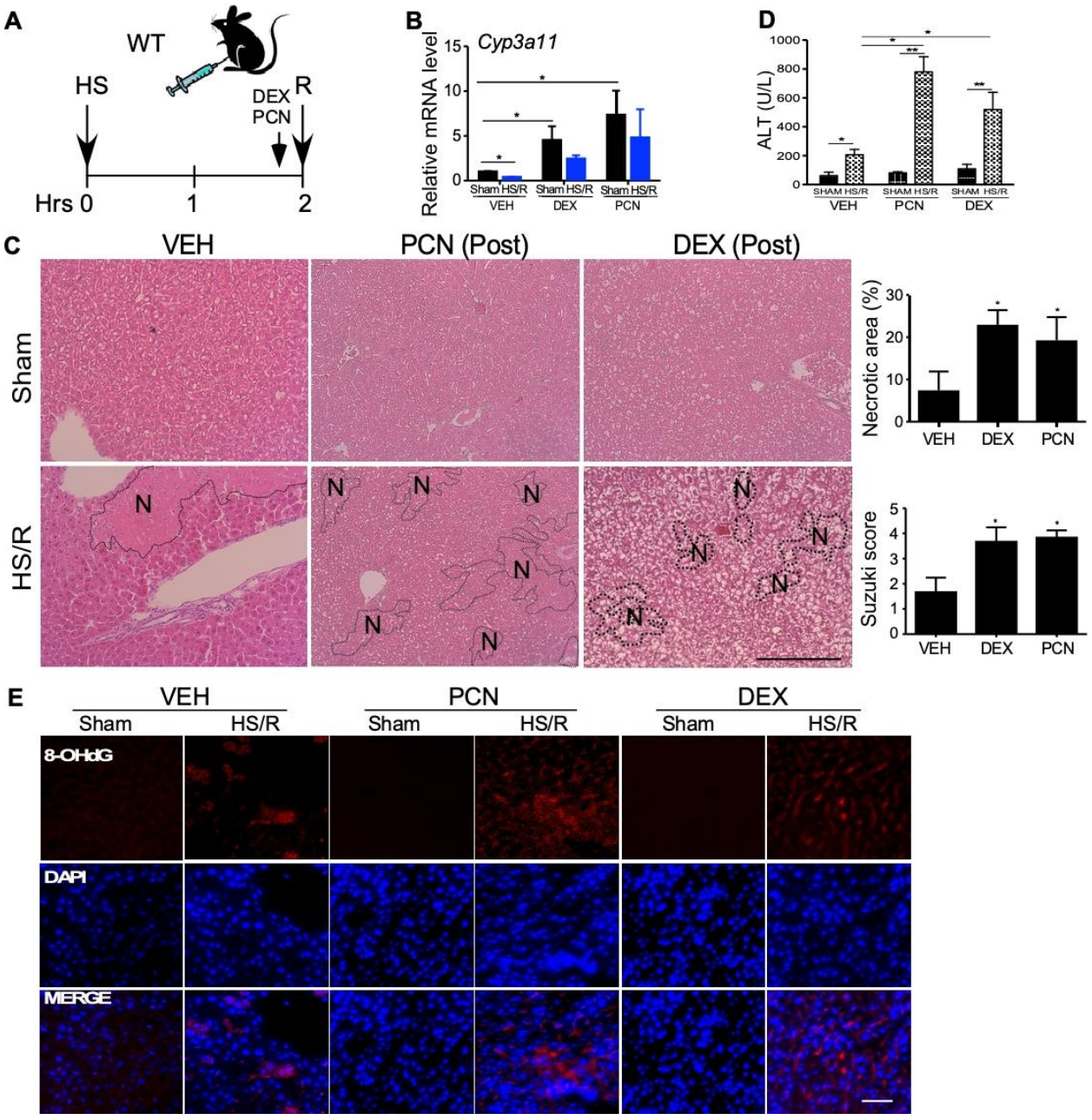

Figure 17. Post-hemorrhagic shock activation of PXR sensitizes mice to HS-induced hepatic injury.

(A) Schematic representation of the model of post-HS treatment of PCN or DEX. WT mice were subject to a 2-h HS and intraperitoneally injected with PCN (40 mg/kg) or DEX (20 mg/kg) before the resuscitation. and the mice were sacrificed 22 h after. **(B)** The hepatic mRNA expression of *Cyp3a11* was measured by qRT-PCR. **(C)** Liver histology was analyzed by H&E staining. Shown on the right are quantification of necrotic areas and Suzuki scores. **(D)** Serum levels of ALT. **(E)** Immunofluorescent staining for 8-OHdG. Bar is 100 μm. n=4~5 for each group. *, $p < 0.05$; **, p

< 0.01, the comparisons are labeled (B and D), or compared to the VEH group (C).

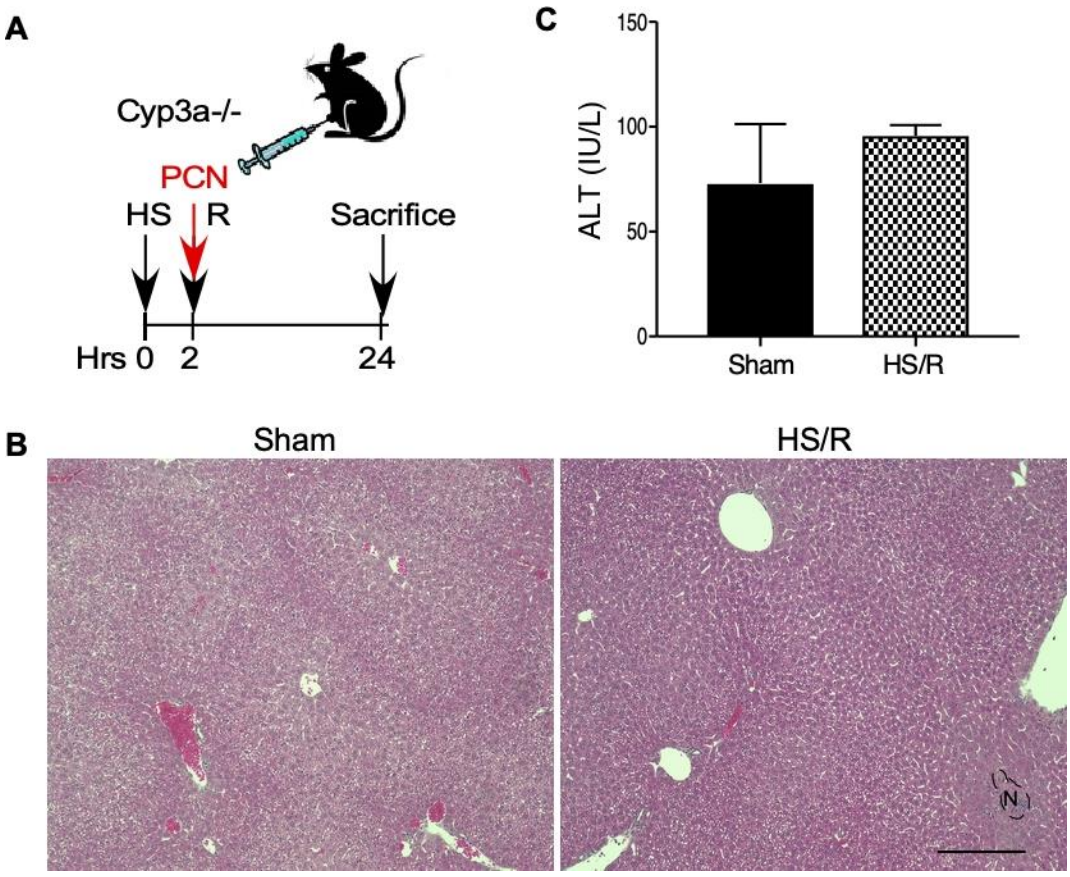

Figure 18. Ablation of Cyp3a abolishes the sensitizing effect of post-hemorrhagic shock treatment of PCN. **(A)** Schematic representation of the PCN post-HS treatment model. Cyp3a$^{-/-}$ mice were intraperitoneally injected with PCN (40 mg/kg) 2 hours after the initiation of HS and right before resuscitation. **(B)** Liver histology was analyzed by H&E staining. Bar is 100 μm. **(C)** Serum levels of ALT. Results are presented as mean ±SE. n=3 for each group.

2.3.7 Treatment with the hPXR antagonist SPA70 protects the hPXR/hCYP3A4 humanized mice from HS-induced hepatic injury in a time-sensitive manner

To determine whether a pharmacological inhibition of PXR can protect mice from HS/R-induced hepatic injury, humanized mice treated with RIF (10 mg/kg), in the absence or presence of a recently reported human-specific PXR antagonist SPA70 (150 mg/kg) (Lin et al., 2017), for

3 days were subject to HS/R (Figure 19A). Treatment with SPA70 efficiently blocked RIF-responsive induction of CYP3A4 as reported (Lin et al., 2017) (Figure 19B). SPA70 also attenuated HS/R-responsive and RIF-exacerbated hepatic injury as shown by histology (Figure 19C) and the serum ALT level (Figure 19D). In addition, SPA70 attenuated HS/R-induced oxidative stress, as shown by immunostaining of 4-HNE (Figure 19E), immunofluorescence of 8-OHdG (Figure 19F), and measurement of the expression of Atf3 and Chop (Figure 19G).

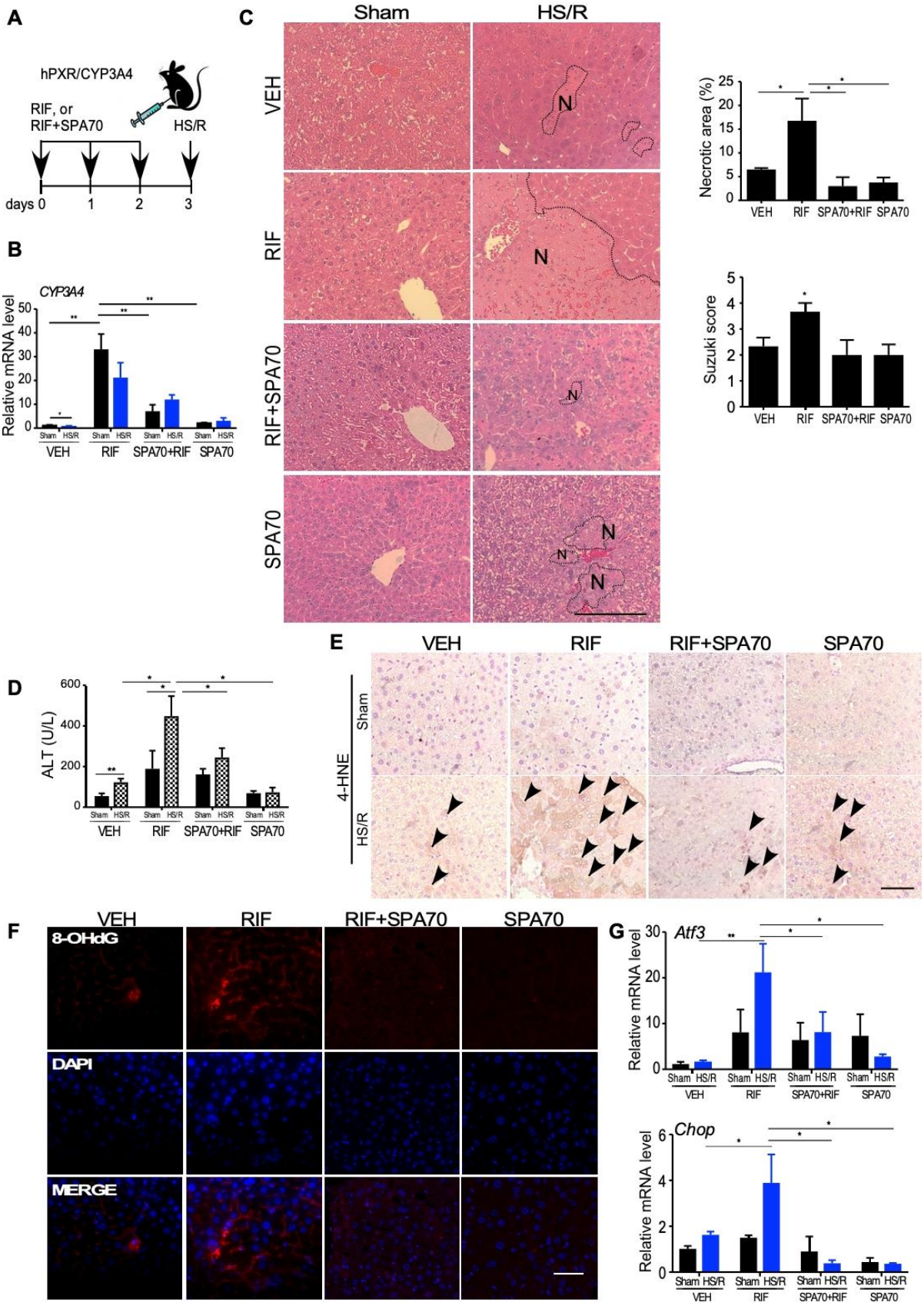
A
hPXR/CYP3A4
RIF, or
RIF+SPA70
HS/R
days 0 1 2 3
B
CYP3A4
Relative mRNA level
Sham HS/R
VEH RIF SPA70+RIF SPA70
C
Sham HS/R
VEH
RIF
RIF+SPA70
SPA70
N
Necrotic area (%)
VEH RIF SPA70+RIF SPA70
Suzuki score
VEH RIF SPA70+RIF SPA70
D
ALT (U/L)
VEH RIF SPA70+RIF SPA70
E
VEH RIF RIF+SPA70 SPA70
4-HNE
Sham
HS/R
F
VEH RIF RIF+SPA70 SPA70
8-OHdG
DAPI
MERGE
G
Atf3
Relative mRNA level
Chop
Relative mRNA level
Sham HS/R
VEH RIF SPA70+RIF SPA70

Figure 19. Treatment with the hPXR antagonist SPA70 protects the hPXR/hCYP3A4 humanized mice from HS-induced hepatic injury.

(A) Schematic representation of the SPA70 pre-treatment model. Mice were intraperitoneally injected with VEH, RIF (10 mg/kg) and SPA70 (150 mg/kg) individually or in combination for 3 days before receiving the sham surgery or HS/R. **(B)** The hepatic mRNA expression of *CYP3A4* was measured by qRT-PCR. **(C)** Liver histology was analyzed by H&E staining. Shown on the right are quantification of necrotic areas and Suzuki scores. **(D)** Serum levels of ALT. **(E and F)** The hepatic levels of 4-HNE (arrowheads indicated the positive staining) (E) and 8-OHdG (F) were measured by immunostaining and immunofluorescence, respectively. **(G)** The hepatic mRNA expression of *Atf3* and *Chop* was measured by qRT-PCR. Bars are 100 μm. n=4~5 for each group. *, $p < 0.05$; **, $p < 0.01$, the comparisons are labeled.

The protective effect of SPA70 was time-sensitive, because when given at 2-h or 12-h after the initiation of HS (Figure 20A), SPA70 failed to protect humanized mice from RIF-induced and HS/R-responsive hepatic injury (Figure 20B-20E). The lack of post-HS effect of SPA70 was likely due to the insufficient time to inhibit RIF-responsive expression of *CYP3A4* (Figure 20F). In the same set of experiments, treatment with KET at the 2-h time point, but not the 12-h time point, was effective to attenuate HS-induced hepatic injury (Figure 20B-20E).

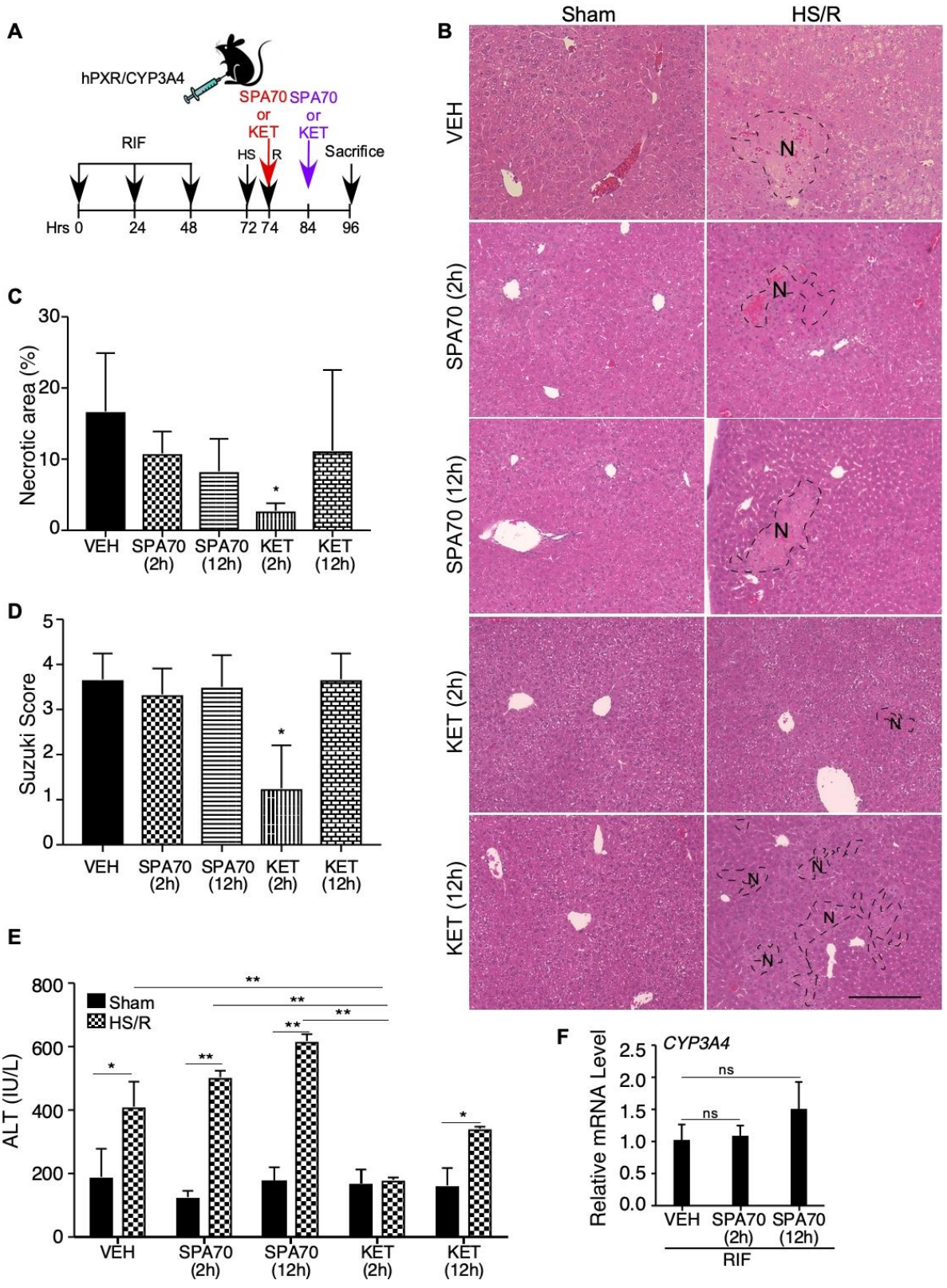
A
hPXR/CYP3A4
SPA70 or KET
SPA70 or KET
RIF
HS
R
Sacrifice
Hrs 0
24
48
72 74
84
96
B
Sham
HS/R
VEH
SPA70 (2h)
SPA70 (12h)
KET (2h)
KET (12h)
N
C
Necrotic area (%)
30
20
10
0
VEH
SPA70 (2h)
SPA70 (12h)
KET (2h)
KET (12h)
D
Suzuki Score
5
4
3
2
1
0
E
ALT (IU/L)
800
600
400
200
0
Sham
HS/R
F
CYP3A4
Relative mRNA Level
2.5
2.0
1.5
1.0
0.5
0.0
ns
RIF

Figure 20. Effects of post-hemorrhagic shock treatment of SPA70 and KET on HS-induced hepatic injury in humanized mice.

(A) Schematic representation of the SPA70/KET post-HS treatment model. Mice were intraperitoneally injected with RIF (10 mg/kg) for three days before receiving the sham surgery or HS/R. SPA70 (150 mg/kg), KET(95 mg/kg), or VEH was administrated either 2-h after the initiation of HS (at 72 h), or 12-h after the initiation of HS (at 84 h). **(B)** Liver histology was analyzed by H&E staining. Bar is 100 μm. **(C-E)** Mice are the same as in (B). Shown are quantification of necrotic areas (C), Suzuki scores (D), and serum levels of ALT (E) in mice subject to HS/R. **(F)** The hepatic mRNA expression of *CYP3A4* in RIF-treated sham groups. Results are presented as mean ±SE. n=3 for each group. *, $p < 0.05$; **, $p < 0.01$, compared to the VEH group (C and D), or the comparisons are labeled (E and F).

2.4 Discussion and conclusion

HS remains a major health concern due to the secondary tissue and organ injuries. A better understanding of the mechanisms by which HS induces tissue injury will help to develop effective therapeutic strategies to reduce the mortality of organ injury, including injury to the liver. Our previous microarray analysis suggested a major suppression in the expression of PXR and its target DMEs (Edmonds et al., 2011), based on which we initially speculated that the suppression of PXR might have contributed to HS-induced hepatic injury. To our surprise, we found that the activation of PXR exacerbated hepatic injury following HS, while Pxr ablation or pharmacological inhibition of PXR in humanized mice by SPA70 protected mice from HS-induced hepatic injury. The pathological role of PXR activation in HS-induced hepatic injury was consistent with our observation that there was an intact expression of Pxr and elevated expression of Cyp3a11 in mice that received the 2-h HS but without a resuscitation. Our results suggest that HS has a dynamic

effect on the expression of Pxr and DMEs, and the HS-responsive suppression of PXR may represent a protective response and/or secondary response to HS-induced hepatic injury.

Our study is of medical significance. This is because seriously injured trauma patients are uniformly prescribed with multiple drugs, many of which are PXR activators and DME inducers in the liver. The unavoidable use of PXR-activating drugs prior to HS or during the clinical management of trauma may restore drug metabolism, but has the potential to exacerbate HS-induced hepatic injury. We showed both pre-HS and post-HS activation of PXR sensitized mice to HS-induced hepatic injury. The pre-treatment with PXR agonists simulates HS patients who happen to take PXR-activating drugs prior to their injury, whereas treatment during resuscitation mimics HS patients who receive PXR-activating medications during their ER visit or ICU stay. The human relevance of this study was also illustrated by our use of the hPXR/hCYP3A4 humanized mice, in which treatment with RIF, an antibiotic to reduce deep surgical site infections (Shiels et al., 2018; Tyas et al., 2018) or to treat tuberculosis, sensitized these mice to HS-induced hepatic injury.

The mechanistic insight revealed from this study may provide translational opportunities. We have presented both pharmacological and genetic evidence that the induction of CYP3A is required for the sensitizing effect of PXR on HS-induced hepatic injury. The initial evidence was that treatment with the CYP3A inhibitor KET attenuated the VP-PXR transgenic mice from HS-induced hepatic injury. In addition to inhibiting Cyp3a enzymes, KET and its derivatives can also function as PXR antagonists (Wang et al., 2007). Therefore, we cannot exclude the possibility that inhibition of both Cyp3a and PXR may have contributed to the protective effect of KET. To more conclusively define the role of CYP3A, we showed that ablation of the Cyp3a genes abolished the sensitizing phenotype in VP-PXR transgenic mice, PCN- or DEX-treated WT mice, or RIF-treated

humanized mice. Pharmacoenhancing by CYP3A inhibition is not uncommon in the clinic. It is interesting to know whether pharmacoenhancers, such as Ritonavir used in the HIV antiretroviral therapy (Saag et al., 2018), can be used to attenuate the sensitizing effect of PXR activation. The use of antioxidant NACA to relieve the sensitizing effect of PXR was also exciting, because the oral formulation of N-acetylcysteine (NAC) is a drug approved for treating APAP overdose whose mechanism of hepatotoxicity also involves oxidative stress (Yan et al., 2018). The use of hPXR antagonist SPA70 to attenuate RIF-induced sensitization in humanized mice provided a proof of concept evidence that a direct use of PXR antagonists may also be used to manage PXR-mediated sensitization of HS-responsive liver injury. Last but not least, it is encouraging that post-HS administration of NACA and KET remained effective in alleviating PXR-induced and HS/R-responsive hepatic injury.

In summary of Chapter II, we have uncovered a previously unrecognized role of PXR in HS-induced hepatic injury (Figure 21). Cautions need to be applied when PXR-activating drugs are used in trauma patients, or when patients were on PXR-activating drugs prior to their traumatic injuries. Our results also suggest that co-administration of anti-oxidative agents, CYP3A inhibitors, and/or PXR antagonists can be used to mitigate the side effect of liver injury associated with the unavoidable use of PXR-activating drugs in trauma patients.

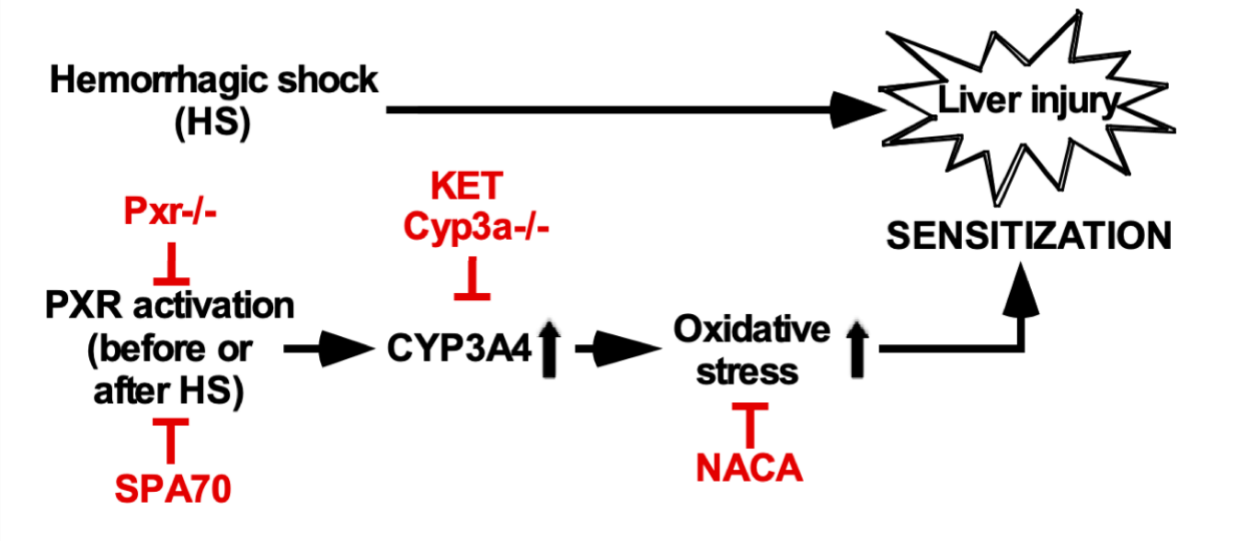

Figure 21. Summary of Chapter II.

3.0 Estrogen sulfotransferase and hemorrhagic shock-induced acute lung injury

3.1 Estrogen sulfotransferase in liver disease

3.1.1 The superfamily of sulfotransferases

Sulfate conjugation (sulfation or sulfonation) is a major conjugating pathway responsible for the deactivation, detoxification and excretion of xenobiotics and endogenous molecules (Falany, 1991). Sulfoconjugation was first recognized as an important metabolic pathway by Baumann in 1876 (Baumann, 1876). At the chemical level, the cytosolic sulfotransferases (SULTs) catalyze the transfer of a negatively charged sulfonate group (SO3-) from the universal sulfate donor 3′- phosphoadenosine-5′-phosphosulfate (PAPS) onto a nucleophilic group of their substrates to generate hydrophilic products, which often promote the urinary excretion of the substrates. The high-energy sulfate donor PAPS can be generated by PAPS synthases, including PAPSS1 and PAPSS2, as well as by ATP sulfurylase and two forms of adenosine 5′-phosphosulfate kinase (APS kinases) (Mueller et al., 2018).

SULTs are widely expressed in the liver, as well as metabolically active or hormonally responsive extrahepatic tissues (Dooley et al., 2000; Gamage et al., 2006). This large family of enzymes are responsible for sulfating a variety of endogenous and exogenous molecules, including pharmaceuticals, procarcinogens, hormones, neurotransmitters, as well as intermediates of endogenous metabolism (Dooley et al., 2000; Glatt et al., 2001; Negishi et al., 2001; Jancova et al., 2010). Sulfation often results in the inactivation of the substrates or reduced potency of ligands (Strott, 2002; Bjerregaard-Olesen et al., 2015) but with some exceptions. Their abundance in the

liver and wide range of substrates suggest SULTs may act as important mediators for the development of liver diseases, such as hepatocellular carcinoma (Xie et al., 2017; Zou et al., 2017), liver fibrosis (Hardwick et al., 2013; Krattinger et al., 2016; Yetti et al., 2018), and drug-induced liver injury (Fang et al., 2016). Therefore, in this review we focus on the roles of the human and rodent SULTs in liver diseases.

The *SULTs superfamily contains* 62 human *SULT* genes and 46 murine homologues as of 2016 (Mueller et al., 2015; Herrero et al., 2016). Among *SULTs*, the aryl-sulfotransferase (SULT1) and the hydroxysteroid sulfotransferase (SULT2) families are two principal sub-families of SULTs that are the major contributors to the sulfonation of many xenobiotics including pharmaceuticals and procarcinogens, and endobiotics including steroids, thyroid, and neurotransmitters (Kauffman, 2004; Reinen and Vermeulen, 2015).

SULT1 family comprises five isoforms: phenol-sulfotransferases (SULT1A1/2) (Raftogianis et al., 1999), catecholamine phenol sulfotransferase (SULT1A3/4) that is only present in humans (Zou et al., 2017), thyroid hormone sulfotransferase (SULT1B1) (Saeki et al., 1998), iodothyronine sulfotransferase (SULT1C2,1C4) (Dubaisi et al., 2019), and estrogen sulfotransferase (EST/SULT1E1) (Zhang et al., 1998; Guo et al., 2015). SULT2 family has two isoforms: SULT2A1 that sulfonates 3-hydroxysteroids (Mueller et al., 2018) and bile acids (Huang et al., 2010), and SULT2B1b that has a greater selectivity for 3-hydroxysteroids, such as cholesterol (Bi et al., 2018), but not for bile acids.

In addition to the SULT1 and SULT2 families of enzymes, the human genome contains two more sulfotransferase gene families, *SULT4* and *SULT6*, encoding enzymes including

SULT4A1 that is a brain-specific sulfotransferase associated with antipsychotic treatment response (Wang et al., 2014) and SULT6B1 whose physiological function is largely unknown.

3.1.2 Estrogen Sulfotransferase in liver diseases

3.1.2.1 EST in liver cancer

Estrogen sulfotransferase (SULT1E1, also known as EST), widely expressed in human tissues such as the liver, lung, adipose tissue, and kidney (Barbosa et al., 2019), is best known for its function in the sulfoconjugation and deactivation of estrogens. This is because sulfonated estrogens fail to bind to the estrogen receptor and thus lose their hormonal activities (Song, 2001). As such, SULT1E1 has long been implicated in female sex hormone related cancer, such as breast, endometrial, and ovarian cancers (Pasqualini, 2009; Mungenast et al., 2017; Sinreih et al., 2017; Xu et al., 2018). Interestingly, SULT1E1 is also reported to be associated with the occurrence of HCC in rats. In a study on inflammatory liver disease, upregulation of *Sult1e1* in diethynitrosamine (DEN)-treated mouse livers was observed compared to the vehicle-treated livers using real time RT-PCR (Lee et al., 2017). However, in the DEN-induced rat model of hepatoma, the expression of *SULT1E1* was decreased with the onset of hepatomas (Albrethsen et al., 2011). The causal relationship remains to be defined, because the expression of *SULT1E1* was increased in regenerating liver (Albrethsen et al., 2011). Moreover, the species difference and the human relevance of *SULT1E1* in liver cancer need to be clarified.

3.1.2.2 EST in non-alcoholic fatty liver disease (NAFLD) and non-alcoholic steatohepatitis (NASH)

Previous study in our lab found that loss of *Sult1e1/Est* in female mice improved metabolic function with improved insulin sensitivity and reduced hepatic steatosis in ob/ob mice lacking *Sult1e1* (also known as the obe mice), compared to the ob/ob (Gao et al., 2012). In an independent study, Sult1e1 was suggested to play a role in sensitizing male mouse to NAFLD/NASH induced

by a 20-wk feeding of a Western diet high in cholesterol and saturated fat diet (HCFD) (Matsushita et al., 2017). The authors found that NASH was attenuated in *IkbkbΔmye* mice with myeloid IKKβ deficiency in both genders but aggravated in male but not female *IkbkbΔhep* mice with hepatocyte IKKβ deficiency. Microarray analysis on liver tissues from male and female WT and *IkbkbΔhep* mice fed HCFD showed a significant upregulation of *Sult1e1* gene in *IkbkbΔhep* mice compared to WT mice. Among the four groups, the male *IkbkbΔhep* mice expressed the highest level of *Sult1e1* gene which was associated with decreased plasma estradiol levels. The authors' mechanism study indicated that the enrichment of LXRα to LXRE on the *Sult1e1* gene promoter of male *IkbkbΔhep* mice might be responsible for their heightened sensitivity to NASH. These results suggest hepatocyte IKKβ is protective in males due at least in part to its ability to repress LXR responsive induction of Sult1e1 (Matsushita et al., 2017).

3.1.2.3 EST in liver injury induced by sepsis and ischemia /reperfusion

SULT1E1 is relatively thoroughly studied in inflammation-based conditions. Sepsis, resulting from the host's deleterious systemic inflammatory response to microbial infections, is a major cause of mortality in the intensive care unit. Although sepsis and its associated inflammation are known to decrease the expression and activity of many drug metabolizing enzymes, we observed a major induction of Sult1e1 and compromised estrogen activity in the liver of mice subjected to the bacterial lipopolysaccharide (LPS) or cecum ligation and puncture (CLP) models of sepsis. The inflammatory induction of *Sult1e1* gene by sepsis was mediated by NF-kB. Reciprocally, the expression and activity of Sult1e1 can impact the clinical outcome of sepsis. Specifically, ablation of the *Sult1e1* gene or pharmacological inhibition of the Sult1e1 enzyme by Triclosan sensitized mice to sepsis-induced death in an estrogen dependent manner. The increased sepsis induced lethality in *Sult1e1* knockout mice was explained to be due to increased estrogen

activity and the resultant attenuated sepsis-induced pro-survival inflammatory response (Chai et al., 2015c).

Hepatic ischemia-reperfusion (I/R) injury is a major cause of liver damage. The pathogenesis of hepatic I/R injury is a dynamic process including the deprivation of blood and oxygen supply during the ischemic phase, followed by their restoration during the reperfusion phase, which is associated with oxidative stress and inflammation. An induction of *Sult1e1* in rats subjected to I/R was reported as early as 2006, but without a clearly defined mechanism or understanding of the biological significance (Svetlov et al., 2006). More recently, we reported a systemic analysis of the effect of liver I/R on the expression of *Sult1e1*. We showed that the expression of *Sult1e1* was markedly induced by I/R in the mouse liver. The ablation of *Sult1e1* protected female mice from the injury in an estrogen dependent manner, but heightened liver injury in male mice in an androgen-dependent manner. Further mechanism study established *Sult1e1* as a direct transcriptional target of nuclear factor erythroid 2-related factor (Nrf2), a key transcriptional factor responsible for the activation of an array of genes to adapt the cells to hypoxic or oxidative damages. Based on these results, we proposed that inhibition of SULT1E1, at least in females, may represent an effective approach to manage hepatic I/R injury (Guo et al., 2015).

3.1.2.4 EST in cystic fibrosis

Cystic fibrosis (CF), characterized by mutations of both copies of the cystic fibrosis transmembrane receptor (CFTR) gene, is an inherited disorder that causes progressive and eventually fatal damage to the lungs, digestive system, and other organs in the body. Liver is an organ that can be affected by CF. A series of papers published from the laboratory of Charles Falany suggested that the hepatic SULT1E1 may play a role in the progression of liver damage in CF patients (Li and Falany, 2007; He et al., 2008; Falany et al., 2009). Specifically, elevated

hepatic SULT1E1 activity was observed in mouse models of CF (Li and Falany, 2007) and HepG2 cells co-cultured with human MMNK-1 cholangiocytes with repressed CFTR (He et al., 2008). The induction of SULT1E1 in CFTR-deficient MMNK-1 cells/HepG2 cells co-culture system was found to be dependent on the activation of LXR, and the SULT1E1 induction led to alterations in the expression of estrogen responsive genes, including IGF-1, GST-P1 and carbonic anhydrase II, due to decreased E_2 levels. These results suggest that the induction of hepatic *SULT1E1* in CF patients may have facilitated the development of CF liver disease (Falany et al., 2009).

3.2 Hepatic estrogen sulfotransferase distantly sensitizes mice to HS-induced acute lung injury

3.2.1 Research Background

As described in **3.1 Estrogen Sulfotransferase in liver disease**, the primary function of EST is to sulfo-conjugate and deactive estrogens, such as estradiol. EST locates in cytosol and catalyzes the transfer of a negatively charged sulfonate group (SO_3^-) from the universal sulfate donor 3′-phosphoadenosine-5′-phosphosulfate (PAPS) to a nucleophilic group of their substrates to generate hydrophilic products.

We previously reported that the expression of EST is highly inducible in the livers of mouse models of multiple disease, including obesity and type 2 diabetes (Gao et al., 2012) , hepatic ischemia and reperfusion (Guo et al., 2015), and sepsis (Chai et al., 2015). Reciprocally, the expression and/or activity of EST have major effects on the outcome of these diseases through varied mechanisms and often in a sex- and tissue-specific manner (Gao et al., 2012; Chai et al., 2015; Guo et al., 2015; Garbacz et al., 2017). Based on these studies, we originally hypothesized that EST might also impact on HS-induced hepatic injury, and we were wondering whether EST expression is upregulated as in other disease models and how the changes in EST expression impact on HS-induced hepatic injury. To this end, we employed the same mouse model of HS/R described in Chapter II. We also found liver EST is highly inducible in both male and female mice however, liver EST showed no impact on HS-induced hepatic injury as described in **3.2.3 Experimental Results**.

Besides HS-induced liver injury, acute lung injury is one of the leading causes of death in surgical and trauma patients with the in-hospital mortality rate as high as 40% (Rubenfeld et al., 2005; Villar et al., 2014). Therefore, we are wondering if the induction of EST would play a pathological role in HS-induced acute lung injury. As a consequence of hemorrhagic shock and resuscitation (HS/R), an exaggerated inflammatory response is initiated and a large number of polymorphonuclear neutrophils (PMNs) are activated and migrate into the lung. The infiltration of PMNs is a hallmark of acute lung injury, and it plays a central role in the development of lung tissue injury (Liu et al., 2009; Wen et al., 2014; Xu et al., 2017). It is interesting to know whether liver EST would impact on inflammation response following HS and it is conceivable that a better understanding of the mechanism by which HS induces acute lung injury will help to develop effective strategies for the clinical management of HS in trauma and surgical patients.

Both clinical and animal studies have shown a sex-dependent response to HS. The levels of female sex hormones, especially 17β-estradiol, are believed to be positively associated with a favorable outcome after HS (Sperry et al., 2012; Yang et al., 2014). In human studies, it has been reported that the male sex is independently associated with 40% higher rate of multiple organ failure (MOF), a 25% higher rate of nosocomial infection (NI), and elevated levels of IL-6 (Sperry et al., 2008) in trauma patients. In contrast, the female patients tend to have lower levels of systemic inflammatory cytokines and they are more resistant to MOF (Frink et al., 2007). However, the role of estrogens in trauma patients is not without controversy. For example, it was reported that elevated serum levels of 17β-estradiol and testosterone in the early time period post-injury have their independent associations with greater risk of MOF and NI (Zolin et al., 2015). In animal studies, it was reported that acute estradiol treatment attenuates lung inflammatory responses, such as reducing the basal expression of platelet endothelial cell adhesion molecule-1 (PECAM-1) and IL-10 levels in male rats subjected to intestinal ischemia (Breithaupt-Faloppa et al., 2014). Treatment with 17 β-estradiol also attenuated acute lung injury induced by oxidant stresses other than HS, such as the herbicide paraquat and acute alveolar anoxia (Hamidi et al., 2011). It was noted that most of the reported roles of estrogens in traumatic injury relied on the administration of pharmacological doses of estrogens. It is unclear whether regulation of endogenous estrogen metabolism can affect the clinical outcome of HS-induced tissue injury. Since EST is a master regulator of estrogen sulfation and deactivation and a pulmonary function of EST has not been reported, it is interesting to know whether and how EST plays a role in HS-induced acute lung injury.

In this study, we uncovered a novel function of EST in HS-induced acute lung injury. HS induces the hepatic expression of Est in mice. The HS-responsive induction of Est may have played

a pathogenic role in HS-induced acute lung injury, because genetic ablation or pharmacological inhibition of Est effectively protected female mice from HS-induced acute lung injury, whereas hepatic reconstitution of EST re-sensitized mice to HS-induced acute lung injury.

3.2.2 Experimental Procedures

Chemicals

The EST inhibitor triclosan, 17β-estradiol, estrone, estrone 3-sulfate sodium salt, β-estradiol 3-sulfate sodium salt, and dansyl chloride were purchased from Sigma-Aldrich (St. Louis, MO). N-butyl chloride was purchased from Fisher Scientific (Ottawa, Ontario, Canada). 17β-estradiol-2,4,16,16,17-d5 and 17β-estradiol-2,4,16,16-d4-3-sulfate were purchased from CDN isotopes (Pointe-Claire, Quebec, Canada).

Animals and mouse model of hemorrhagic shock and resuscitation

Est$^{-/-}$ mice have been described previously (Qian et al., 2001). KOLE mice are Est-knockout (KO) and Lap-EST (LE) transgenic mice that were generated by cross-breeding Est$^{-/-}$ mice with Lap-tTA/TetRE-EST (Lap-EST) transgenic mice. The Lap-EST transgene overexpresses the human EST exclusively in the liver/hepatocytes under the control of the liver-enriched activator protein (Lap) gene promoter (Chai et al., 2015). All mice were maintained in C57/BL6 background. The majority of the experiments were performed on mice of 8 weeks of age except those specified for ovariectomy (5-weeks old). Hemorrhagic shock and resuscitation was performed as we have previously described (Xie et al., 2019), and the serum and tissues were collected 4, 6 or 24 hours after HS. The use of mice in this study has complied with all relevant federal guidelines and institutional policies, and has been approved by the University of Pittsburgh Institutional Animal Care and Use Committee.

Bronchoalveolar lavage fluid (BALF) collection

This was performed essentially as described (Jhingran et al., 2016). In brief, 4 hours after HS/R, mice were anesthetized by i.p. injections of 150 mg/kg ketamine and 10 mg/kg xylazine. A BALF catheter was inserted into the trachea and repeatedly injected with 0.5 ml of ice-cold PBS (from the "input" syringe filled with 3 ml of PBS) and then BALF was aspirated from the inflated lungs into the initially unfilled "output" syringe via a 3-way stopcock. We typically injected a total of 3 ml and recovered 2.5 ml of BALF in the output syringe. The 3-way stopcock is adjusted after each injection and aspiration round to ensure that BALF was captured in the output syringe. The recovered BALF were centrifuged at 300 g for 5 minutes. The cell free supernatants of BALF were collected and subjected to the measurement of protein concentration using a BCA protein assay kit from ThermoFisher Scientific (Waltham, MA).

Measurement of lung wet/dry ratio

Mice were sacrificed, and lungs were excised 4 hours after the HS/R. Blood was removed by blotting the lungs with filter papers until dry, and the lungs were then weighed for their wet weight. The lungs were subsequently placed in an oven at 65°C for 72 hours, and the dry weight was recorded. The wet/dry weight ratio was calculated to assess tissue edema.

Measurement of IL-6 in BALF and serum

These were measured using enzyme-linked immunosorbent assay kits from Pierce/Thermo Fisher Scientific, according to the manufacturer's instructions.

Histology, immunohistochemistry, and immunofluorescence

The lungs were freshly harvested and fixed in 10% neutral-buffered formalin for 24 hours. The tissues were histologically processed, embedded in paraffin, sectioned at 4 μm, and stained with hematoxylin and eosin for general histology. For myeloperoxidase (MPO) immunostaining,

de-paraffinized sections were incubated with anti-MPO antibody from Abcam (Cambridge, MA) at 1:25 dilution overnight at 4 °C. The antibody signal was visualized by peroxidase reaction using 3,3′-diaminobenzidine as the chromogen. Hematoxylin was used as a nuclear counterstain. For estrogen sulfotransferase (EST) immunofluorescence, liver and lung paraffin sections were incubated with anti-estrogen sulfotransferase from Abcam at 1:100 dilution overnight at 4 °C. The secondary antibody used was a Cyanine 5 (Cy5) conjugated donkey anti-rabbit polyclonal antibody from MilliporeSigma (Danvers, MA) at 1:500 dilution. DAPI-Fluoromount-G purchased from Southern Biotech, Birmingham, AL, was used as a nuclear counterstain. For immunohistochemistry and immunofluorescence, at least three mice were used for each treatment group, and for each sample at least four noncontiguous regions were photographed and analyzed.

Real-time PCR and Western blotting

Real-time PCR is performed as described in Chapter II. For Western blotting, 30 μg of total proteins for each sample were separated on 13% SDS-polyacrylamide gel. The primary antibodies were polyclonal rabbit anti-SULT1E1 from Proteintech at 1:200 dilution and monoclonal mouse anti-β-actin from Sigma-Aldrich at 1:5000 dilution. The secondary antibodies were anti-rabbit antibody and anti-mouse antibody from Cell Signaling Technology at 1:5000 dilution. Detection was achieved by using an ECL system from Amersham (Piscataway, NJ).

Flow cytometry

Tissue dissection and digestion were performed as described (Jhingran et al., 2016). Mouse bone marrow neutrophils were isolated and purified as described (Swamydas and Lionakis, 2013). Flow cytometry was performed as described (Liu et al., 2009; Jhingran et al., 2016). In brief, 200 μL suspended cells (approx. 2.5 million cells) or 100ul peripheral blood were stained with anti-CD45 buv395, anti-CD11b-APC antibody, anti-Gr-1-PE antibody, and anti-CXCR2(CD182)-

FITC antibody for the detection of neutrophils. The stained cells were applied for data acquisition on BD STI LSRII Cytometer and re-analyzed with BD FACSDIVA software.

Estradiol extraction and derivatization

Estradiol was extracted by liquid-liquid extraction using n-Butyl chloride and then derivatized with dansyl chloride as previously described by Li, et al (Li et al., 2016). Samples were first spiked with internal standard 20 μL17β-estradiol-2,4,16,16,17-d5 (1 ng/ml in methanol). 3 ml n-Butyl chloride was then added and vortexed for 1 min. The tubes were then centrifuged at 4770g at room temperature for 10 min and the organic layer was transferred to salinized culture tubes and dried down under a soft steam of nitrogen at 37 °C for 20 min. Residues were derivatized in 0.1 ml buffered dansyl chloride solution (a 1:1 mix of acetonitrile: water, pH 10.5), heated at 60 °C for 3 min, and then transferred to glass vials for UPLC-MS/MS analysis.

Estradiol sulfate extraction

Estrogen sulfates in lung tissue were extracted in 75% methanol before drying down. Sediment were removed after recovering with 1 ml PBS and centrifuging for 20 min (8000 g, 4 °C). For both lung tissue samples and serum samples, internal standard 17β-estradiol-2,4,16,16-d4-3-sulfate (100 pg) were added. Solid-phase extraction using Oasiss MCX (3 cc/60 mg, Waters) extraction cartridges was performed under gravity. Prior to loading the tissue or serum samples, the cartridges were conditioned with methanol (1 ml), followed by water (1 ml). The sample was loaded and allowed to pass through the cartridges and the eluate discarded. Next, the cartridges were washed with methanol (5% v/v, 3 ml) and again the eluate discarded. Finally, the estrogen sulfates were eluted in methanol (3 ml). Extracts were reduced to dryness under oxygen-free nitrogen at 40 °C.

UPLC–MS/MS analysis of estradiol and estradiol sulfate

We used published UPLC–MS/MS methods for the detection of estradiol (Li et al., 2016) and estradiol sulfate (Chai et al., 2015) with minor modifications. Liquid chromatography was performed using an Acquity ultra performance LC autosampler from Waters (Milford, MA). Analytes were separated on a UPLC BEH C-18, 1.7 mm (2.1 × 150 mm) reverse-phase column from Waters. Column temperature was maintained at 55 °C. For estradiol detection, mobile phases, delivered at a flow rate of 0.3 ml/min, consisted of (A) acetonitrile and (B) 0.1% formic acid in water, at an initial mixture of 50:50 A and B. Mobile phase B was maintained at 50% for 1 min and then increased to 85% in a linear gradient over 3 min, where it remained for 1 min. This was followed by a linear return to initial conditions over 1.5 min. For the detection of estradiol sulfate, mobile phase B was maintained at 80%. Total run time per sample was 6.5 min and all injection volumes were 7.5 μl. Mass spectrometric analysis of analyte formation was performed using a TSQ Quantum Ultra from Thermo Fisher Scientific (San Jose, CA) triple quadrupole mass spectrometer coupled with heated electrospray ionization source (HESI) operated in negative selective reaction monitoring (SRM) mode with unit resolutions at both Q1 and Q3 set at 0.70 full width at half maximum. Quantification by SRM analysis of estradiol and estradiol sulfate were performed by monitoring the m/z transitions.

PMNs isolation from bone marrow

This experiment was performed as described (Swamydas et al., 2015). In brief, PMNs were isolated and purified from bone marrow cells using Histopaque-based density gradient centrifugation. 3 ml of Histopaque 1077 (density, 1.077 g/ml) were overlaid on 3 ml of Histopaque 1119 (density, 1.119 g/ml) in a 15-ml conical centrifuge tube, and the bone marrow cell suspension were added on top of the Histopaque 1077 layer. Collect the neutrophils at the interface of the Histopaque 1119 and Histopaque 1077 layers after centrifuging for 30 minutes at 872 × g at room

temperature without brake. The collected PMNs were washed twice with RPMI 1640 1X supplemented with 10% FBS and 1% penicillin/streptomycin and centrifuged at 1400 rpm for 7 minutes at 4°C before cell plating.

Statistical analysis

Results are expressed as mean ± SE. Differences between two individual groups were determined by Student's *t* test. Differences between multiple groups were evaluated using two-way analysis of variance followed by post-hoc multiple comparison according to the Tukey's test. Statistical significance was accepted at $p < 0.05$.

3.2.3 Experimental Results

3.2.3.1 Hemorrhagic shock (HS) tissue specifically induces the expression of Est in the liver

To determine whether liver EST is inducible after HS, we performed the same HS model here and harvested the tissue at 24 h after HS. We found the mRNA expression of *Est* was markedly induced in the liver, but not in the lung of female mice subjected to HS/R (Figure 22A). HS/R also induced the mRNA expression of *Est* in male mice, but the fold induction was not as dramatic as in female mice (Figure 22B). The induction of Est protein in the liver and lack of induction in the lung of female and male mice were further verified by immunofluorescence (Figure 22C). The expression of Est in the lung was barely detectable, consistent with a previous report (Riches et al., 2009). The HS/R-responsive inductions of Est protein in the liver of female and male mice were also confirmed by Western blotting (Figure 22D).

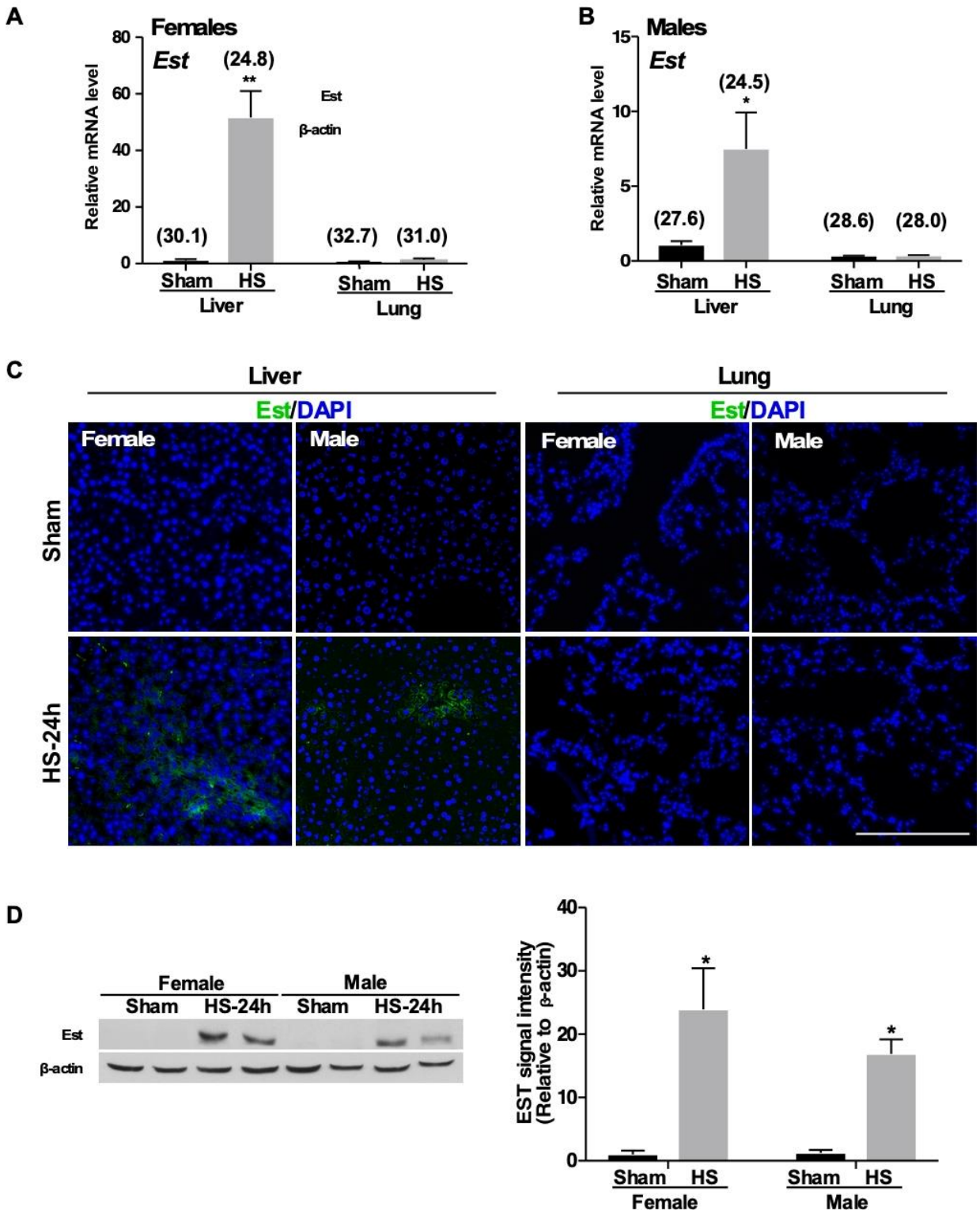

Figure 22. Hemorrhagic shock (HS) specifically induces the expression of Est in the liver.

Female and male WT mice were subjected to Sham surgery or HS/R. Serum and tissue were harvested at 24 hours after HS. **(A and B)** The mRNA expression of *Est* in the liver and lung of female (A) and male (B) mice was measured by real-time PCR. **(C)** The protein expression of Est in the liver and lung in female and male mice was measured by immunofluorescence staining of DAPI (blue) and Est (green). Bar is 100 μm. **(D)** The protein expression of Est in the liver of female and male mice was measured by Western Blotting. Shown to the right is the quantification of the Western results. Numbers in parentheses in A and B are average real-time PCR cycle numbers. Results are presented as mean ±SE. n=3 for each group. *, $p < 0.05$; **, $p < 0.01$, compared to the Sham groups.

Because of the significant induction of liver Est after HS/R surgery, we sought to know if the induction of liver Est play a pathological role in HS-induced hepatic injury similar to the diseased models we reported before. To our surprise, Est ablation in female mice had little effect on hepatic injury at different time points after HS. Here showing is the liver histology at 24 h after HS (Figure 23A) and serum level of alanine aminotransferase (ALT) (Figure 23B).

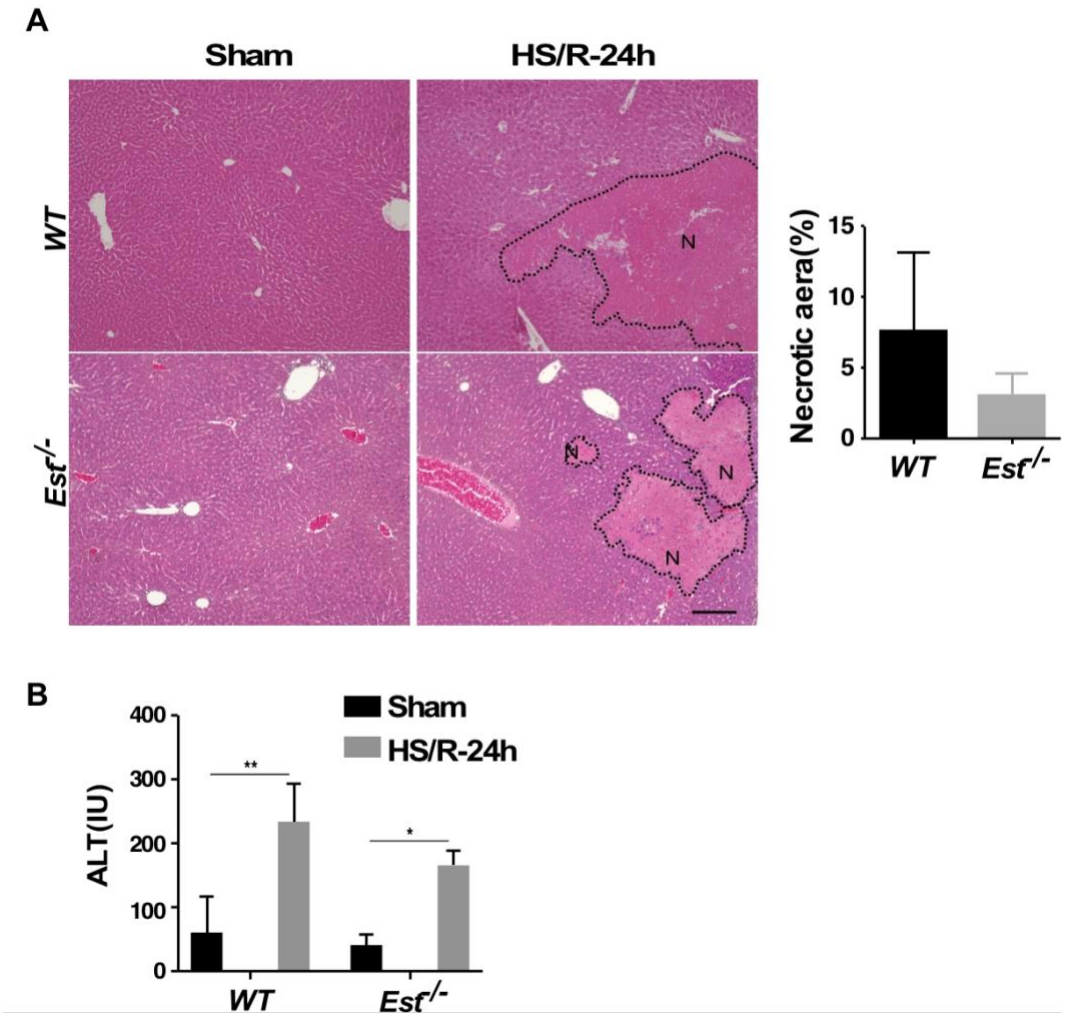

Figure 23. Est ablation has no effect on HS-induced hepatic injury.

Female WT and *Est-/-* mice were subjected to HS/R. Mice were sacrificed 24 hours after the initiation of HS. **(A)** H&E the liver sections (left) and quantification of the necrotic areas (right). The Ns within the dotted circle indicate the necrotic areas. Bar is 100 μm. **(B)** Serum levels of ALT. Results are presented as mean ±SE. n=4~5 for each group. *, $p < 0.05$; **, $p < 0.01$, with the comparisons labeled.

3.2.3.2 Genetic ablation or pharmacological inhibition of Est protects female, but not male mice from HS-induced acute lung injury

Since lung is sensitive to HS-induced acute immune responses which participants tissue injury immediately after HS, we measured acute lung injury at different time points, including 4 or 24 hours after HS in female wild-type (WT) and Est$^{-/-}$ mice to determine the functional relevance of Est induction in HS-induced acute lung injury. The liver expression of Est was efficiently induced at both time points (Figure 24). When acute lung injury was evaluated, female Est$^{-/-}$ mice were found to be protected from HS-induced acute lung injury at both time points, including decreased pulmonary interstitial edema and infiltration of cells into the interstitium and alveolar spaces at the histological level (Figure 25A), decreased bronchoalveolar lavage fluid (BALF) protein concentrations, a marker for tissue leakage (Figure 25B), and decreased lung wet to dry (W/D) ratio, the marker for water retention, (Figure 25C). In an independent model of pharmacological inhibition of Est, treatment of female WT mice with the EST inhibitor triclosan (5-chloro-2(2,4-dichlorophenoxy)-phenol) (Wang et al., 2004) also inhibited the 4-hour HS-induced acute lung injury, as shown by histology (Figure 25D) and measurements of BALF protein concentration (Figure 25E) and W/D ratio (Figure 25F). Interestingly, we noticed triclosan treatment itself tended to induce an increase in BALF protein and W/D ratio in the sham condition (Figure 25E and 25F). It has been reported that triclosan can trigger colonic inflammation in mice, so it is possible triclosan may have also induced mild inflammation in the lung and caused a mild induction of the total BALF protein level in the sham group. However, the inhibition of EST by triclosan which results in the elevation of estrogens overrided the pro-inflammatory activity of triclosan, leading to an overall protective effect, including decreased total protein in BALF.

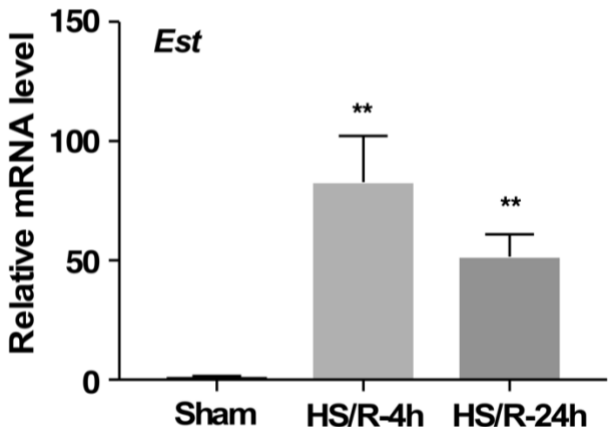

Figure 24. Expression of liver Est at different time point following HS/R.

The mRNA expression of *Est* was measured by real-time PCR. Results are presented as mean ±SE. n=4~5 for each group. *, $p < 0.05$; **, $p < 0.01$, compared to the Sham group.

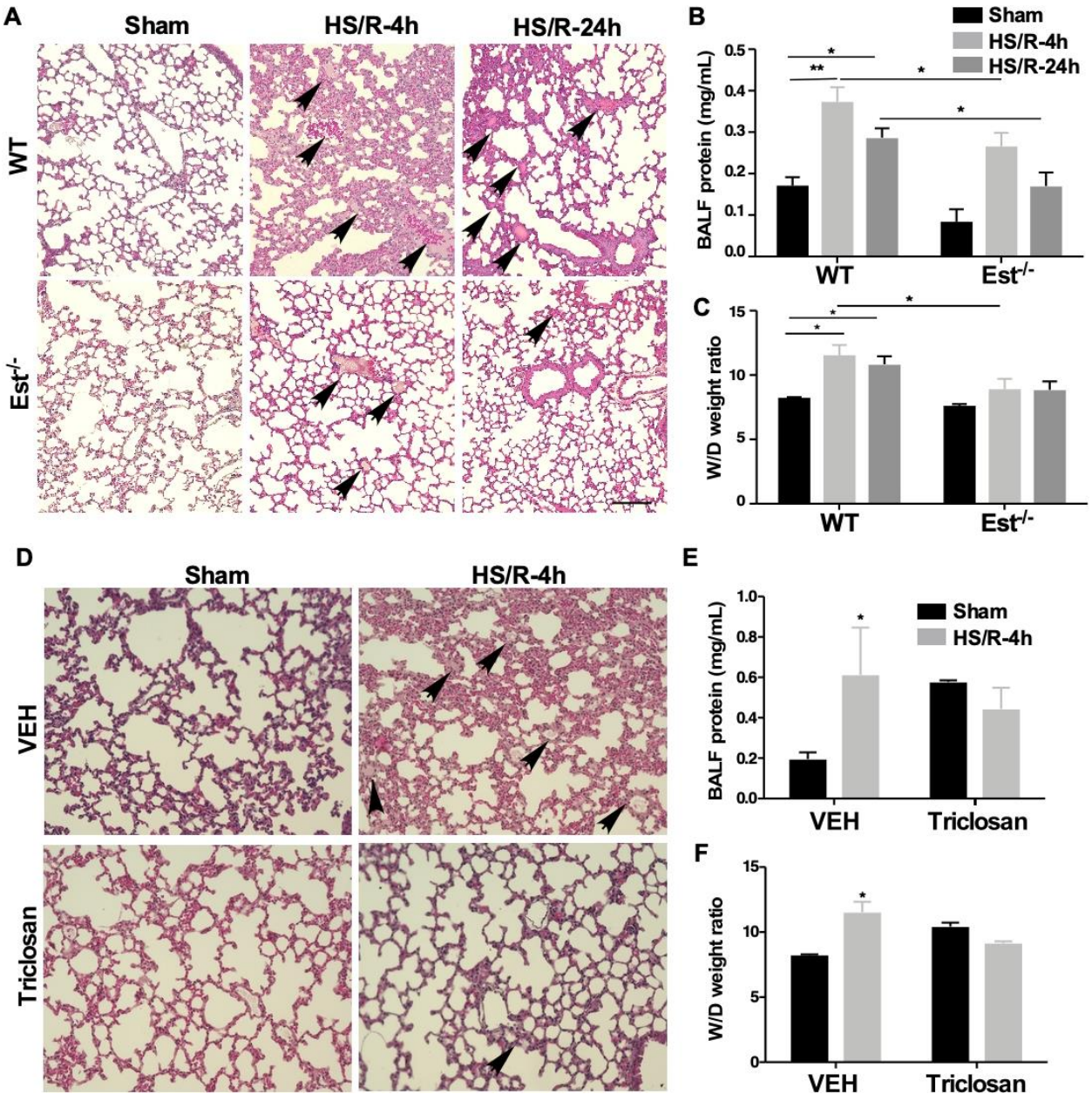

Figure 25. Genetic ablation or pharmacological inhibition of Est protects female, but not male mice from HS-induced acute lung injury.

(A-C) Female WT and *Est-/-* mice were subjected to HS/R. The mice were sacrificed 4 or 24 h after the initiation of HS. Shown are H&E staining of the lung sections (A, Bar is 100 μm). The section shows interstitial edema and infiltrated blood cells in the lung tissue (arrow-head). Protein concentrations in the cell free bronchoalveolar lavage fluid (BALF) (B), and wet/dry (W/D) weight ratio of the lung tissues (C) were also shown. **(D-F)** Female WT mice were subcutaneous injected daily with triclosan (10 mg/kg) beginning 3 days before HS/R surgery. Mice were

sacrificed 4 h after the initiation of HS. Shown are H&E staining of the lung sections (D, original magnification 200x), BALF protein concentrations (E), and lung W/D ratio (F). Results are presented as mean ±SE. n=4-5 for each group. *, $p < 0.05$; **, $p < 0.01$, with the comparisons among groups as labeled (B, C, E and F).

3.2.3.3 The pulmonoprotective effect of Est ablation is estrogen dependent

Consistent with the notion that a primary function of EST is to sulfonate and deactivate estrogens, we found the circulating (Figure 26A) and lung tissue (Figure 26B) levels of estradiol were elevated in sham-treated female Est$^{-/-}$ mice. In contrast, the circulating level of estradiol sulfate was decreased in sham-treated female Est$^{-/-}$ mice (Figure 26C). The dropped levels of estradiol and estradiol sulfate in 4-hour HS-treated Est$^{-/-}$ mice were likely accounted for by the withdrawal of a large volume of blood during HS, and insufficient time to replenish estrogens within 4 hours before the mice were sacrificed. Consistent with the increased lung tissue concentration of estradiol, the pulmonary expression of the estrogen-responsive gene *Areg*, encoding the amphiregulin protein (Deroo et al., 2009), was increased in Est$^{-/-}$ mice subjected to sham surgery (Figure 26D). Since estrogens are known for their pulmonoprotective effect (Breithaupt-Faloppa et al., 2014), we speculated that the elevated circulating and lung tissue estrogen levels might have accounted for the pulmonoprotective phenotype in the female Est$^{-/-}$ mice. To evaluate the estrogen dependence, we performed ovariectomy (OVX) on female Est$^{-/-}$ mice before subjecting them to HS/R. Indeed, OVX attenuated the pulmonoprotective phenotype as shown by histology (Figure 26E), and measurements of BALF protein concentration (Figure 26F) and lung W/D ratio (Figure 26G), suggesting that the pulmonoprotective effect of *Est* ablation was estrogen dependent.

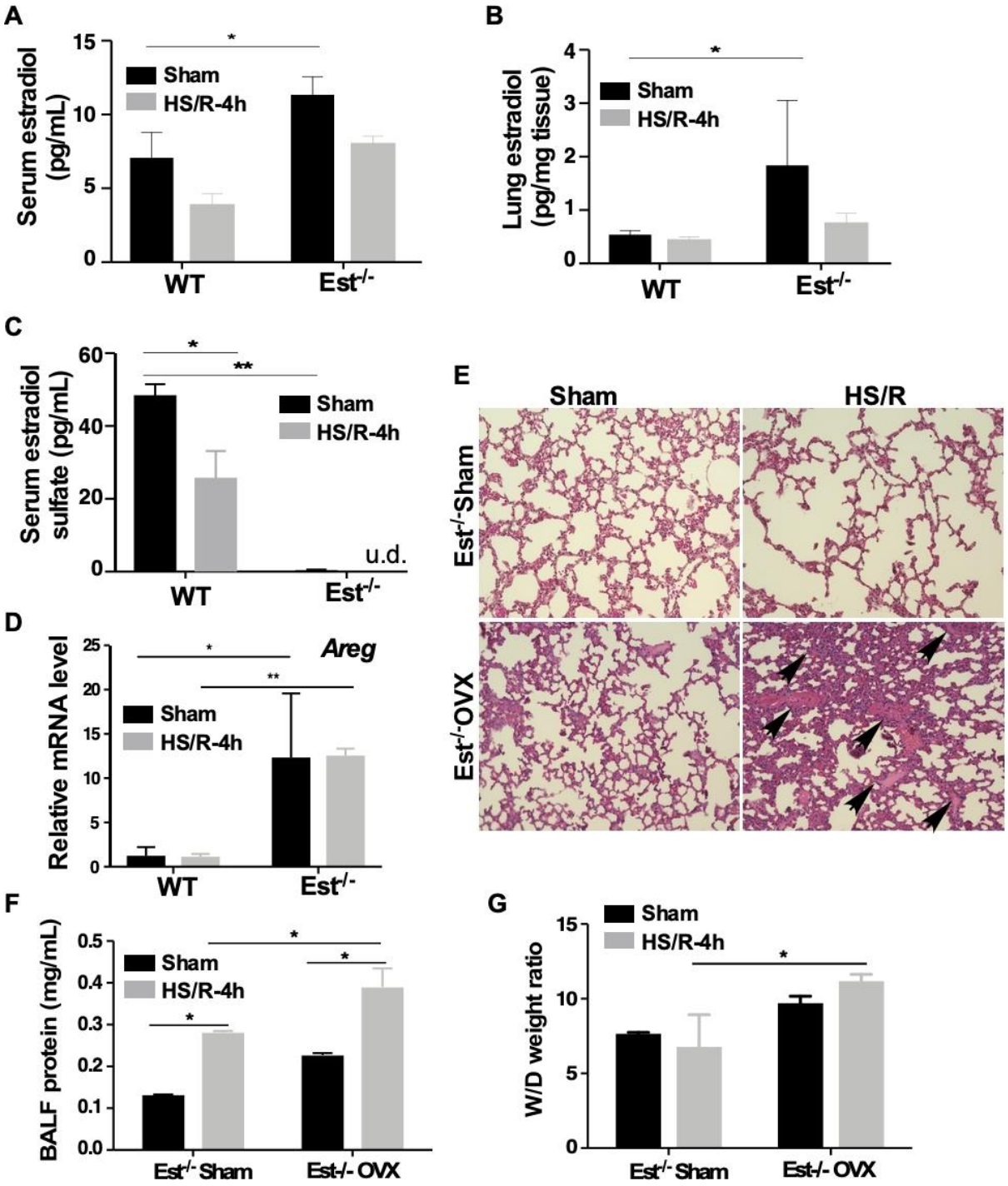

Figure 26. The pulmonoprotective effect of Est ablation is estrogen dependent.

(A-D) Mice are the same 4-h HS/R mice described in Fig. 2A. Shown are serum estradiol levels (A), lung estradiol levels (B), serum estradiol sulfate levels (C), and pulmonary mRNA expression of *Areg* (D). **(E-G)** Female Est-/- mice were subjected to sham surgery or ovariectomy (OVX) at 5 weeks old before being subjected to sham surgery or HS/R

when the mice were 8 weeks old. Mice were sacrificed 4 h after the initiation of HS. Shown are H&E staining of the lung sections (E, original magnification 200x). The section shows interstitial edema and infiltrated blood cells in the lung tissue (arrow-head). BALF protein concentrations (F), and lung W/D ratio (G) were also shown. Results are presented as mean ±SE. n=4-5 for each group. *, $p < 0.05$; **, $p < 0.01$, with the comparisons labeled.

Interestingly, treatment of female Est$^{-/-}$ mice with Fulvestrant, an ERα/β antagonist that destabilizes ER (Casa et al., 2015; Gorska et al., 2016; Win et al., 2019), failed to abolish the pulmonoprotective effect as shown by histology (Figure 27A) and measurements of BALF protein concentration (Figure 27B) and W/D ratio (Figure 27C). As expected, the pulmonary mRNA expression of *Areg* was inhibited by Fulvestrant (Figure 27D). These results suggested that although the protective effect of *Est* ablation was estrogen dependent, it might be ER independent. Hemorrhagic shock had little effect on the pulmonary expression of other enzymes involved in the local estrogen homeostasis, such as aromatase (*Cyp19a1*) (Figure 28A), 17β-hydroxysteroid dehydrogenase (HSD) 17β1 (*Hsd17b1*) (Figure 28B), and steroid sulfatase (*Sts*) (Figure 28C), regardless of the *Est* genotypes.

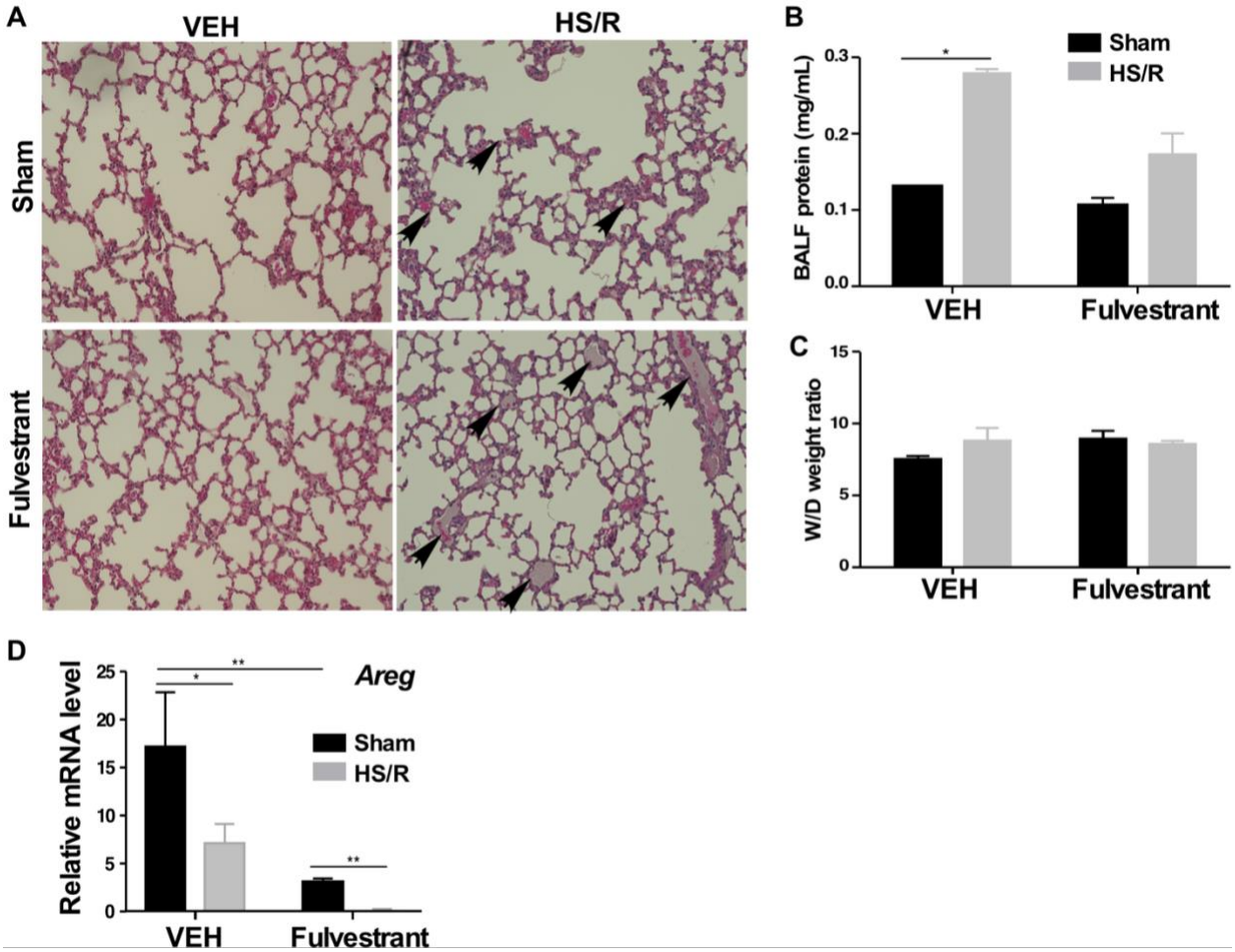

Figure 27. Treatment with the ER antagonist Fulvestrant fails to re-sensitize Est-/- mice to HS-induced acute lung injury.

(A to D) Female Est$^{-/-}$ mice were weekly and subcutaneously injected with Fulvestrant (5 mg/kg) for 3 weeks before being subjected to the Sham surgery or HS/R. Mice were sacrificed 4 h after the initiation of HS. Shown are H&E staining of the lung sections (A, with arrowheads indicating interstitial edema and cell infiltrations, original magnification 200x), BALF protein concentrations (B), and lung W/D ratio (C), and pulmonary mRNA expression of *Areg* (D). Results are presented as mean ±SE. n=4~5 for each group. *, $p < 0.05$; **, $p < 0.01$, with the comparisons labeled.

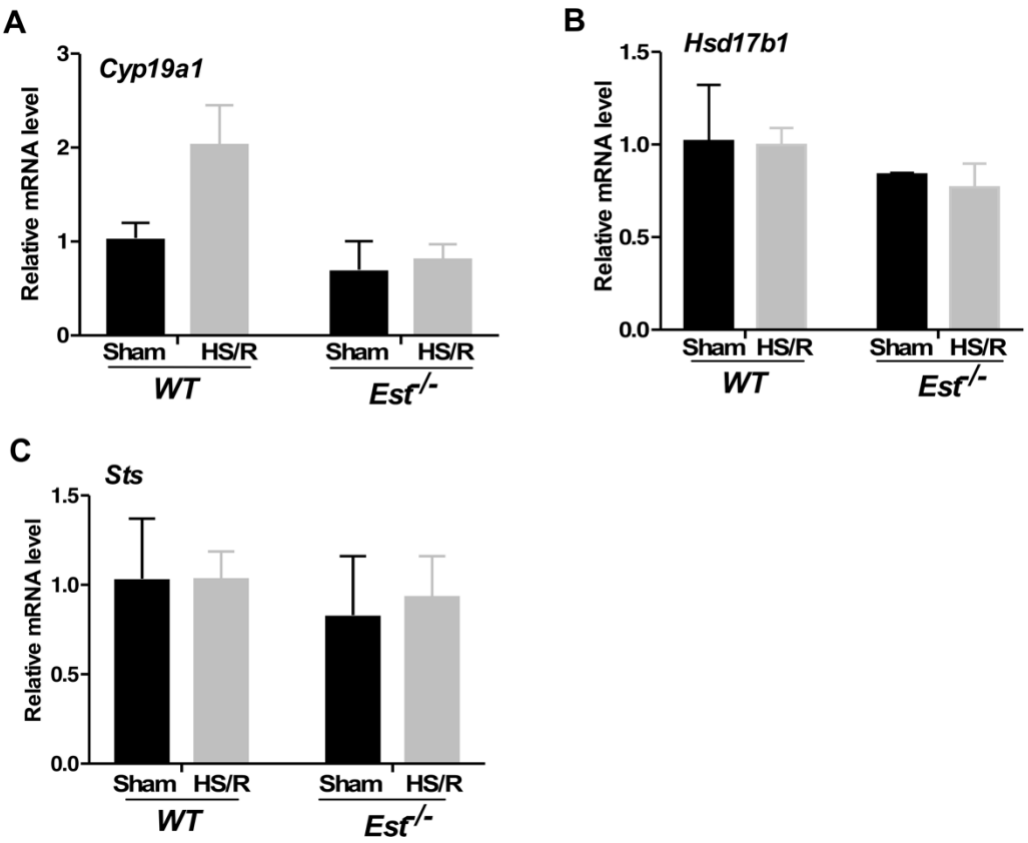

Figure 28. Local estrogen synthesis in the lung is not affected by HS/R.

(A-C) The mRNA expression of genes related to estrogen synthesis, *Cyp19a1* (A), *Hsb17b1* (B), *and Sts* (C) was measured by real-time PCR. Results are presented as mean ±SE. n=3 for each group.

3.2.3.4 Reconstitution of EST to the liver abolishes the pulmonoprotective effect of Est ablation

Since the expression of Est in the lung was barely detectable and it was not inducible by HS/R, we speculated that the phenotype in female Est$^{-/-}$ mice may have resulted from the loss of Est in an extrapulmonary tissue. Knowing that hepatic expression of Est was induced by HS/R in WT mice, we wanted to determine whether EST in the liver played a pathogenic role in HS-induced acute lung injury. For this purpose, we generated the KOLE mice that are Est knockout (KO) and Lap-EST (LE) transgenic. The KOLE mice were generated by breeding the liver-specific

Lap-EST transgene (18) into the Est$^{-/-}$ background as outlined in Figure 29A. The LE transgenic mice express the human EST/SULT1E1 exclusively in the liver under the control of the liver-enriched activator protein (Lap) gene promoter (Chai et al., 2015). The reconstitution of *EST* in the liver, but not in the lung, was verified by Western blotting (Figure 29B). Compared to the acute lung injury resistant female Est$^{-/-}$ mice, the female KOLE mice showed sensitivity to HS/R-induced acute lung injury, as evidence by their increased pulmonary interstitial edema (Figure 29C), BALF protein contents (Figure 29D), and lung W/D ratio (Figure 29E). Consistent with their reconstitution of EST, the sham-treated female KOLE mice showed decreased levels of serum (Figure 29F) and lung tissue (Figure 29G) estradiol, and an increased circulating level of estradiol sulfate (Figure 29H) compared to their Est$^{-/-}$ counterparts.

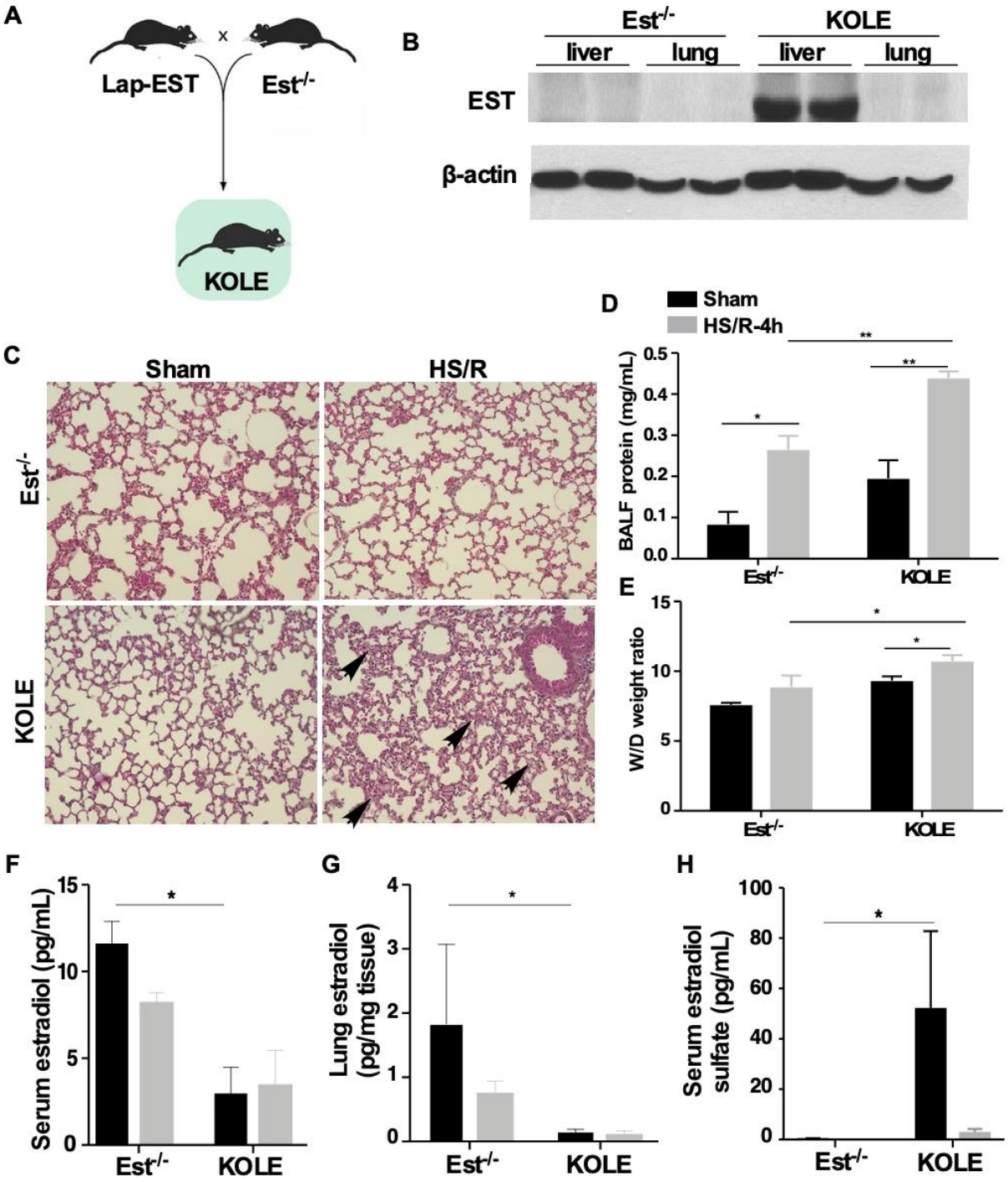

Figure 29. Reconstitution of EST to the liver abolishes the pulmonoprotective effect of Est ablation.

(A) Schematic representation of the creation of the KOLE transgenic mice. **(B)** Expression of EST in the liver and lung as measured by Western blotting. **(C-H)** Female Est-/- and KOLE mice were subjected to the Sham surgery or HS/R. Mice were sacrificed 4 h after the initiation of HS. Shown are H&E staining of the lung sections (C, original

magnification 200x). The section shows interstitial edema and infiltrated blood cells in the lung tissue (arrow-head). BALF protein concentrations (D), lung W/D ratio (E), serum estradiol levels (F), lung estradiol levels (G), serum estradiol sulfate levels (H) were also shown. Data of estradiol and estradiol sulfate levels in Est$^{-/-}$ mice are from the same mice in Figure 23. Results are presented as mean ±SE. n=4-5 for each group. *, $p < 0.05$; **, $p < 0.01$, with the comparisons labeled.

3.2.3.5 Est ablation attenuates, whereas liver reconstitution of EST restores HS-induced lung local and systemic inflammation

Estrogens are known for their anti-inflammatory activities. To determine whether the inhibition of HS-induced acute lung injury in female Est$^{-/-}$ mice was accompanied by the attenuation of inflammation, we evaluated pulmonary infiltration of PMNs, another hallmark of acute lung injury (Matute-Bello et al., 2008), by measuring the number of lung PMNs by flow cytometry and the level of myeloperoxidase (MPO) by immunohistochemistry. Myeloperoxidase is a widely used index of polymorphonuclear neutrophil sequestration that reflects the infiltration of lung parenchymal phagocytes (Bradley et al., 1982). Since PMNs is the most abundant cell type included in CD45^{+}/CD11b^{+}/Gr-1^{+} myeloid cells, we used CD11b and Gr-1 as markers representing PMNs infiltration in this current study. Compared to HS-treated female WT mice, HS-treated female Est$^{-/-}$ mice showed a reduced level of lung CD45^{+}/CD11b^{+}/Gr-1^{+} cells as shown by flow cytometry (Figure 30A) and its quantification (Figure 30B), as well as MPO immunostaining (Figure 30C), and these effects were abolished in ovariectomized Est$^{-/-}$ mice and intact KOLE mice (Figure 30A-30C). Consistent with the results of flow cytometry and histology, the reductions in the pulmonary mRNA expression of *ICAM-1* (Figure 30D) and *IL-6* (Figure 30E), and in the serum (Figure 30F) and BALF (Figure 30G) levels of IL-6 observed in HS-treated female Est$^{-/-}$ mice were attenuated or abolished in ovariectomized Est$^{-/-}$ mice or intact KOLE mice. ICAM-1 contributes

to the firm adhesion and emigration of PMNs (Bullard et al., 1995), whereas IL-6 is known to regulate neutrophil trafficking and function (Fielding et al., 2008). One exception is that ovariectomy did not increase the BALF IL-6 level, suggesting that there might be other yet to be identified substrates or metabolites of Est that may have also contributed to the protective effect *Est* ablation.

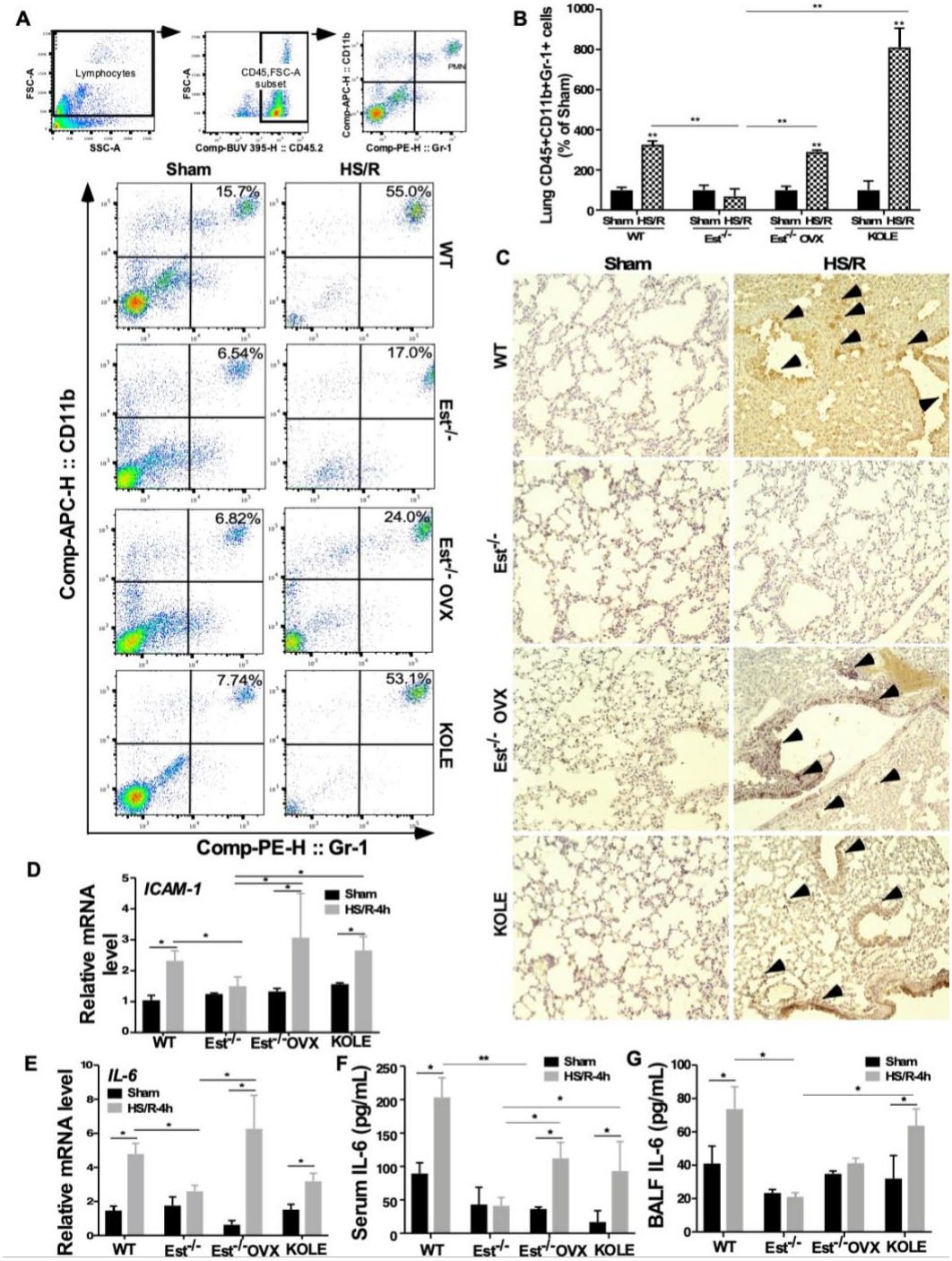

Figure 30. Est ablation attenuates, whereas liver reconstitution of EST restores HS-induced lung local and systemic inflammation.

(A and B) Polymorphonuclear neutrophils (PMN) were quantified by flow cytometry in the lung collected from female WT, Est-/-, Est-/- OVX, and KOLE mice subjected to the Sham surgery or HS/R. Mice were sacrificed 4 h after the initiation of HS. Shown are gating strategy (upper three panels) and representative density plots (bottom panels)

of flow cytometry (A) and quantification of lung $CD45^{+}/CD11b^{+}/Gr\text{-}1^{+}$ PMN cells normalized by PMNs in Sham group (B). **(C)** Myeloperoxidase (MPO) immunohistochemical staining on lung paraffin sections. Arrowheads indicate positive MPO staining. Original magnification 200x. **(D and E)** The mRNA expression of *ICAM-1* (D) and *IL-6* (E) was measured by real-time PCR. **(F and G)** The serum (F) and BALF (G) levels of IL-6 were measured ELISA. Results are presented as mean ±SE. n=4~5 for each group. *, $p < 0.05$; **, $p < 0.01$, with the comparisons labeled.

3.2.3.6 Est ablation attenuates HS-induced PMN mobilization from the bone marrow

Besides the PMN migration to the lung, we also wondered whether Est ablation also affected HS-responsive mobilization of PMNs from the bone marrow (BM) to the circulation. To this end, we went on to measure the numbers of PMNs in peripheral blood and BM collected at multiple time points including 4 and 6 hours after HS by flow cytometry. Based on our result (Figure 31), the change of PMNs peaks at 6 hours after HS rather than 4 hours after HS in WT mice, indicating the release of PMNs from the BM to peripheral blood happens later than the recruitment of PMNs to the lung tissue. Therefore, we continued to measure the changes of PMNs at 6 hours after HS in both WT and $Est^{-/-}$ mice.

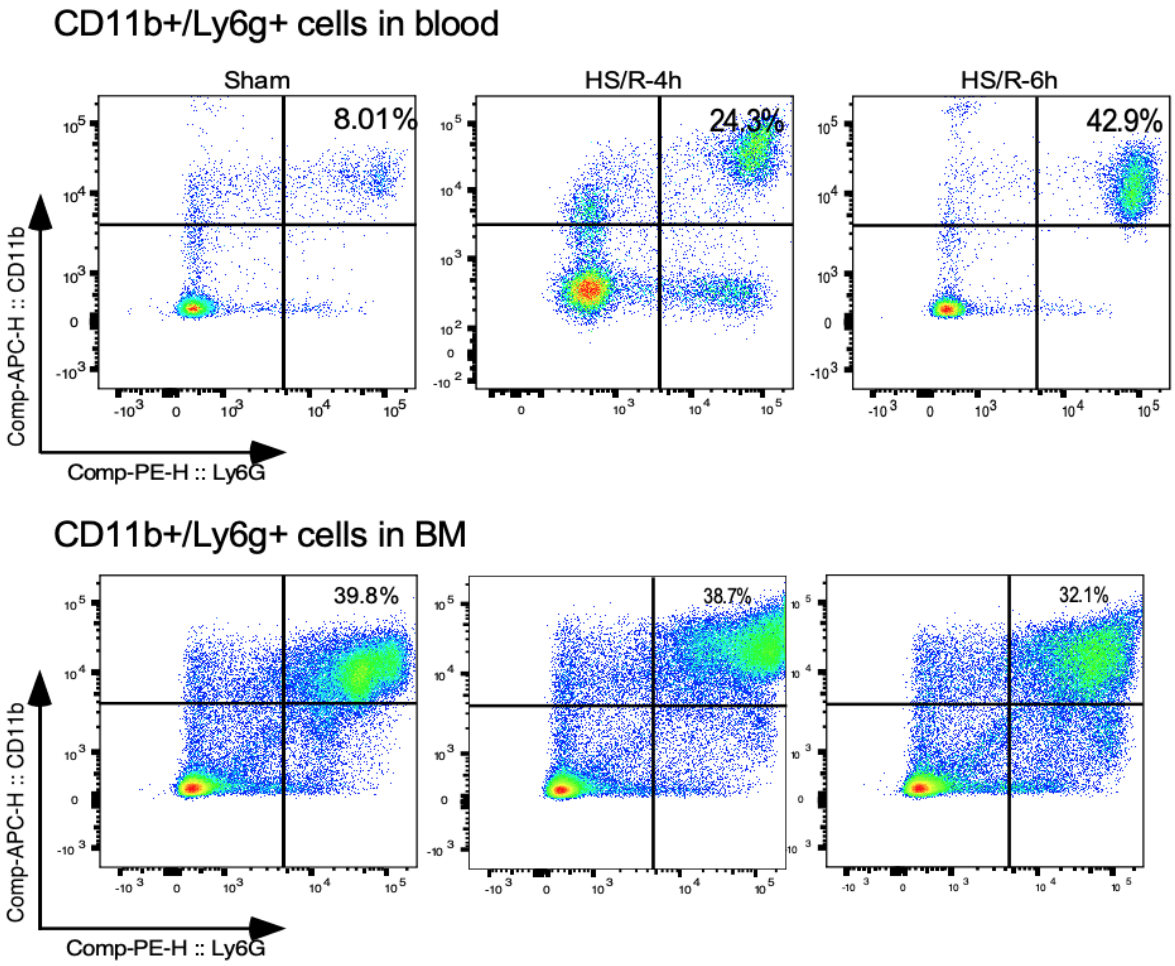

Figure 31. Dynamic changes of PMNs in blood and BM after HS.

Consistent with their attenuation of acute lung injury, HS-treated Est-/- mice showed reduced PMNs mobilization as shown by decreased PMN induction in peripheral blood (Figure 31A and 31B) and attenuated PMN reduction in BM (Figure 31C and 31D) as compared to WT mice at 6 hours after HS. We observed a slightly higher level of blood PMNs in Est-/- mice than WT mice in the sham group. As reported by others, there is an unresolved paradox with respect to the immunomodulating role of estrogens, either suppression of inflammation during trauma and sepsis or the pro-inflammatory effects in some chronic autoimmune diseases in humans. It has been suggested that E_2 can stimulate the expression and secretion of IL-1β and IL-6 in certain cell

or tissue types (35). Future studies are necessary to further define the role of *EST* and estradiol in HS-induced lung inflammation. The C-X-C chemokine receptor type 2 (CXCR2) is an important PMN surface receptor that contributes to PMN release from BM (Eash et al., 2010). There was a 5-fold induction of CXCR2 positive PMNs in the peripheral blood of HS-treated WT mice, but this induction was abolished in HS-treated Est$^{-/-}$ mice (Figure 31E), further suggesting that *Est* ablation inhibited the mobilization of PMN from BM. CXCR4, a chemokine receptor important for PMNs retention in BM was also measure by flow cytometry (data is not shown)(Martin et al., 2003). However, no significant correlation between Est and CXCR4 positive PMNs was found.

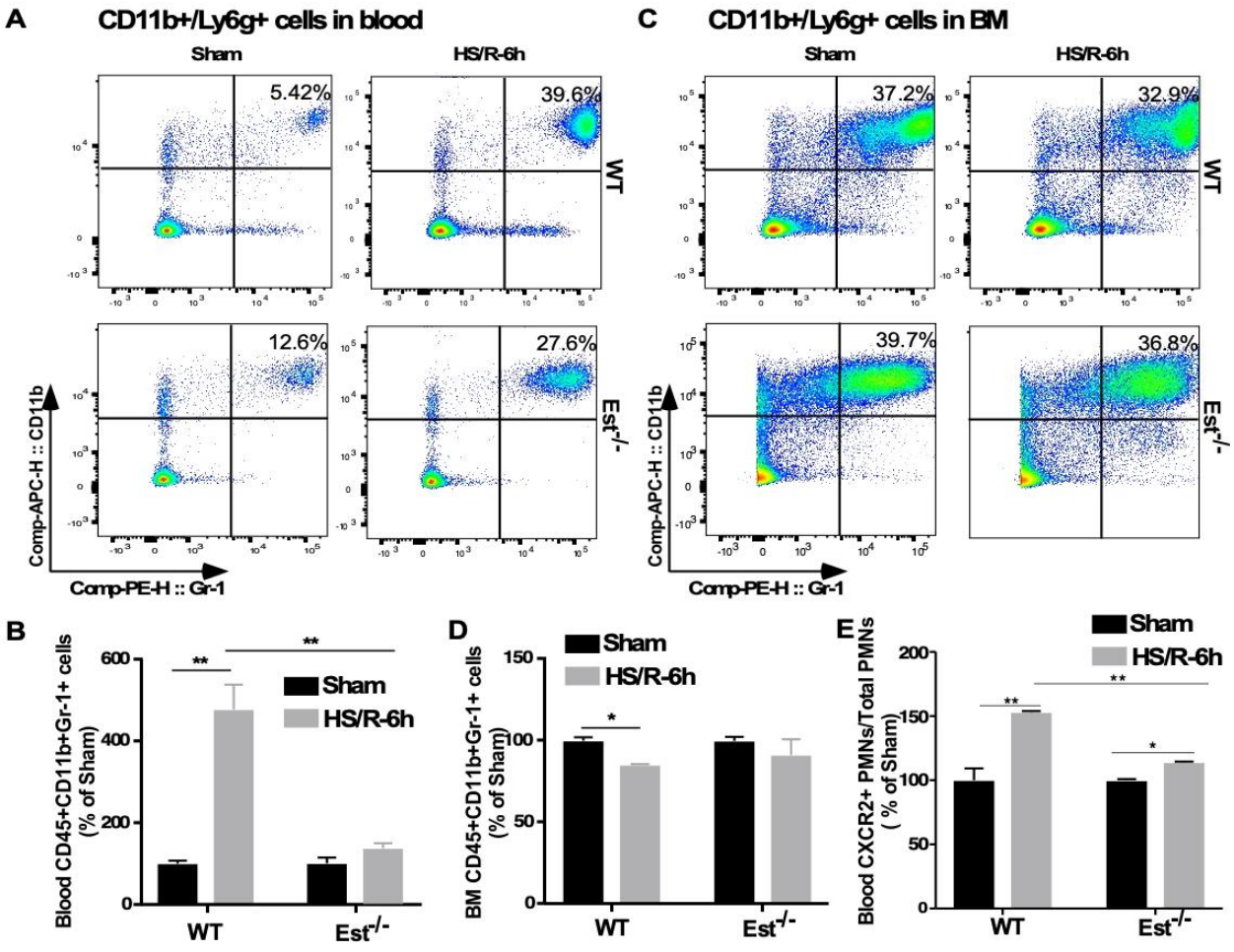

Figure 32. Est ablation attenuates HS-induced PMN mobilization from the bone marrow.

(A-D) PMNs in peripheral blood and bone marrow (BM) of female WT and Est$^{-/-}$ mice subjected to HS/R are quantified by flow cytometry. Mice were sacrificed 6 h after the initiation of HS. Shown are representative density plots (A) and quantification of CD45^{+}/CD11b^{+}/Gr-1^{+} PMN cells normalized by PMNs in Sham group (B) in peripheral blood, as well as representative density plots (C) and quantification of CD45^{+}/CD11b^{+}/Gr-1^{+} PMN cells normalized by PMNs in Sham group (D) in BM. **(E)** Quantification of CXCR2^{+} PMNs in peripheral blood by flow cytometry. Results are presented as mean ±SE. n=3 for each group. *, $p < 0.05$; **, $p < 0.01$, with the comparisons labeled.

3.2.4 Discussion and Conclusion

Hemorrhagic shock remains a major health concern largely due to the secondary tissue and organ injuries. A better understanding of the pathophysiology of HS and the mechanisms by which HS induces tissue injury, including lung injury, will help to develop better therapeutic strategies to reduce the morbidity and mortality of HS. In this study, we have uncovered a novel function of liver EST in HS-induced acute lung injury.

One of our interesting findings was the estrogen dependence and sex-specific effect of *Est* inhibition on HS-induced acute lung injury. Sex-specific differences in pulmonary morbidity in humans have been well documented. The mortality of acute lung injury was higher in male patients compared to female patients (Sperry et al., 2012; Yang et al., 2014). The female protection was postulated to be due to the protective effect of estrogens in pre-menopausal patients (Staren and Omer, 2004; Sperry et al., 2008; Yang et al., 2014), a notion consistent with our finding that the female Est$^{-/-}$ mice were protected from HS-induced acute lung injury and this protection was estrogen dependent. Knowing ER mediates many of the estrogen functions, we were surprised to find that treatment with the ERα/β antagonist Fulvestrant had little effect on the pulmonoprotective effect of Est ablation, suggesting the protection was ER independent. Estrogens are known to exert their functions through multiple pathways in either an ER dependent or independent manner (Hall

et al., 2001; Yue et al., 2013). Future use of ER α and/or β knockout mice will further clarify the role of ER in mediating the *EST* effect. Most of the reported roles of estrogens in traumatic injury relied on the administration of pharmacological doses of estrogens. Our results suggested that the benefit of estrogens in organ protection can also be achieved through the regulation of endogenous estrogen homeostasis, such as that mediated by EST and its regulation. Modulation of estrogen activity by regulating the metabolism of endogenous estrogens has the potential benefit of avoiding side effects associated with pharmacological estrogen therapies (Staren and Omer, 2004).

The inhibition of PMN mobilization from BM by Est ablation was also interesting. The HS-responsive mobilization of PMNs from BM was at least in part contributed to by the induction of CXCR2, a chemokine receptor important for PMN release from BM. The HS-responsive induction of CXCR2 positive PMNs was abolished in Est$^{-/-}$ mice, which may have contributed to the inhibition of PMN mobilization. The effect of Est on the number of CXCR2 positive PMNs was unlikely intrinsic, because PMNs isolated from BM had no detectable expression of *Est* (data not shown). Rather, the induction of CXCR2 positive PMNs may have been explained by the induction of hepatic Est and decreased circulating level of estrogens, because CXCR2 is known to be negatively regulated by estradiol (Lei et al., 2003; Lasarte et al., 2016). Based on literature studies, we were suspecting that estrogens might influence the expression, translocation or intrinsic activity of G protein-coupled receptor kinase (GRK) (probably GRK-2, or 6), and thereby mediating the desensitize and internalize of the CXCR2 (Raghuwanshi et al., 2012; Miyoshi et al., 2013). However, more studies are needed to build the link between circulating estrogens and the expression of CXCR2 on PMNs.

Interestingly, ablation of *Est* had little effect on HS-induced acute lung injury in male mice. The mechanism for the lack of pulmonoprotective effect in male Est$^{-/-}$ mice remains to be

understood. Est ablation had little detectable effect on the circulating and lung tissue levels of estrogens in male mice, which may be due to the extremely low levels of endogenous estrogens that were beyond the detections by LC/MS (data not shown). Nevertheless, the sex-specific effect of *EST* was not uncommon. Sex-specific effects of Est ablation were also observed in our previous studies of metabolic disease and liver ischemia-reperfusion induced liver injury. We reported that Est ablation protected female ob/ob (leptin deficient, or *Lep^{ob}*) mice from obesity and type II diabetes, but sensitized male ob/ob mice to metabolic syndrome (Gao et al., 2012). In a mouse model of liver ischemia-reperfusion, Est ablation conferred hepatoprotection to female mice, whereas the male Est$^{-/-}$ mice were further sensitized (Guo et al., 2015). Interestingly, unlike in the ob/ob mice or in the liver ischemia-reperfusion models, Est ablation did not sensitize male mice to HS-induced acute lung injury.

Another interesting finding was the evidence of organ crosstalk and the tissue-specific effect of EST on HS-induced acute lung injury. Different from liver I/R which blocks the blood flow in the liver and resulted in the damage primarily in the liver, HS is a systemic condition of deprivation of blood and impact on multiple organs including lung, liver and etc. Similar to liver I/R, HS significantly induces liver Est, however, Est ablation surprisingly had little effect on HS-induced hepatic injury. The lack of Est knockout effect on HS-induced hepatic injury was reminiscent of the lack of effect of Est ablation on obesity and type 2 diabetes, despite a marked hepatic induction of this enzyme in metabolic disease (Gao et al., 2012; Garbacz et al., 2017). An even more interesting finding is that the hepatic EST can distantly sensitize mice to HS-induced acute lung injury, which was supported by two key pieces of evidence: 1) There was no appreciable expression or induction of Est in the lung in response to HS; and 2) Reconstitution of EST to the liver of KOLE mice was sufficient to re-sensitize female Est$^{-/-}$ mice to HS-induced acute lung

injury. The distal effect of hepatic EST on HS-induced acute lung injury was likely mediated by hepatic metabolism of estrogens, which led to decreased circulating and lung tissue levels of active estrogens. The lack of HS effect on the pulmonary expression of other enzymes involved in local estrogen homeostasis suggested that the increased estrogen activity in the lung was independent of local estrogen production.

In summary of Chapter III (Figure 32), we have uncovered a novel contribution of liver EST to HS-induced acute lung injury. EST has been shown to affect the structure and function of several tissues, including the male and female reproductive tissues, liver, and adipose tissue. To our best knowledge, the current study represents the first report on the pulmonary function of EST, and the pulmonary effect of EST was achieved via the liver-to-lung organ crosstalk. Our results suggested that pharmacological inhibition of EST, at least in females, might represent a novel therapeutic approach to manage HS-induced acute lung injury.

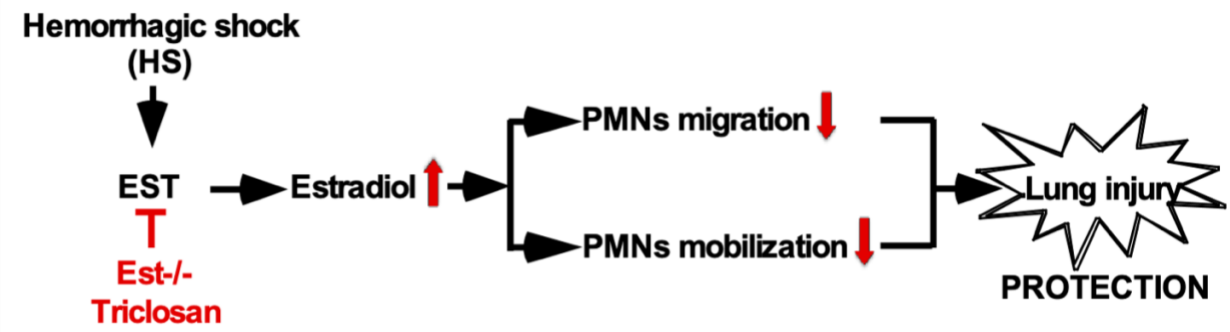

Figure 33. Summary of Chapter III.

4.0 Summary and Perspectives

Over the past 50 years or so, significant advances have been achieved in our emergency management of HS. Despite of the development of modern resuscitation techniques which led to an improved immediate survival, the occurence of subsequent organ failure remains a major health issue that may lead to late death (Minei et al., 2012). Among HS-induced tissue injuries, hepatic injury and acute lung injury are of high incidence (Yu et al., 2008; Wetzel et al., 2014). Acute lung injury is also one of the leading causes of death in surgical and trauma patients with the in-hospital mortality rate as high as 40% (Rubenfeld et al., 2005; Villar et al., 2014). The pathogenesis of HS-induced tissue injury is dynamic, including the deprivation of blood and oxygen supply in the acute phase, followed by blood volume restoration upon resuscitation, or re-establishment of the circulation, which resulted in exaggerated inflammatory responses and oxidative stress. A better understanding of the mechanism by which HS induces tissue injury will help to develop effective strategies for the clinical management of HS in trauma and surgical patients, here we conducted mechanism studies on HS-induced hepatic injury and acute lung injury.

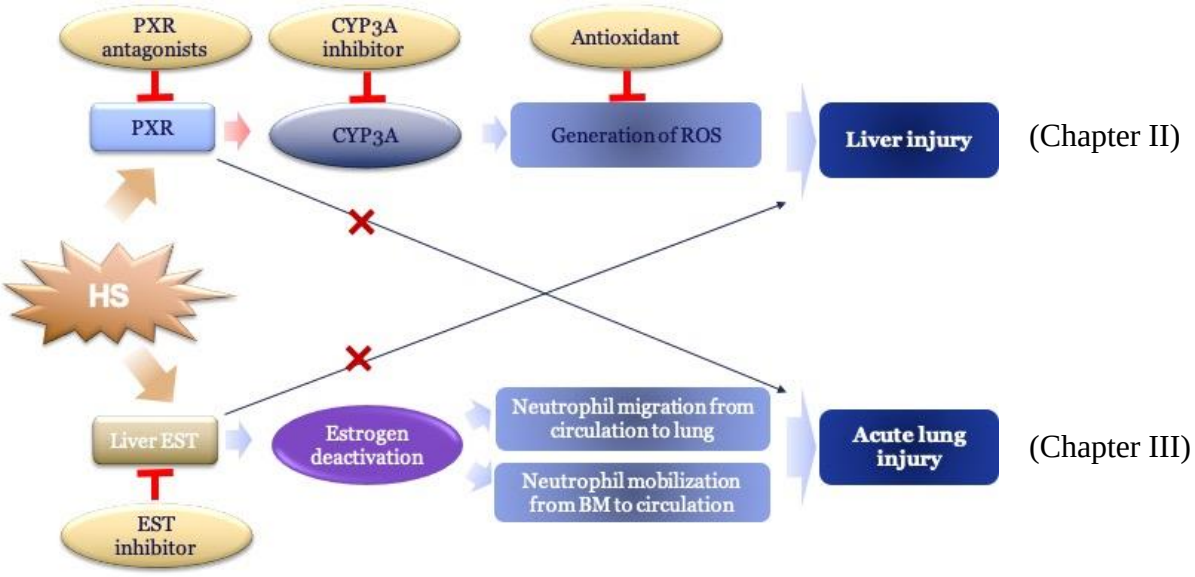

Figure 34. Overall Summary

As summarized in Figure 29, in Chapter II we have investigated the role of PXR in the setting of HS-induced hepatic injury. Since PXR is a species-specific xenobiotic receptor that regulates the expression of DMEs with CYP3A as its primary target gene (Yan and Xie, 2016) and seriously injured trauma patients are often prescribed with medications that can activate PXR and induce CYP3A, including DEX as an ICU medication, fibrates for trauma patients with hyperlipidemia, and the antibiotic RIF for reducing deep surgical site infections (Shiels et al., 2018; Tyas et al., 2018) or for the treatment of tuberculosis. We focused our study on whether and how the activation of PXR plays a role in HS-induced hepatic injury. Through utilizing different pharmacologic and genetic mouse models, we showed that activation of PXR sensitized mice to HS-induced hepatic injury in a CYP3A-dependent manner. The sensitizing effect of PXR on HS-induced hepatic injury can be mitigated by inhibition of CYP3A, or treatment with an antioxidant, or a PXR antagonist. However, manipulation of PXR had little impact on HS-induced acute lung injury. The lack of impact of PXR on HS-induced acute lung injury might because the extremely low expression of PXR in the lung.

As described in Chapter III, we investigated the role of EST in the setting of HS-induced acute lung injury. At the beginning, we were expecting ablation of Est would also show a primary protective effect on HS-induced hepatic injury similar to the results in other liver injury/disease models, including sepsis (Chai et al., 2015), liver I/R (Guo et al., 2015), type II diabetes (Gao et al., 2012), reported in our previous studies since we observed a significant upregulation of Est expression by HS. However, limited protective effect on liver in Est$^{-/-}$ mice subjected to HS were found. In contrast, a significant pulmonoprotective effect was observed in Est$^{-/-}$ mice as early as 4 hours after HS surgery, even though Est expression was barely detectable in the lung. On the other hand, hepatic reconstitution of EST re-sensitized mice to HS-induced ALI. Besides tissue-specific effect, we also demonstrated the sex-specific effect of EST on the outcome of HS-induced acute lung injury. Only female mice responded to Est ablation associated pulmonoprotective effect. Further mechanism study established a link between EST and the mobilization/migration of PMNs into lung following HS mediated by the changes in circulating estrogens, especially 17β-estradiol. The ablation or inhibition of EST resulted in the elevated circulating level of 17β-estradiol, which is believed to be positively associated with a favorable outcome with attenuated lung inflammation after HS (Sperry et al., 2012; Breithaupt-Faloppa et al., 2014; Yang et al., 2014), and thereby reducing the mobilization/migration of PMNs following HS.

Besides mechanisms discussed in this dissertation study, a complex cascade of posttraumatic events related to inflammatory and immune responses, such as complement activation(Younger et al., 2001), contribute the adverse immune consequences of HS. Autophagy can also be induced under stress conditions, which on one hand facilitates cell survival by removing damaged subcellular debris and on the other hand triggers cell death pathways through apoptosis (He and Simon, 2013). Although the current study provides novel insights into the roles

of PXR and EST in HS-induced tissue injury, more studies are needed to take more comprehensive mechanisms into consideration, such as 1) complement activation, autophagy, and their causal relationship with PXR and/or EST; 2) the identification of previously unknown molecular mechanisms underlying the roles of PXR and EST in impacting tissue damage and establishing the link between EST/estrogen signaling and surface CXCR2 expression on neutrophil; 3) the crosstalk between PXR or EST and toll-like receptors (TLRs), TLR4 and TLR2, who have been demonstrated to be key factors impacting tissue injury induced by HS (Li et al., 2009; McDonald et al., 2015; Ding et al., 2017) and sepsis (Chai et al., 2015); as well as 4) the crosstalk between PXR and other nuclear receptors, such as liver X receptor (LXR) and constitutive androstane receptor (CAR).

In summary, in this dissertation study, we uncovered novel functions of PXR and EST in HS-induced tissue injuries in a tissue-specific manner. PXR and EST work through different mechanisms in HS-induced tissue injuries, 1) PXR works as a xenobiotic transcription factor mediating the induction of CYP3A which contributes to HS-induced hepatic injury, but not acute lung injury, through the generation of ROS; 2) Liver EST works as an enzyme catalyzing the sulfation and deactivation of estrogens which distantly impacts on HS-induced lung injury via the recruitment of PMNs to the lung, whereas lack of impacts on HS-induced hepatic injury. Despite of the different mechanisms of PXR and EST in HS-induced tissue injury, both of them are master regulators that control the exogenous and endogenous metabolism, and they are the potential therapeutic targets in preventing of HS-induced tissue injury. Clinical studies are urgently needed for the clinically evaluation of the effectiveness of PXR and EST antagonists or inhibitors in HS patients.

Appendix A

Table 1. Oligonucleotide sequences of primers used for real-time PCR

Gene Name	NCBI Reference	Sequences
mEst	NM_023135.2	Forward: 5'- GGAACGCCAAAGATGTCGCCG -3' Reverse: 5'- ACCATACGGAACTTGCCCTTGCA -3'
mIcam-1	NM_010493.3	Forward: 5'- TTCACACTGAATGCCAGCTC -3' Reverse: 5'- GTCTGCTGAGACCCCTCTTG -3'
mCyp19a1	NM_001348171.1	Forward: 5'- AGCCTGTTGTGGACTTGGTC -3' Reverse: 5'- ACTCGAGCCTGTGCATTCTT -3'
mIl-6	NM_031168.2	Forward: 5'- CGACGGCCTTCCCTACTT -3' Reverse: 5'- TGGGAGTGGTATCCTCTGTGAA -3'
mAreg	NM_009704.4	Forward: 5'- TGGCAGTGAACTCTCCACAG -3' Reverse: 5'- CAATTGCATGTCACCACCTC -3'
mSts	NM_009293.1	Forward: 5'- GCTCGTCTACTTCACCTCGG -3' Reverse: 5'- GTGGGGAAGACGTCCATGAG -3'
mCyclophilin	NM_011149.2	Forward: 5'- GGCTCCGTCGTCTTCCTTTT -3' Reverse: 5'- TGACACGATGGAACTTGCTGT -3'
mCyp3a11	NM_007818.3	Forward: 5'- AGGGAAGCATTGAGGAGGAT -3' Reverse: 5'- GGTAGAGGAGCACCAAGCTG -3'
mCyp2b10	NM_009999.4	Forward: 5'- CGCATGGAGAAGGAGAAGTC -3' Reverse: 5'- CTCTGCAACATGGGGTACT -3'

mCyp2c29	NM_007815.3	Forward: 5’- CATGCAAGACAGGAGCCACA -3’
		Reverse: 5’- CTGCATCAGGCAGGCTAGTG -3’
mCyp2d22	NM_019823.4	Forward: 5’- GGGCCTTTGTTACCATGTTGG -3’
		Reverse: 5’- TACTCGGCGCTGCACATCTG -3’
mPxr	NM_010936.3	Forward: 5’- GGGATAGGGTTACAGCACGA -3’
		Reverse: 5’- TCTGAAAAACCCCTTGCATC -3’
mCatalase	NM_009804.2	Forward: 5’- CACTGACGAGATGGCACACT-3’
		Reverse: 5’- CACTGACGACGAGATGGCACACT-3’
Sod2	NM_013671.3	Forward: 5’- TCTGTGGGAGTCCAAGGTTC-3’
		Reverse: 5’- TAAGGCCTGTTGTTCCTTGC-3’
mGst-α	NM_008181.3	Forward: 5’- GCAGGGGTGGAGTTTGAAGA-3’
		Reverse: 5’- TCTCTTTGGTCTGGGGGACA-3’
mGst-mu	NM_008183.3	Forward: 5’- TTCCCAATCTGCCCTACTTG-3’
		Reverse: 5’- TGCCATAGCCTGGTTCTCC-3’
mGst-pi	NM_013541.1	Forward: 5’- TGCCACCATACACCATTGTC-3’
		Reverse: 5’- CCAGCCTTGCATCCAGGTAT-3’
hPXR	NM_003889.3	Reverse: 5’- ACTCCCCTCACCTGCCATAA -3’
		Reverse: 5’- CTCTTGGACTGCTTGGTGGT -3’
hCYP3A4	NM_017460.5	Forward: 5’-GTCTTTGGGGCCTACAGCAT -3’
		Reverse: 5’- GGGATGAGGAATGGAAAGACTGTT -3’

Table 2. Oligonucleotide sequences of primers used for genotyping

Gene Name	Sequences
hPXR	Forward: 5'-GCA CCT GCT GCT AGG GAA TA-3'
	Reverse: 5'-CTC CAT TGC CCC TCC TAA GT-3'
mPXR	Forward: 5'-CTG GTC ATC ACT GTT GCT GTA CCA-3'
	Reverse-1: 5'- GCA GCA TAG GAC AAG TTA TTC TAG AG -3'
	Reverse-2: 5'-CTA AAG CGC ATG CTC CAG ACT GC -3'
FABP promoter (FABP-VP-PXR)	Forward: 5′-CCATCGATAATTCTCAGAATACAAAACAGT-3′
	Reverse: 5′-CCCAAGCTTCTGACCACAACAGCTCTGTCTGC-3′
mCyp3a11	Forward: 5'-GGTAGCTAGTATAGCAGAACC-3'
	Reverse: 5'-GTACATACAGCTCAGAGCCTG-3'
	Wild-type Cyp3a11 Forward: 5'-CCACCAAATTGACATGAGTCC-3'

Appendix B

Table 3. Antibody information

Antigen	Company	Identifier	Application*	Dilution
4-HNE	Abcam	Ab48506	IHC/WB	1:25/1:200
8-OHdG	Abcam	Ab48508	IF	1:200
Cyp2b10	Abcam	Ab9916	WB	1:200
Cyp3a11/CYP3A4	Obtained from Dr. Frank J. Gonzalez (National Cancer Institute, NIH)		WB	1:200
MPO	Abcam	AB_9353	IHC	1:25
EST	Abcam	AB_197674	IF	1:100
Cyanine 5 conjugated donkey anti-rabbit polyclonal antibody	MilliporeSigma	AP182SA6MI	IF	1:500
Cyanine 3 conjugated donkey anti-mouse polyclonal antibody	MilliporeSigma	AP192C	IF	1:500
DAPI-Fluoromount-G	Southern Biotech	0100-20	IF	-
SULT1E1	Proteintech	12522-1-AP	WB	1:200
β-actin	Sigma-Aldrich	A1978	WB	1:5000

anti-rabbit antibody	Cell Signaling Technology	7074S	WB	1:5000
anti-mouse antibody	Cell Signaling Technology	7076S	WB	1:5000
anti-CD45 buv395	BD Biosciences	564279	Flow	1:100
anti-CD11b-APC	Biolegend	101212	Flow	1:100
anti-Gr-1-PE	Biolegend	108407	Flow	1:100
anti-CXCR2-FITC	Biolegend	149309	Flow	1:100

*: WB, Western blot; IF, Immunofluorescence; IHC, Immunohistochemistry; Flow, Flow cytometry.

Bibliography

Abel RM and Reis RL (1971) Intravenous diazepam for sedation following cardiac operations: clinical and hemodynamic assessments. *Anesth Analg* **50:**244-248.

Albrethsen J, Miller LM, Novikoff PM, and Angeletti RH (2011) Gel-based proteomics of liver cancer progression in rat. *Biochim Biophys Acta* **1814:**1367-1376.

Anderson JE and Blaschke TF (1986) Ketoconazole inhibits cyclosporine metabolism in vivo in mice. *J Pharmacol Exp Ther* **236:**671-674.

Barbosa ACS, Feng Y, Yu C, Huang M, and Xie W (2019) Estrogen sulfotransferase in the metabolism of estrogenic drugs and in the pathogenesis of diseases. *Expert Opin Drug Metab Toxicol* **15:**329-339.

Bi Y, Shi X, Zhu J, Guan X, Garbacz WG, Huang Y, Gao L, Yan J, Xu M, Ren S, Ren S, Liu Y, Ma X, Li S, and Xie W (2018) Regulation of Cholesterol Sulfotransferase SULT2B1b by Hepatocyte Nuclear Factor 4alpha Constitutes a Negative Feedback Control of Hepatic Gluconeogenesis. *Mol Cell Biol* **38**.

Bjerregaard-Olesen C, Bossi R, Bech BH, and Bonefeld-Jorgensen EC (2015) Extraction of perfluorinated alkyl acids from human serum for determination of the combined xenoestrogenic transactivity: a method development. *Chemosphere* **129:**232-238.

Blumberg B, Sabbagh W, Jr., Juguilon H, Bolado J, Jr., van Meter CM, Ong ES, and Evans RM (1998) SXR, a novel steroid and xenobiotic-sensing nuclear receptor. *Genes Dev* **12:**3195-3205.

Bradley PP, Priebat DA, Christensen RD, and Rothstein G (1982) Measurement of cutaneous inflammation: estimation of neutrophil content with an enzyme marker. *J Invest Dermatol* **78:**206-209.

Breithaupt-Faloppa AC, Thais Fantozzi E, Romero DC, Rodrigues Ada S, de Sousa PT, Lino Dos Santos Franco A, Oliveira-Filho RM, Boris Vargaftig B, and Tavares de Lima W (2014) Acute effects of estradiol on lung inflammation due to intestinal ischemic insult in male rats. *Shock* **41:**208-213.

Bullard DC, Qin L, Lorenzo I, Quinlin WM, Doyle NA, Bosse R, Vestweber D, Doerschuk CM, and Beaudet AL (1995) P-selectin/ICAM-1 double mutant mice: acute emigration of neutrophils into the peritoneum is completely absent but is normal into pulmonary alveoli. *J Clin Invest* **95:**1782-1788.

Casa AJ, Hochbaum D, Sreekumar S, Oesterreich S, and Lee AV (2015) The estrogen receptor alpha nuclear localization sequence is critical for fulvestrant-induced degradation of the receptor. *Mol Cell Endocrinol* **415:**76-86.

Chai X, Guo Y, Jiang M, Hu B, Li Z, Fan J, Deng M, Billiar TR, Kucera HR, Gaikwad NW, Xu M, Lu P, Yan J, Fu H, Liu Y, Yu L, Huang M, Zeng S, and Xie W (2015) Oestrogen sulfotransferase ablation sensitizes mice to sepsis. *Nat Commun* **6:**7979.

Dai F, Lee H, Zhang Y, Zhuang L, Yao H, Xi Y, Xiao ZD, You MJ, Li W, Su X, and Gan B (2017) BAP1 inhibits the ER stress gene regulatory network and modulates metabolic stress response. *Proc Natl Acad Sci U S A* **114:**3192-3197.

Deroo BJ, Hewitt SC, Collins JB, Grissom SF, Hamilton KJ, and Korach KS (2009) Profile of estrogen-responsive genes in an estrogen-specific mammary gland outgrowth model. *Mol Reprod Dev* **76:**733-750.

Ding X, Jin S, Tong Y, Jiang X, Chen Z, Mei S, Zhang L, Billiar TR, and Li Q (2017) TLR4 signaling induces TLR3 up-regulation in alveolar macrophages during acute lung injury. *Sci Rep* **7:**34278.

Dooley TP, Haldeman-Cahill R, Joiner J, and Wilborn TW (2000) Expression profiling of human sulfotransferase and sulfatase gene superfamilies in epithelial tissues and cultured cells. *Biochem Biophys Res Commun* **277:**236-245.

Dubaisi S, Caruso JA, Gaedigk R, Vyhlidal CA, Smith PC, Hines RN, Kocarek TA, and Runge-Morris M (2019) Developmental Expression of the Cytosolic Sulfotransferases in Human Liver. *Drug Metab Dispos* **47:**592-600.

Eash KJ, Greenbaum AM, Gopalan PK, and Link DC (2010) CXCR2 and CXCR4 antagonistically regulate neutrophil trafficking from murine bone marrow. *J Clin Invest* **120:**2423-2431.

Edagawa M, Kawauchi J, Hirata M, Goshima H, Inoue M, Okamoto T, Murakami A, Maehara Y, and Kitajima S (2014) Role of activating transcription factor 3 (ATF3) in endoplasmic reticulum (ER) stress-induced sensitization of p53-deficient human colon cancer cells to tumor necrosis factor (TNF)-related apoptosis-inducing ligand (TRAIL)-mediated apoptosis through up-regulation of death receptor 5 (DR5) by zerumbone and celecoxib. *J Biol Chem* **289:**21544-21561.

Edmonds RD, Vodovotz Y, Lagoa C, Dutta-Moscato J, Yang Y, Fink MP, Levy RM, Prince JM, Kaczorowski DJ, Tseng GC, and Billiar TR (2011) Transcriptomic response of murine liver to severe injury and hemorrhagic shock: a dual-platform microarray analysis. *Physiol Genomics* **43:**1170-1183.

Falany CN (1991) Molecular enzymology of human liver cytosolic sulfotransferases. *Trends Pharmacol Sci* **12:**255-259.

Falany CN, He D, Li L, Falany JL, Wilborn TW, Kocarek TA, and Runge-Morris M (2009) Regulation of hepatic sulfotransferase (SULT) 1E1 expression and effects on estrogenic activity in cystic fibrosis (CF). *J Steroid Biochem Mol Biol* **114:**113-119.

Fang JL, Wu Y, Gamboa da Costa G, Chen S, Chitranshi P, and Beland FA (2016) Human Sulfotransferases Enhance the Cytotoxicity of Tolvaptan. *Toxicol Sci* **150:**27-39.

Fang WB, Lofwall MR, Walsh SL, and Moody DE (2013) Determination of oxycodone, noroxycodone and oxymorphone by high-performance liquid chromatography-electrospray ionization-tandem mass spectrometry in human matrices: in vivo and in vitro applications. *J Anal Toxicol* **37:**337-344.

Fielding CA, McLoughlin RM, McLeod L, Colmont CS, Najdovska M, Grail D, Ernst M, Jones SA, Topley N, and Jenkins BJ (2008) IL-6 regulates neutrophil trafficking during acute inflammation via STAT3. *J Immunol* **181:**2189-2195.

Frink M, Pape HC, van Griensven M, Krettek C, Chaudry IH, and Hildebrand F (2007) Influence of sex and age on mods and cytokines after multiple injuries. *Shock* **27:**151-156.

Gamage N, Barnett A, Hempel N, Duggleby RG, Windmill KF, Martin JL, and McManus ME (2006) Human sulfotransferases and their role in chemical metabolism. *Toxicol Sci* **90:**5-22.

Gao J, He J, Shi X, Stefanovic-Racic M, Xu M, O'Doherty RM, Garcia-Ocana A, and Xie W (2012) Sex-specific effect of estrogen sulfotransferase on mouse models of type 2 diabetes. *Diabetes* **61:**1543-1551.

Garbacz WG, Jiang M, Xu M, Yamauchi J, Dong HH, and Xie W (2017) Sex- and Tissue-Specific Role of Estrogen Sulfotransferase in Energy Homeostasis and Insulin Sensitivity. *Endocrinology* **158:**4093-4104.

Glatt H, Boeing H, Engelke CE, Ma L, Kuhlow A, Pabel U, Pomplun D, Teubner W, and Meinl W (2001) Human cytosolic sulphotransferases: genetics, characteristics, toxicological aspects. *Mutat Res* **482:**27-40.

Gong H, Singh SV, Singh SP, Mu Y, Lee JH, Saini SP, Toma D, Ren S, Kagan VE, Day BW, Zimniak P, and Xie W (2006) Orphan nuclear receptor pregnane X receptor sensitizes oxidative stress responses in transgenic mice and cancerous cells. *Mol Endocrinol* **20:**279-290.

Gorska M, Wyszkowska RM, Kuban-Jankowska A, and Wozniak M (2016) Impact of Apparent Antagonism of Estrogen Receptor β by Fulvestrant on Anticancer Activity of 2-Methoxyestradiol. *Anticancer Res* **36:**2217-2226.

Grinstein-Nadler E and Bottoms GD (1976) Dexamethasone treatment during hemorrhagic shock: changes in extracellular fluid volume and cell membrane transport. *Am J Vet Res* **37:**1337-1343.

Guo Y, Hu B, Huang H, Tsung A, Gaikwad NW, Xu M, Jiang M, Ren S, Fan J, Billiar TR, Huang M, and Xie W (2015) Estrogen Sulfotransferase Is an Oxidative Stress-responsive Gene That Gender-specifically Affects Liver Ischemia/Reperfusion Injury. *J Biol Chem* **290:**14754-14764.

Hall JM, Couse JF, and Korach KS (2001) The multifaceted mechanisms of estradiol and estrogen receptor signaling. *J Biol Chem* **276:**36869-36872.

Hamidi SA, Dickman KG, Berisha H, and Said SI (2011) 17beta-estradiol protects the lung against acute injury: possible mediation by vasoactive intestinal polypeptide. *Endocrinology* **152:**4729-4737.

Hardwick RN, Ferreira DW, More VR, Lake AD, Lu Z, Manautou JE, Slitt AL, and Cherrington NJ (2013) Altered UDP-glucuronosyltransferase and sulfotransferase expression and function during progressive stages of human nonalcoholic fatty liver disease. *Drug Metab Dispos* **41:**554-561.

He D, Wilborn TW, Falany JL, Li L, and Falany CN (2008) Repression of CFTR activity in human MMNK-1 cholangiocytes induces sulfotransferase 1E1 expression in co-cultured HepG2 hepatocytes. *Biochim Biophys Acta* **1783:**2391-2397.

He Z and Simon HU (2013) Autophagy protects from liver injury. *Cell Death Differ* **20:**850-851.

Herrero J, Muffato M, Beal K, Fitzgerald S, Gordon L, Pignatelli M, Vilella AJ, Searle SM, Amode R, Brent S, Spooner W, Kulesha E, Yates A, and Flicek P (2016) Ensembl comparative genomics resources. *Database (Oxford)* **2016**.

Hrycay EG and Bandiera SM (2015) Involvement of Cytochrome P450 in Reactive Oxygen Species Formation and Cancer. *Adv Pharmacol* **74:**35-84.

Huang J, Bathena SP, Tong J, Roth M, Hagenbuch B, and Alnouti Y (2010) Kinetic analysis of bile acid sulfation by stably expressed human sulfotransferase 2A1 (SULT2A1). *Xenobiotica* **40:**184-194.

Jaeschke H (2011) Reactive oxygen and mechanisms of inflammatory liver injury: Present concepts. *J Gastroenterol Hepatol* **26 Suppl 1:**173-179.

Jancova P, Anzenbacher P, and Anzenbacherova E (2010) Phase II drug metabolizing enzymes. *Biomed Pap Med Fac Univ Palacky Olomouc Czech Repub* **154:**103-116.

Jhingran A, Kasahara S, and Hohl TM (2016) Flow Cytometry of Lung and Bronchoalveolar Lavage Fluid Cells from Mice Challenged with Fluorescent Aspergillus Reporter (FLARE) Conidia. *Bio Protoc* **6**.

Kauffman FC (2004) Sulfonation in pharmacology and toxicology. *Drug Metab Rev* **36:**823-843.

Kliewer SA, Moore JT, Wade L, Staudinger JL, Watson MA, Jones SA, McKee DD, Oliver BB, Willson TM, Zetterstrom RH, Perlmann T, and Lehmann JM (1998) An orphan nuclear receptor activated by pregnanes defines a novel steroid signaling pathway. *Cell* **92:**73-82.

Kohut LK, Darwiche SS, Brumfield JM, Frank AM, and Billiar TR (2011) Fixed volume or fixed pressure: a murine model of hemorrhagic shock. *J Vis Exp*.

Krattinger R, Bostrom A, Lee SML, Thasler WE, Schioth HB, Kullak-Ublick GA, and Mwinyi J (2016) Chenodeoxycholic acid significantly impacts the expression of miRNAs and genes involved in lipid, bile acid and drug metabolism in human hepatocytes. *Life Sci* **156:**47-56.

Krug EG, Sharma GK, and Lozano R (2000) The global burden of injuries. *Am J Public Health* **90:**523-526.

Lasarte S, Samaniego R, Salinas-Munoz L, Guia-Gonzalez MA, Weiss LA, Mercader E, Ceballos-Garcia E, Navarro-Gonzalez T, Moreno-Ochoa L, Perez-Millan F, Pion M, Sanchez-Mateos P, Hidalgo A, Munoz-Fernandez MA, and Relloso M (2016) Sex Hormones Coordinate Neutrophil Immunity in the Vagina by Controlling Chemokine Gradients. *J Infect Dis* **213:**476-484.

Lee SR, Lee SY, Kim SY, Ryu SY, Park BK, and Hong EJ (2017) Hydroxylation and sulfation of sex steroid hormones in inflammatory liver. *J Biomed Res* **31:**437-444.

Lei ZB, Fu XJ, Lu ZT, Wang BC, Liu XL, and You NZ (2003) Effect of estradiol on chemokine receptor CXCR2 expression in rats: implications for atherosclerosis. *Acta Pharmacol Sin* **24:**670-674.

Li J, Oberly PJ, Poloyac SM, and Gibbs RB (2016) A microsomal based method to detect aromatase activity in different brain regions of the rat using ultra performance liquid chromatography-mass spectrometry. *J Steroid Biochem Mol Biol* **163:**113-120.

Li L and Falany CN (2007) Elevated hepatic SULT1E1 activity in mouse models of cystic fibrosis alters the regulation of estrogen responsive proteins. *J Cyst Fibros* **6:**23-30.

Li Y, Xiang M, Yuan Y, Xiao G, Zhang J, Jiang Y, Vodovotz Y, Billiar TR, Wilson MA, and Fan J (2009) Hemorrhagic shock augments lung endothelial cell activation: role of temporal alterations of TLR4 and TLR2. *Am J Physiol Regul Integr Comp Physiol* **297:**R1670-1680.

Lin W, Wang YM, Chai SC, Lv L, Zheng J, Wu J, Zhang Q, Wang YD, Griffin PR, and Chen T (2017) SPA70 is a potent antagonist of human pregnane X receptor. *Nat Commun* **8:**741.

Liu Y, Yuan Y, Li Y, Zhang J, Xiao G, Vodovotz Y, Billiar TR, Wilson MA, and Fan J (2009) Interacting neuroendocrine and innate and acquired immune pathways regulate neutrophil mobilization from bone marrow following hemorrhagic shock. *J Immunol* **182:**572-580.

Logsdon AF, Lucke-Wold BP, Nguyen L, Matsumoto RR, Turner RC, Rosen CL, and Huber JD (2016) Salubrinal reduces oxidative stress, neuroinflammation and impulsive-like behavior in a rodent model of traumatic brain injury. *Brain Res* **1643:**140-151.

Ma X, Cheung C, Krausz KW, Shah YM, Wang T, Idle JR, and Gonzalez FJ (2008) A double transgenic mouse model expressing human pregnane X receptor and cytochrome P450 3A4. *Drug Metab Dispos* **36:**2506-2512.

Martin C, Burdon PC, Bridger G, Gutierrez-Ramos JC, Williams TJ, and Rankin SM (2003) Chemokines acting via CXCR2 and CXCR4 control the release of neutrophils from the bone marrow and their return following senescence. *Immunity* **19:**583-593.

Matsubara T, Prough RA, Burke MD, and Estabrook RW (1974) The preparation of microsomal fractions of rodent respiratory tract and their characterization. *Cancer Res* **34:**2196-2203.

Matsushita N, Hassanein MT, Martinez-Clemente M, Lazaro R, French SW, Xie W, Lai K, Karin M, and Tsukamoto H (2017) Gender difference in NASH susceptibility: Roles of hepatocyte Ikkbeta and Sult1e1. *PLoS One* **12:**e0181052.

Matute-Bello G, Frevert CW, and Martin TR (2008) Animal models of acute lung injury. *Am J Physiol Lung Cell Mol Physiol* **295:**L379-399.

McDonald KA, Huang H, Tohme S, Loughran P, Ferrero K, Billiar T, and Tsung A (2015) Toll-like receptor 4 (TLR4) antagonist eritoran tetrasodium attenuates liver ischemia and reperfusion injury through inhibition of high-mobility group box protein B1 (HMGB1) signaling. *Mol Med* **20:**639-648.

Minei JP, Cuschieri J, Sperry J, Moore EE, West MA, Harbrecht BG, O'Keefe GE, Cohen MJ, Moldawer LL, Tompkins RG, Maier RV, Inflammation, and the Host Response to Injury Collaborative Research P (2012) The changing pattern and implications of multiple organ failure after blunt injury with hemorrhagic shock. *Crit Care Med* **40:**1129-1135.

Miyoshi T, Otsuka F, and Shimasaki S (2013) GRK-6 mediates FSH action synergistically enhanced by estrogen and the oocyte in rat granulosa cells. *Biochem Biophys Res Commun* **434:**401-406.

Mueller JW, Gilligan LC, Idkowiak J, Arlt W, and Foster PA (2015) The Regulation of Steroid Action by Sulfation and Desulfation. *Endocr Rev* **36:**526-563.

Mueller JW, Idkowiak J, Gesteira TF, Vallet C, Hardman R, van den Boom J, Dhir V, Knauer SK, Rosta E, and Arlt W (2018) Human DHEA sulfation requires direct interaction between PAPS synthase 2 and DHEA sulfotransferase SULT2A1. *J Biol Chem* **293:**9724-9735.

Mungenast F, Aust S, Vergote I, Vanderstichele A, Sehouli J, Braicu E, Mahner S, Castillo-Tong DC, Zeillinger R, and Thalhammer T (2017) Clinical significance of the estrogen-modifying enzymes steroid sulfatase and estrogen sulfotransferase in epithelial ovarian cancer. *Oncol Lett* **13:**4047-4054.

Negishi M, Pedersen LG, Petrotchenko E, Shevtsov S, Gorokhov A, Kakuta Y, and Pedersen LC (2001) Structure and function of sulfotransferases. *Arch Biochem Biophys* **390:**149-157.

Pasqualini JR (2009) Estrogen sulfotransferases in breast and endometrial cancers. *Ann N Y Acad Sci* **1155:**88-98.

Puntarulo S and Cederbaum AI (1998) Production of reactive oxygen species by microsomes enriched in specific human cytochrome P450 enzymes. *Free Radic Biol Med* **24:**1324-1330.

Qian YM, Sun XJ, Tong MH, Li XP, Richa J, and Song WC (2001) Targeted disruption of the mouse estrogen sulfotransferase gene reveals a role of estrogen metabolism in intracrine and paracrine estrogen regulation. *Endocrinology* **142:**5342-5350.

Raftogianis RB, Wood TC, and Weinshilboum RM (1999) Human phenol sulfotransferases SULT1A2 and SULT1A1: genetic polymorphisms, allozyme properties, and human liver genotype-phenotype correlations. *Biochem Pharmacol* **58:**605-616.

Raghuwanshi SK, Su Y, Singh V, Haynes K, Richmond A, and Richardson RM (2012) The chemokine receptors CXCR1 and CXCR2 couple to distinct G protein-coupled receptor kinases to mediate and regulate leukocyte functions. *J Immunol* **189:**2824-2832.

Reinen J and Vermeulen NP (2015) Biotransformation of endocrine disrupting compounds by selected phase I and phase II enzymes--formation of estrogenic and chemically reactive metabolites by cytochromes P450 and sulfotransferases. *Curr Med Chem* **22:**500-527.

Riches Z, Stanley EL, Bloomer JC, and Coughtrie MW (2009) Quantitative evaluation of the expression and activity of five major sulfotransferases (SULTs) in human tissues: the SULT "pie". *Drug Metab Dispos* **37:**2255-2261.

Rubenfeld GD, Caldwell E, Peabody E, Weaver J, Martin DP, Neff M, Stern EJ, and Hudson LD (2005) Incidence and outcomes of acute lung injury. *N Engl J Med* **353:**1685-1693.

Saag MS, Benson CA, Gandhi RT, Hoy JF, Landovitz RJ, Mugavero MJ, Sax PE, Smith DM, Thompson MA, Buchbinder SP, Del Rio C, Eron JJ, Jr., Fatkenheuer G, Gunthard HF, Molina JM, Jacobsen DM, and Volberding PA (2018) Antiretroviral Drugs for Treatment and Prevention of HIV Infection in Adults: 2018 Recommendations of the International Antiviral Society-USA Panel. *JAMA* **320:**379-396.

Saeki Y, Sakakibara Y, Araki Y, Yanagisawa K, Suiko M, Nakajima H, and Liu MC (1998) Molecular cloning, expression, and characterization of a novel mouse liver SULT1B1 sulfotransferase. *J Biochem* **124:**55-64.

Shiels SM, Tennent DJ, and Wenke JC (2018) Topical Rifampin Powder for Orthopaedic Trauma Part I: Rifampin powder reduces recalcitrant infection in a delayed treatment musculoskeletal trauma model. *J Orthop Res*.

Sinreih M, Knific T, Anko M, Hevir N, Vouk K, Jerin A, Frkovic Grazio S, and Rizner TL (2017) The Significance of the Sulfatase Pathway for Local Estrogen Formation in Endometrial Cancer. *Front Pharmacol* **8:**368.

Song WC (2001) Biochemistry and reproductive endocrinology of estrogen sulfotransferase. *Ann N Y Acad Sci* **948:**43-50.

Sperry JL, Friese RS, Frankel HL, West MA, Cuschieri J, Moore EE, Harbrecht BG, Peitzman AB, Billiar TR, Maier RV, Remick DG, Minei JP, Inflammation, and the Host Response

to Injury I (2008) Male gender is associated with excessive IL-6 expression following severe injury. *J Trauma* **64:**572-578; discussion 578-579.

Sperry JL, Vodovotz Y, Ferrell RE, Namas R, Chai YM, Feng QM, Jia WP, Forsythe RM, Peitzman AB, and Billiar TR (2012) Racial disparities and sex-based outcomes differences after severe injury. *J Am Coll Surg* **214:**973-980.

Staren ED and Omer S (2004) Hormone replacement therapy in postmenopausal women. *Am J Surg* **188:**136-149.

Strott CA (2002) Sulfonation and molecular action. *Endocr Rev* **23:**703-732.

Suzuki S, Toledo-Pereyra LH, Rodriguez FJ, and Cejalvo D (1993) Neutrophil infiltration as an important factor in liver ischemia and reperfusion injury. Modulating effects of FK506 and cyclosporine. *Transplantation* **55:**1265-1272.

Svetlov SI, Xiang Y, Oli MW, Foley DP, Huang G, Hayes RL, Ottens AK, and Wang KK (2006) Identification and preliminary validation of novel biomarkers of acute hepatic ischaemia/reperfusion injury using dual-platform proteomic/degradomic approaches. *Biomarkers* **11:**355-369.

Swamydas M and Lionakis MS (2013) Isolation, purification and labeling of mouse bone marrow neutrophils for functional studies and adoptive transfer experiments. *J Vis Exp***:**e50586.

Swamydas M, Luo Y, Dorf ME, and Lionakis MS (2015) Isolation of Mouse Neutrophils. *Curr Protoc Immunol* **110:**3 20 21-23 20 15.

Tien YC, Liu K, Pope C, Wang P, Ma X, and Zhong XB (2015) Dose of Phenobarbital and Age of Treatment at Early Life are Two Key Factors for the Persistent Induction of Cytochrome P450 Enzymes in Adult Mouse Liver. *Drug Metab Dispos* **43:**1938-1945.

Tjalkens RB, Cook LW, and Petersen DR (1999) Formation and export of the glutathione conjugate of 4-hydroxy-2, 3-E-nonenal (4-HNE) in hepatoma cells. *Arch Biochem Biophys* **361:**113-119.

Toklu HZ and Tumer N (2015) Oxidative Stress, Brain Edema, Blood-Brain Barrier Permeability, and Autonomic Dysfunction from Traumatic Brain Injury, in: *Brain Neurotrauma: Molecular, Neuropsychological, and Rehabilitation Aspects* (Kobeissy FH ed), Boca Raton (FL).

Tsai YF, Yu HP, Chung PJ, Leu YL, Kuo LM, Chen CY, and Hwang TL (2015) Osthol attenuates neutrophilic oxidative stress and hemorrhagic shock-induced lung injury via inhibition of phosphodiesterase 4. *Free Radic Biol Med* **89:**387-400.

Tyas B, Marsh M, Oswald T, Refaie R, Molyneux C, and Reed M (2018) Antibiotic resistance profiles of deep surgical site infections in hip hemiarthroplasty; comparing low dose single antibiotic versus high dose dual antibiotic impregnated cement. *J Bone Jt Infect* **3:**123-129.

Valavanidis A, Vlachogianni T, and Fiotakis C (2009) 8-hydroxy-2' -deoxyguanosine (8-OHdG): A critical biomarker of oxidative stress and carcinogenesis. *J Environ Sci Health C Environ Carcinog Ecotoxicol Rev* **27:**120-139.

van Herwaarden AE, Wagenaar E, van der Kruijssen CM, van Waterschoot RA, Smit JW, Song JY, van der Valk MA, van Tellingen O, van der Hoorn JW, Rosing H, Beijnen JH, and Schinkel AH (2007) Knockout of cytochrome P450 3A yields new mouse models for understanding xenobiotic metabolism. *J Clin Invest* **117:**3583-3592.

Villar J, Sulemanji D, and Kacmarek RM (2014) The acute respiratory distress syndrome: incidence and mortality, has it changed? *Curr Opin Crit Care* **20:**3-9.

Wang D, Li Q, Favis R, Jadwin A, Chung H, Fu DJ, Savitz A, Gopal S, and Cohen N (2014) SULT4A1 haplotype: conflicting results on its role as a biomarker of antipsychotic response. *Pharmacogenomics* **15:**1557-1564.

Wang H, Huang H, Li H, Teotico DG, Sinz M, Baker SD, Staudinger J, Kalpana G, Redinbo MR, and Mani S (2007) Activated pregnenolone X-receptor is a target for ketoconazole and its analogs. *Clin Cancer Res* **13:**2488-2495.

Wang LQ, Falany CN, and James MO (2004) Triclosan as a substrate and inhibitor of 3'-phosphoadenosine 5'-phosphosulfate-sulfotransferase and UDP-glucuronosyl transferase in human liver fractions. *Drug Metab Dispos* **32:**1162-1169.

Wen Z, Fan L, Li Y, Zou Z, Scott MJ, Xiao G, Li S, Billiar TR, Wilson MA, Shi X, and Fan J (2014) Neutrophils counteract autophagy-mediated anti-inflammatory mechanisms in alveolar macrophage: role in posthemorrhagic shock acute lung inflammation. *J Immunol* **193:**4623-4633.

Wetzel G, Relja B, Klarner A, Henrich D, Dehne N, Bruhne B, Lehnert M, and Marzi I (2014) Myeloid knockout of HIF-1 alpha does not markedly affect hemorrhage/resuscitation-induced inflammation and hepatic injury. *Mediators Inflamm* **2014:**930419.

Willson TM and Kliewer SA (2002) PXR, CAR and drug metabolism. *Nat Rev Drug Discov* **1:**259-266.

Win S, Min RW, Chen CQ, Zhang J, Chen Y, Li M, Suzuki A, Abdelmalek MF, Wang Y, Aghajan M, Aung FW, Diehl AM, Davis RJ, Than TA, and Kaplowitz N (2019) Expression of mitochondrial membrane-linked SAB determines severity of sex-dependent acute liver injury. *J Clin Invest.*

Xie C, Yan TM, Chen JM, Li XY, Zou J, Zhu LJ, Lu LL, Wang Y, Zhou FY, Liu ZQ, and Hu M (2017) LC-MS/MS quantification of sulfotransferases is better than conventional immunogenic methods in determining human liver SULT activities: implication in precision medicine. *Sci Rep* **7:**3858.

Xie W, Barwick JL, Downes M, Blumberg B, Simon CM, Nelson MC, Neuschwander-Tetri BA, Brunt EM, Guzelian PS, and Evans RM (2000a) Humanized xenobiotic response in mice expressing nuclear receptor SXR. *Nature* **406:**435-439.

Xie W, Barwick JL, Simon CM, Pierce AM, Safe S, Blumberg B, Guzelian PS, and Evans RM (2000b) Reciprocal activation of xenobiotic response genes by nuclear receptors SXR/PXR and CAR. *Genes Dev* **14:**3014-3023.

Xie Y, Xu M, Deng M, Li Z, Wang P, Ren S, Guo Y, Ma X, Fan J, Billiar TR, and Xie W (2019) Activation of Pregnane X Receptor Sensitizes Mice to Hemorrhagic Shock-Induced Liver Injury. *Hepatology*.

Xu J, Guardado J, Hoffman R, Xu H, Namas R, Vodovotz Y, Xu L, Ramadan M, Brown J, Turnquist HR, and Billiar TR (2017) IL33-mediated ILC2 activation and neutrophil IL5 production in the lung response after severe trauma: A reverse translation study from a human cohort to a mouse trauma model. *PLoS Med* **14:**e1002365.

Xu Y, Lin X, Xu J, Jing H, Qin Y, and Li Y (2018) SULT1E1 inhibits cell proliferation and invasion by activating PPARgamma in breast cancer. *J Cancer* **9:**1078-1087.

Xue Y, Moore LB, Orans J, Peng L, Bencharit S, Kliewer SA, and Redinbo MR (2007) Crystal structure of the pregnane X receptor-estradiol complex provides insights into endobiotic recognition. *Mol Endocrinol* **21:**1028-1038.

Yan J and Xie W (2016) A brief history of the discovery of PXR and CAR as xenobiotic receptors. *Acta Pharm Sin B* **6:**450-452.

Yan M, Huo Y, Yin S, and Hu H (2018) Mechanisms of acetaminophen-induced liver injury and its implications for therapeutic interventions. *Redox Biol* **17:**274-283.

Yang KC, Zhou MJ, Sperry JL, Rong L, Zhu XG, Geng L, Wu W, Zhao G, Billiar TR, and Feng QM (2014) Significant sex-based outcome differences in severely injured Chinese trauma patients. *Shock* **42:**11-15.

Yetti H, Naito H, Yuan Y, Jia X, Hayashi Y, Tamada H, Kitamori K, Ikeda K, Yamori Y, and Nakajima T (2018) Bile acid detoxifying enzymes limit susceptibility to liver fibrosis in female SHRSP5/Dmcr rats fed with a high-fat-cholesterol diet. *PLoS One* **13:**e0192863.

Younger JG, Sasaki N, Waite MD, Murray HN, Saleh EF, Ravage ZB, Hirschl RB, Ward PA, and Till GO (2001) Detrimental effects of complement activation in hemorrhagic shock. *J Appl Physiol (1985)* **90:**441-446.

Yu HP, Hsu JC, Hwang TL, Yen CH, and Lau YT (2008) Resveratrol attenuates hepatic injury after trauma-hemorrhage via estrogen receptor-related pathway. *Shock* **30:**324-328.

Yue W, Yager JD, Wang JP, Jupe ER, and Santen RJ (2013) Estrogen receptor-dependent and independent mechanisms of breast cancer carcinogenesis. *Steroids* **78:**161-170.

Zingarelli B, Caputi AP, and Di Rosa M (1994) Dexamethasone prevents vascular failure mediated by nitric oxide in hemorrhagic shock. *Shock* **2:**210-215.

Zolin SJ, Vodovotz Y, Forsythe RM, Rosengart MR, Namas R, Brown JB, Peitzman AP, Billiar TR, and Sperry JL (2015) The early evolving sex hormone environment is associated with significant outcome and inflammatory response differences after injury. *J Trauma Acute Care Surg* **78:**451-457; discussion 457-458.

Zou J, Li H, Huang Q, Liu X, Qi X, Wang Y, Lu L, and Liu Z (2017) Dopamine-induced SULT1A3/4 promotes EMT and cancer stemness in hepatocellular carcinoma. *Tumour Biol* **39:**1010428317719272.